*Center for Alternative Fuels, Engines, & Emissions*

*West Virginia University*

**Contract No. 11611**

**Final Report**

# In-Use Emissions Testing and Demonstration of Retrofit Technology for Control of On-Road Heavy-Duty Engines


**Principal Investigators:**

**Daniel K Carder**
**Mridul Gautam Ph.D**
**Robert C. Byrd Professor of Mechanical and Aerospace Engineering, and**
**Associate Vice President for Research and Economic Development**
**West Virginia University, Morgantown, WV 26506**
**(304) 293-5913 (office); (304) 293-7498 (fax); mgautam@mail.wvu.edu**

**Co-investigators**

**Arvind Thiruvengadam**
**Marc C. Besch**
**Mechanical and Aerospace Engineering, West Virginia University**


**Prepared for:**

**Adewale Oshinuga**
**Project Officer**
**South Coast Air Quality Management District**
**Diamond Bar, CA- 91765**
**E-mail: aoshinuga@aqmd.gov**

**July 2, 2014**

## ACKNOWLEDGEMENTS

WVU would like to thank Ralphs Grocery Distribution Center, Riverside, CA for being a vital partner in this study. We thank Ralphs for hosting the WVU transportable emissions laboratory for over two years and contributing various resources to the success of this study.

WVU thanks SCAQMD and Ports of LA and Long Beach for providing the funding for this research project.

WVU would also like to thank the following individuals and institutions for their time, effort and unconditional support to the success of the study:

- **Ralphs distribution a Kroger Co.- Greg Peterson**
- **United Parcel Service- Mike Britt**
- **Ryder Truck Rental-Heather Kreminszki**
- **Los Angeles Sanitation Bureau- Dr. Kim Tran**
- **Orange County Transit Authority**
- **Total Transportation Services Inc (TTSI)- Deigo Duenas**
- **Hayday Farms- LA Ichida, Dale Tyson**
- **Border Valley Trading- Preston Richter, Greg Braun**
- **Westport Innovations-Aaron Sandstrom**
- **University California Riverside- Ce-CERT**

# TABLE OF CONTENTS

# LIST OF TABLES

# LIST OF FIGURES

## EXECUTIVE SUMMARY

The global objective of this study was to assess the in-use emissions rate of regulated pollutants from heavy-duty diesel, natural gas, propane, and combination of liquefied natural gas and ultra- low sulfur diesel (dual-fuel) technology vehicles. The secondary objectives of the study included the characterization of in-use emissions of ammonia, nitrous oxide ($N_2O$), benzene, toluene, ethyl-benzene, xylene (BTEX), carbonyls and elemental carbon/organic carbon (EC/OC). The secondary objectives also included the evaluation of emission reduction potential of retrofit technology for ammonia emissions from heavy-duty natural gas engines. The study also characterized in-use emissions of oxides of nitrogen (NOx) and greenhouse gas (GHG) from a heavy-duty diesel truck equipped with DPF and SCR during a long-haul operation across the country.

In December 2010 and October 2011, the South Coast Air Quality Management District (SCAQMD) Board awarded contracts to West Virginia University (WVU) and University of California Riverside (UCR) to conduct chassis dynamometer testing of 24 model year (MY) 2007-2012 heavy-duty vehicles from different vocations and fueling technologies, and if necessary, to evaluate emission-reduction potential of retrofit technology for ammonia emission from a natural gas heavy-duty engine. The test vehicle vocation included goods movement, refuse truck, transit bus and school bus applications, and the test cycles used for the specific vocations were port drayage cycles for goods movement, orange county transit authority (OCTA) cycle and central business district (CBD) for transit bus and SCAQMD refuse truck cycles for the refuse trucks. The heavy-duty urban dynamometer driving schedule (UDDS) was a common cycle for all vocations. The test matrix involved five natural gas and four dual-fuel vehicles to be chassis dynamometer tested by WVU, eight diesel and two propane vehicles tested by UCR, and five diesel vehicles tested by both WVU and UCR for inter laboratory comparison. The heavy-duty natural gas engines included both stoichiometric fueled, three-way catalyst (TWC) equipped engines; and lean burn high-pressure direct injection (HPDI) engines equipped with diesel particulate filter (DPF) and selective catalytic reduction (SCR). Diesel engines tested include US-EPA 2007 emissions compliant engines and US-EPA 2010 emissions compliant engines. The USEPA 2007 emissions compliant engines were equipped with exhaust gas recirculation (EGR) and DPF, while the USEPA 2010 emissions compliant engines were of two types: a) with EGR and DPF only b) with DPF and SCR.

Additionally, the WVU's contract also included the in-use characterization of NOx and GHG emissions from a MY 2011 heavy-duty Mack diesel vehicle equipped with DPF and SCR. The Mack vehicle was used to transport a WVU transportable emissions measurement system (TEMS) across the country while continuously measuring emission through a 40 CFR Part 1065 compliant CVS system for over a 2,500-mile route between Morgantown, WV and Riverside, CA. The vehicle was instrumented to

monitor after-treatment NOx and particulate matter (PM) emissions performance and conduct a thorough analysis of the effect of road-grade on real-world emissions rate.

The in-use emissions test results show that the TWC equipped stoichiometric natural gas vehicles emit significantly lower NOx emissions compared to SCR equipped diesel vehicles for all vocations. The stoichiometric air-fuel ratio contributes to a sustained NOx reduction activity by the TWC, unlike the SCR technology that is affected by vehicle operation that results in exhaust temperature lower than 250°C. For example stoichiometric natural gas drayage vehicles emitted 91% lower NOx emissions than a SCR equipped diesel over a near-dock driving cycle characterized by extended idle and creep operation. The SCR catalyst activity profile suggested the after-treatment system was active less than 40% of the time during all types of drayage operation. The HPDI vehicle exhibited a SCR catalyst activity profile similar to that of the diesel technology vehicles. However, the lower in-cylinder NOx formation due to dual-fuel combustion resulted in an overall reduction in NOx emissions compared to SCR equipped diesel vehicles. In addition, the natural gas refuse truck emitted 20% lower NOx emissions than a comparable SCR equipped diesel refuse truck. The PM emissions from both natural gas engines and diesel engines equipped with DPF were close to the detection limits of the gravimetric method.

The activity of the TWC contributes to the formation of ammonia and as a result the stoichiometric natural gas vehicles were characterized by ammonia emissions close to 1 g/mi over all driving cycles. $N_2O$ emissions were observed only during the warm-up period of the TWC. No significant ammonia emissions were detected from SCR equipped diesel vehicles. WVU also conducted preliminary testing to evaluate a retrofit technology for ammonia abatement in stoichiometric natural gas vehicles. The passive SCR technology tested by WVU showed close to 70% reduction in ammonia and 27% further reduction in NOx over the UDDS cycle. As an extension to this study, WVU will be conducting extensive after-treatment development research for ammonia reductions from stoichiometric natural gas engines.

Emissions comparison between stoichiometric natural gas vehicles and SCR equipped diesel vehicles show the TWC after-treatment system to be superior in NOx reduction compared to the SCR system. Since the TWC is dependent on control of the air-fuel ratio close to stoichiometric rather than exhaust temperature characteristics, the activity of the TWC is extended even to idle and creep mode operations. Therefore, natural gas engines can be viewed as better alternatives to diesel technology in certain applications such as refuse trucks and port drayage trucks that are characterized by extended idle and creep mode operations. The fuel range limitation of stoichiometric natural gas engines may limit its operation to smaller geographical ranges. However, the dual-fuel HPDI vehicles with the lean-burn technology provide the same range advantage of a diesel with a relatively lower NOx emissions profile.

The test results also showed that the $NO_2$ fraction of total NOx emissions was lowest for stoichiometric natural gas vehicle with TWC (<2%) and highest for HPDI vehicle equipped with DPF and SCR (average of 50%). The diesel vehicle equipped with DPF and SCR showed an average 14% $NO_2$ fraction in NOx emissions.

Natural gas vehicles equipped with TWC and the HPDI vehicles equipped with SCR showed lower NOx emissions rate during cold start emissions in comparison to diesel vehicles.

Particle size distribution and concentration measurements showed that number concentrations from both diesel vehicles equipped with DPF and natural gas vehicles equipped with TWC were close to ambient levels. The presence of EC in the PM fraction further corroborates the PM size distribution results which showed a particle emissions in the accumulation mode. Since, natural gas combustion is relatively soot free, the presence of EC and the accumulation mode particles could suggest the contribution of lubrication oil to PM emissions from natural gas heavy-duty vehicles.

The tailpipe exhaust global warming potential (GWP) of heavy-duty natural gas vehicles with TWC was lower than the USEPA 2010 emissions compliant diesel vehicles by 6% for the goods movement application. Tailpipe methane emissions was not a significant contributor to GWP in comparison to $CO_2$ contribution from the exhaust. The GWP of natural gas refuse truck was 22% lower than a DPF and SCR equipped diesel refuse truck.

The inter-laboratory comparisons between WVU and UCR served as a quality check for the emissions data from the two laboratories. PM and NOx after-treatment systems can induce high degree of test-to-test variability within a laboratory and between laboratories. Therefore, brake-specific $CO_2$ and total engine work were chosen as the primary metrics to perform the inter-laboratory comparison between WVU and UCR. The inter-laboratory comparison of emissions data between WVU and UCR showed very good agreement between the two laboratories. The brake-specific $CO_2$ emissions and the work comparison between the two laboratories were within 5% and 3% respectively of each other. Brake-specific NOx emissions between the two laboratories also showed good agreement with differences between the laboratories being within 3% of each other for all vehicles with exception of the two diesel refuse trucks.

The results from this study provide a comprehensive understanding of heavy-duty vehicle emissions rates from different fuel and engine technologies. One of the important outcomes of the study is that, it provides accurate emissions inventory of heavy-duty natural gas and diesel vehicles operating in the drayage vocation using driving cycles that closely represent actual vehicle operation. The results illustrate the emission rate as a function of exhaust aftertreatment activity based on driving cycle properties.

Although this test campaign is not representative of engine certification procedure, the results from the brake-specific emissions from HD-UDDS test cycle showed goods movement vehicles from all technologies to have NOx emissions below 0.20 gms/bhp-hr.

Results of the cross-country study showed that the NOx conversion efficiency of the SCR after-treatment system to be an average 83-88% during the course of the test campaign. Sustained temperatures of greater than 250°C contributed to high SCR activity at highway driving conditions. One of the shortcomings of the cross-country study was the lack of high traffic densities in major sections of the route. Therefore the effect of extended idling and stop-and-go traffic on SCR activity was seldom noticed A one-hour duration of a “high NOx” event observed in the state of Kansas contributed to about 92% of the total NOx emitted during a five-hour duration micro trip. The “high NOx” event can be attributed to SCR regeneration strategies adopted by the OEM to burn adsorbed hydrocarbons and/or prevent urea crystallization. . To address the gap in data related heavy-traffic conditions, WVU has been contracted by SCAQMD and CARB to conduct a real-world emissions test campaign focused on vehicle operation within Southern California.

# 1 - INTRODUCTION

United States Environmental Protection Agency (US-EPA) 2010 emissions limits for heavy-duty engines seek to reduce the NOx and PM emissions to near zero levels. The current regulations stipulate the brake-specific NOx and PM emissions from heavy-duty diesel engines tested over the federal test procedure (FTP) engine dynamometer cycle to be at or below 0.20 grams per brake-horsepower (g/bhp-hr) and 0.01 g/bhp-hr, respectively. With the promulgation of the US-EPA 2010 emissions limits, the majority of the heavy-duty engine manufacturers adopted a SCR based after-treatment system with liquid reluctant injection (i.e. urea) for NOx reduction, except one that adopted a complete in-cylinder based NOx reduction strategy using high rates of EGR. Based on the fuel and after-treatment systems, current model year heavy-duty engines can be broadly classified as 1) natural gas engines operating with a TWC; 2) HPDI dual-fuel engines operating with an SCR system; 3) Diesel engines with advanced exhaust gas recirculation (EGR) system and DPF; 4) Diesel engines with DPF and urea-based SCR systems.

Heavy-duty engine certifications are based on the FTP engine dynamometer cycle. Real-world engine operation results in engine operating load conditions that differ from certification engine dynamometer cycles. As a result, a significant difference in the mass rate of emissions of regulated pollutants can be observed between certification value and during in-use operation. As part of the consent decrees settlement in the late 1990's engine manufacturers are required to demonstrate in-use compliance of their engine during normal vocation operating conditions to 1.25 times the FTP standard of 0.20 g/bhp-hr NOx under the engine's lug curve referred to as the Not-To-Exceed (NTE) region. A series of engine torque and speed conditions define the NTE control area (Aneja et al., 2003). Within the NTE control area, manufacturers are provided several allowances to establish a valid NTE event (USEPA, 2004), one of which, is for the temperature of the engine after-treatment system to be above 250 °C. The temperature allowance excludes a majority of emissions resulting during lower load operating conditions for in-use emissions compliance assessment. It is a well-known fact that SCR after-treatment systems require exhaust temperature conditions of at least 250 °C for optimal NOx reductions. Hence, certain heavy-duty applications such as refuse truck and port drayage truck operation might frequently result in periods of non-operation of the SCR after-treatment system, thereby resulting in higher brake-specific NOx emissions compared to their FTP engine certification limits. However, engine emissions during such low exhaust temperature conditions are exempt from in-use emissions compliance by the OEM.

The introduction of current technology heavy-duty diesel and dual-fuel HPDI vehicles has largely contributed to a decrease in both NOx and PM emissions. Technology advancement in the form of DPF

and SCR after-treatment systems has largely contributed to this overall reduction in NOx and PM emissions. However, it should be noted that certain engine operating conditions are not conducive for the sustained operation of urea-SCR systems. These operating conditions are characterized by extended idling time and low load creep mode operations. Therefore it is imperative to understand the effect of different vocations on the emissions rates of regulated pollutants from current technology heavy-duty vehicles.

Current technology heavy-duty natural gas vehicles are available in two platforms, namely the lean burn dual-fuel and the dedicated stoichiometric natural gas engines. The dual-fuel lean burn natural gas engine is developed by Westport Innovations Inc. and is equipped with a proprietary high pressure direct injection (HPDI) natural gas fuel system with diesel pilot injection to initiate the combustion. The pre-2010 model year engine is equipped only with a DPF and the US-EPA 2010 certified engine is equipped with a DPF and urea-SCR after-treatment system. The dedicated stoichiometric fueled natural gas engine manufactured by Cummins Inc. is spark ignited and is equipped with a three-way catalyst for NOx reduction. Studies had shown the presence of ammonia in the exhaust of stoichiometric natural gas engines, therefore it was important for regulatory agencies to investigate the secondary environmental impacts of alternative fuel technology that are primarily favored for their NOx and PM benefits.

SCAQMD has provided various incentives for the procurement, research, development and demonstration of clean alternative fueled transportation and goods movement technologies. Many of these programs have specifically focused on the development of natural gas as a clean alternative fuel for heavy-duty applications. Research and development from these programs have resulted in advancing technology of natural gas engines to reach near-zero NOx and PM emission rates.

### 1.1 OBJECTIVES

The objective of this study was to:

1. Assess in-use emissions rates of carbon monoxide (CO), carbon dioxide ($CO_2$), non-methane hydrocarbons (NMHC), methane ($CH_4$), NOx and PM emissions from heavy-duty diesel, natural gas, and dual fueled vehicles operating as port drayage application, transit buses, and refuse trucks.
2. Characterize in-use ammonia emission rates from stoichiometric fueled natural gas vehicles and urea-SCR diesel vehicles.
3. Characterize in-use particulate number concentrations and Formaldehyde, Benzene, Toluene, Ethyl Benzene and o-p Xylene (BTEX) emissions.
4. Develop a retrofit strategy for reduction of ammonia emissions from natural gas engines.

5. Conduct an in-use cross country evaluation of a heavy-duty diesel truck equipped with DPF and SCR to assess NOx and GHG emissions rates.

WVU and UCR were contracted by SCAQMD to conduct heavy-duty chassis dynamometer testing to achieve the above mentioned objectives. The test matrix included vehicles from 8 engine technology categories distributed among 4 different vocations. A total of 24 heavy-duty vehicles were tested as part of this study. Table 1 shows the matrix of vehicles tested for this study. Table 1 also shows the distribution of test vehicles between WVU and UCR and round-robin test vehicles for cross verification of the two laboratories.

**Table 1 Vehicle test matrix of engine technologies and vehicle vocations**

| Engine/Technology | | Vehicle Vocation/Number of Vehicle | | | |
|---|---|---|---|---|---|
| | | **Transit** | **School Bus** | **Refuse** | **Goods Movement** |
| I. | Natural Gas Engine with 3-Way Catalyst | 1[1] | - | 1[1] | 3[1] |
| II. | HPDI Engine with EGR and DPF at 0.8g NOx | | - | - | 3[1] |
| III. | HPDI Engine with EGR, DPF, and SCR at 0.2g NOx | | | | 1[1] |
| IV. | Diesel Engine Certified at 1.2g NOx | | - | 1[2] | 1[3]+2[2] |
| V. | Propane and Diesel School Bus | - | 2[2] | - | - |
| VI. | Propane engine certified at or below 0.2g NOx | | | 1[2] | |
| VII. | Diesel Engine certified above 0.2g NOx w/o SCR | | - | 1[3] | 1[3]+1[2] |
| VIII. | Diesel Engine certified at or below 0.2g NOx w/SCR | | - | 1[3]+1[2] | 1[3]+2[2] |

***[1] WVU test vehicles; [2] UCR test vehicles; [3] Round-robin test vehicles***

This report includes results from only five natural gas and four dual-fueled vehicles tested by only WVU and five round robin vehicles tested by both WVU and UCR.

## 1.2 ENGINE TECHNOLOGY DISCUSSION

Three broad categories of engine technology were tested by WVU as part of this study. They are as follows:

1. Stoichiometric natural gas engine with TWC
2. HPDI dual fuel engine
3. Diesel engines with DPF and SCR

### *1.2.1 STOICHIOMETRIC NATURAL GAS ENGINES WITH TWC*

US-EPA 2007 emissions compliant natural gas engines were primarily based on a spark ignited lean burn technology. Although the clean burning characteristics of natural gas resulted in orders of magnitude lower PM emissions than comparable diesel engines, the lean burn combustion does not aid lowering

NOx emissions (Ayala et al., 2002). These legacy engine technologies were equipped with only an oxidation catalyst for reduction of CO and NMHC emissions.

Heavy-duty natural gas engines compliant with US-EPA 2010 NOx and PM standards are based on a stoichiometric fueling strategy and NOx control achieved with the use of a TWC. The TWC technology has been historically used in light- and medium-duty gasoline engines for simultaneous reduction of NOx, CO, and hydrocarbons while operating under a stoichiometric fueling strategy. The NOx reduction efficiency of a TWC approaches 100% for slightly rich air-fuel ratio operations and drops significantly toward the leaner side of stoichiometric air-fuel ratios (Defoort et al., 2003). Frequently, engine manufactures adopt a strategy of rapidly changing the air-fuel ratio towards the rich and lean side of the stoichiometric point (i.e. dithering) to optimize the efficiency of TWC to remove all three components over its operating range.

The dedicated heavy-duty natural gas vehicles tested as part of this study were powered by a Cummins ISL-G stoichiometric fueled, cooled EGR and TWC equipped engine. The goods movement and refuse trucks were powered by the 320 hp engine and the transit buses were powered by the 280 hp engine. The Cummins ISL-G engines are the most widely used dedicated natural-gas heavy-duty engines that have been certified to meet the US-EPA 2010 NOx and PM standards.

Natural-gas combustion is relatively soot free in comparison to diesel fuel combustion. Therefore dedicated natural gas engines are capable of meeting the 0.01 g/bhp-hr PM standard without the use of a particulate filter. However, recent studies have shown increased PM emissions due to lubrication oil combustion (Thiruvengadam, 2013). The entry of lubrication oil into the combustion chamber can be attributed to engine deterioration and momentary decrease in piston-cylinder sealing due to changes in in-cylinder pressures. The oil transport mechanism into the combustion chamber is prevalent both in diesel and natural gas engines. However, the absence of a DPF better highlights the contribution of lube oil to PM emissions from natural gas engines. As natural gas engines experience wear from operation, PM number and mass emissions rates may increase. Therefore, it is important to evaluate the impact of natural gas engine deterioration as a result of vehicle duty-cycle on PM number and mass emissions rates.

### *1.2.2 DUAL-FUEL HPDI TECHNOLOGY*

Current model year heavy-duty dual-fueled engines are based on the HPDI technology developed by Westport Innovations Inc. The Westport HPDI fuel system consists of single fuel injectors capable of injecting both natural-gas and diesel fuel directly into the combustion chamber. The first generation HPDI engines were developed on a Cummins ISX platform in 2001. The engine was developed with a non-EGR strategy at brake-specific NOx certification levels of 2.5 g/bhp-hr. The second generation HPDI engines

came into existence on the Cummins ISX EGR diesel engine platform with a brake-specific NOx certification of 1.2 g/bhp-hr. The third generation MY 2009 ISX-G 450 engines are equipped with a DPF and certified at 0.01 g/bhp-hr PM and 0.8 g/bhp-hr NOx . Finally the US-EPA 2010 certified ISX-G 450 is equipped with a DPF and urea-SCR.

Soot emissions from the HPDI engines are primarily from the combustion of the diesel pilot injection. The MY 2009 and MY 2011 HPDI engines are equipped with a DPF to reduce tailpipe soot emissions and meet the 0.01 g/bhp-hr PM standard.

The HPDI dual-fuel engines are very similar in their torque characteristics to diesel engines and offer a greater range than dedicated stoichiometric natural gas engines. The scope of this study included the emissions testing of both the MY 2009 and MY 2011 HPDI dual-fuel engines.

### *1.2.3 DIESEL ENGINES WITH DPF AND SCR*

Brake-specific PM emission standard of 0.01 g/bhp-hr has been in effect since 2007, while the US-EPA decided to phase-in the 0.20 g/bhp-hr NOx emission standard as two phases between 2007 and 2010. Engines developed during the phase-in period were certified at 1.2 g/bhp-hr NOx. As of 2010 all engines were designed to meet the NOx emissions limit of 0.20 g/bhp-hr.

The engines developed under the phase-in period were equipped only with a DPF and NOx control was achieved entirely through an EGR and combustion optimization strategy. All engine manufacturers with the exception of Navistar adopted the SCR pathway to achieve the US-EPA 2010 NOx emissions limit. Navistar adopted the high EGR rate coupled with an advanced combustion strategy to achieve NOx standards. With this strategy, Navistar 2010 engines were certified by US-EPA and CARB at or above 0.5 g/bhp-hr NOx. However, with the use of emissions credits, Navistar was able to meet the US-EPA 2010 NOx emission standard of 0.20 g/bhp-hr.

Manufacturers utilizing the SCR technology were able to certify engines below the 0.20 g/bhp-hr NOx emission standard. The SCR technology injects aqueous urea into the exhaust stream (Diesel Exhaust Fluid-DEF) to release ammonia through a process of thermal hydrolysis in the hot exhaust. The SCR catalyst in the presence of the ammonia reduces NOx to nitrogen and water. However, the efficiency of the SCR after-treatment system is strongly dependent on exhaust gas temperatures. A temperature threshold of 250 °C has been identified as the lower operating temperature of the SCR after-treatment system. Manufacturers refrain from urea injection below this temperature threshold to prevent urea deposits and undesired secondary emissions.

The minimum operating temperature requirement of an SCR system could contribute to significant mass emission rates of NOx from certain applications that are characterized by extended idle and creep

mode operation. Traffic conditions and vehicle vocation can contribute to significant differences between certification NOx values and in-use NOx emissions from heavy-duty SCR equipped diesel vehicles. Hence, it is important to understand the tailpipe emissions rates of SCR equipped heavy-duty diesel vehicles operating in multiple vocations. One of the focuses of this study was to evaluate the NOx emissions profile of heavy-duty vehicles operating as port drayage trucks. This study used drayage driving cycles developed by TIAX LLC to represent three types of drayage operation namely: near-dock, local, and regional type operation (Couch and Leonard, 2011).

Diesel particulate filters are instrumental in removing tailpipe soot emissions from diesel engines to close to the detection limit (0.1 microgram filter loading) of gravimetric measurement systems. Regeneration of a DPF involves the controlled incineration of trapped soot to reduce the plugging of the filter to prevent filter damage and reduce engine back-pressures. Periodic DPF regeneration to burn the trapped soot is vital to the optimum performance and durability of the after-treatment system. DPF filtration efficiencies are largely dependent on the soot cake layer built up over the filter substrate. Studies have shown that regeneration events result in increased PM mass and number emissions due to a loss in filtration efficiency as the soot cake layer is burnt (Ardanese et al., 2009). Manufacturers change DPF regeneration strategies based on the vocation and expected use of the engine. Manufacturers adopt a passive catalyzed regeneration strategy when they know that the exhaust stream of the engine will periodically be hot enough to burn away the trapped soot. An active non-catalyzed regeneration using fuel injection is required for engines where the exhaust stream does not reach temperatures high enough (above 350°C) for DPF regeneration.

### 1.3 VEHICLE AND ENGINE SELECTION

A total of 24 heavy-duty vehicles were chassis dynamometer tested in this study, of which, five natural gas and four dual-fuel vehicles were tested by WVU, and eight diesel and two propane vehicles were tested by UCR. The remaining five vehicles (diesel) were tested by both WVU and UCR for inter laboratory comparison. Table 1 shows the engine technologies and vocations of test vehicles. Table 2 shows the test vehicle and engine specifications.

## Table 2 Vehicle and Engine Specifications of Test Vehicles

| Category | Testing Lab | Vehicle Vocation | Fleet Name | Fuel | Engine | | | | | | Vehicle | | | | Cert. Level NOX (g/bhp-hr) |
|---|---|---|---|---|---|---|---|---|---|---|---|---|---|---|---|
| | | | | | Family | OEM | MY | Model | Disp. (L) | Max Power (HP)@RPM | MY | GVWR | ODO miles | Test Wt. | |
| I | WVU | Transit Bus | OCTA | CNG | 8CEXH054.0LBD | Cummins | 2008 | ISLG280 | 8.9 | 280@2200 | 2008 | 42540 | 116232 | 35000 | 0.2 |
| I | WVU | Refuse Truck | LA Sanitation Bureau | LNG | 8CEXH054.6LBL | Cummins | 2008 | ISLG320 | 8.9 | 320@2100 | 2008 | 58000 | 21465.2 | 56000 | 0.2 |
| I | WVU | Goods Movement | Ryder Truck Rental | CNG | BCEXH054.0LBH | Cummins | 2011 | ISLG320 | 8.9 | 320@2100 | 2011 | 52000 | 191.9 | 69500 | 0.2 |
| I | WVU | Goods Movement | TTSI Drayage Company | LNG | BCEXH054.0LBH | Cummins | 2008 | ISLG320 | 8.9 | 320@2100 | 2008 | 52000 | 45563 | 69500 | 0.2 |
| I | WVU | Goods Movement | TTSI Drayage Company | LNG | BCEXH054.0LBH | Cummins | 2009 | ISLG320 | 8.9 | 320@2100 | 2010 | 50000 | 63256 | 69500 | 0.2 |
| II | WVU | Goods Movement | Border Valley | LNG & ULSD | 8WFSH0912XAL | Westport Innovations | 2008 | ISXG 450 | 14.9 | 450@1800 | 2008 | 48000 | 196562 | 69000 | 0.8 |
| II | WVU | Goods Movement | HayDay | LNG & ULSD | 8WFSH0912XAL | Westport Innovations | 2008 | ISXG 450 | 14.9 | 450@1800 | 2009 | 48000 | 368080 | 69000 | 0.8 |
| II | WVU | Goods Movement | HayDay | LNG & ULSD | 8WFSH0912XAL | Westport Innovations | 2008 | ISXG 450 | 14.9 | 450@1800 | 2008 | 48000 | 379860 | 69000 | 0.8 |
| III | WVU | Goods Movement | UPS | LNG & ULSD | BWFSH0912XAL | Westport Innovations | 2011 | GX 450 | 14.9 | 450@1800 | 2011 | 34700 | 12300 | 69000 | 0.2 |
| IV | WVU UCR | Goods Movement | Ryder Truck Rental | ULSD | 9NVXH0757AGA | Navistar Inc. | 2009 | MAXX FORCE13 | 12.4 | 430@1700 | 2010 | 52000 | 80412 | 69500 | 1.2 |
| IV | UCR | Goods Movement | Container Freight Port | ULSD | 8DDXH14.0ELC | DDC | 2008 | DDC/60 | 14 | 425@1800 | 2009 | 52000 | 129815 | 69500 | 1.07 |
| IV | UCR | Goods Movement | Container Freight Port | ULSD | 8DDXH14.0ELC | DDC | 2008 | DDC/60 | 14 | 425@1800 | 2009 | 52000 | 121766 | 69500 | 1.07 |

| Category | Testing Lab | Vehicle Vocation | Fleet Name | Fuel | Engine | | | | | | Vehicle | | | | Cert. Level NOX (g/bhp-hr) |
|---|---|---|---|---|---|---|---|---|---|---|---|---|---|---|---|
| | | | | | Family | OEM | MY | Model | Disp. (L) | Max Power (HP)@RPM | MY | GVWR | ODO miles | Test Wt. | |
| IV | UCR | Refuse | District 11 CalTrans | ULSD | BNVXH04666AGC | Navistar Inc. | 2008 | GDT260 | 7.6 | 260@2200 | 2009 | 33000 | 9754 | 56000 | 0.82 |
| V | UCR | School Bus | Moreno Valley SD | Propane | 8GMXH08.1502 | GM | 2008 | LPI | 8.1 | 330@1800 | 2009 | 30280 | 55570 | 20000 | * |
| V | UCR | School Bus | A-Z Bus Sales | ULSD | 7CEXH0408BAC | Cummins | 2007 | IS | 6.7 | 220@1800 | 2008 | 31000 | 3357 | 20000 | 2.0* |
| VI | UCR | Goods Movement | Port/China Shipping | Propane | 9BPTE08.1601 | GM | 2009 | P | 8.1 | 325@4000 | 2005 | 52000 | 103608 | 69500 | 0.2 |
| VII | UCR | Goods Movement | Ryder | ULSD | ANVXH0757AGA | Navistar Inc. | 2010 | 12WZJ/B | 12.4 | 430@1700 | 2011 | 52000 | 80651 | 69500 | 0.46 |
| VII | WVU UCR | Goods Movement | Idealease of Los Angeles | ULSD | BNVXH07570GB | Navistar Inc. | 2011 | MAXX FORCE13 | 12.4 | 475@1700 | 2011 | 52350 | 67373 | 69500 | 0.5 |
| VII | WVU UCR | Refuse | CalTrans | ULSD | BNVZH0466AGA | Navistar Inc. | 2011 | MAXX FORCE A260 | 7.6 | 260@2200 | 2012 | 33000 | 10014 | 56000 | 0.5 |
| VIII | UCR | Refuse | Waste Connection | ULSD | BCEXH0540LAQ | Cummins | 2011 | ISL9 370 | 8.9 | 370@2100 | 2012 | 36000 | 2500 | 56000 | 0.2 |
| VIII | WVU UCR | Refuse | EDCO | ULSD | BCEXH0505CAC | Cummins | 2011 | ISC 8.3 300 | 8.3 | 300@2000 | 2011 | 60000 | 14269.4 | 56000 | 0.2 |
| VIII | UCR | Goods Movement | Pac Lease | ULSD | BCEXH0729XAC | Cummins | 2011 | ISX15-485 | 11.9 | 425@1800 | 2011 | 80000 | 4769 | 69500 | 0.12 |
| VIII | UCR | Goods Movement | Coca Cola | ULSD | ACEXH0505CAC | Cummins | 2010 | ISC-300 | 8.3 | 300@2100 | 2011 | 52000 | 13918 | 65000 | 0.2 |
| *VIII | WVU UCR | Goods Movement | Worldwide Rentals | ULSD | BVPTH12.8S01 | Mack | 2011 | MP8-445C | 12.8 | 445@1500 | 2011 | 52000 | 36982 | 69500 | 0.2 |

*Vehicle used for cross-country trip

## 1.4 TEST CYCLES

The objective of the study was to quantify the emissions rates of regulated and unregulated pollutants from heavy-duty vehicles operating under different vocations with different fuel technology. Hence, the test protocol adopted the respective driving cycles that are representative of real-world driving pattern to simulate on-road activity. Table 3 shows the test cycles used for the different vocation vehicles. The drayage port cycles consisted of three individual cycles, independently tested. The Central Business District (CBD) cycle was exercised as a double length to increase the mass loading on sample media used for PM and unregulated pollutant analysis. The heavy-duty Urban Dynamometer Driving Schedule (HD-UDDS) was the common cycle used for all vocations. The HD-UDDS was used as an indicator for evaluating the emissions compliance of the engine with respect to FTP engine dynamometer certification.

**Table 3 List of test cycles for different vehicle vocations**

| Vehicle Vocation | HD-UDDS | Drayage Port Cycles (Near-dock, Regional, Local) | SCAQMD Refuse truck cycles | Orange County Transit Authority (OCTA) | Double length CBD |
|---|---|---|---|---|---|
| Refuse Truck | X | | X | | |
| Transit Bus | X | | | X | X |
| Goods Movement | X | X | | | |

### *1.4.1 DRAYAGE PORT CYCLES*

The drayage port cycles were developed by TIAX LLC (Couch and Leonard, 2011) and characterized the duty cycle of on-road heavy-duty vehicles operating in a port drayage goods movement application. In developing the port cycles, TIAX logged over 1,000 vehicles to statistically create a representative test cycle for chassis dynamometer evaluation of drayage vehicles. The TIAX study categorized a typical drayage vehicle operation into three cycles including, near-dock, local, and regional. The three cycles were created by combining 7 modal trip data sets characterized by periods of creep, low speed transient, short high speed transient, long high speed transient, high speed cruise segment 1, high speed cruise segment 2, and high speed cruise segment 3 operations (Couch, 2011b). The drayage cycles were used to test only goods movement vehicles shown in Table 2.

#### *1.4.1.1 NEAR-DOCK CYCLE*

The near-dock cycle represents heavy-duty vehicle operation within the confines of the port in transporting goods in and out of the port. The cycle is characterized by extended idle times and creep mode operation. The near-dock chassis cycle has a duration of 3,049 seconds with a distance of 5.6 miles

(Couch, 2011a). Table 4 shows the chassis dynamometer cycle metrics for the near-dock cycle. It can be seen that for 98% of the total cycle duration the inlet gas temperatures to the SCR catalyst was below its activation threshold of 250 °C. Although this cycle is an appropriate candidate for a low temperature cycle, the extended duration of idle and its representativeness of inside port operation would bias the representation of the cycle to only port vehicle applications. Figure 1 shows the vehicle speed-time trace for the near-dock port drayage test cycle.

**Table 4 Chassis Cycle Metrics for Near-Dock Operation**

| | |
|---|---|
| Average Vehicle Speed (MPH) | 6.56 |
| Average Engine Torque (N-m) | 314 |
| Average Engine Speed (rpm) | 1038 |
| Average SCR Inlet Temperature (°C) | 168 |
| Duration of engine operation below after-treatment temperature of 250°C (sec) | 3000 |
| Percentage of engine operation below after-treatment temperature of 250°C (%) | 98.4 |

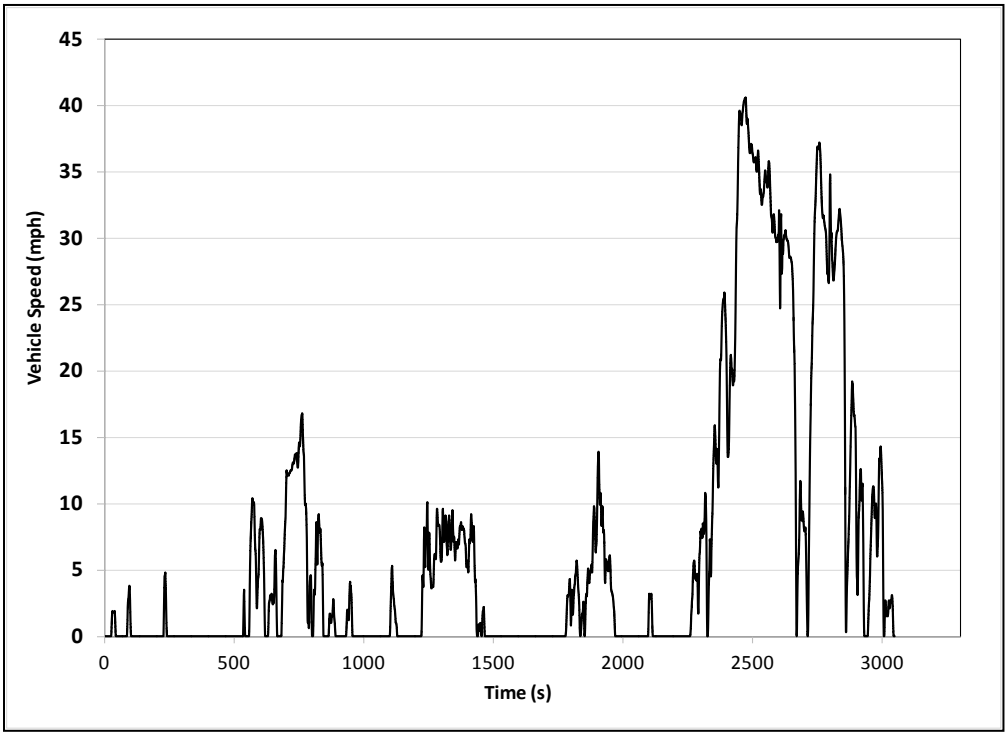


**Figure 1 Speed trace for near-dock drayage test cycle**

#### *1.4.1.2 LOCAL CYCLE*

The local cycle operation is representative of goods transportation by heavy-duty vehicles within a radius of 20 miles of the ports to warehouses and truck distribution centers. Since the location of the

warehouses and truck distribution centers are within the urban region of Los Angeles, the vehicle operation is characterized by highly transient low speed operation with frequent idles. The duration of this chassis dynamometer cycle is 4,643 seconds with a total distance of 8.7 miles (Couch, 2011a). Table 5 shows the chassis dynamometer cycle metrics for the local cycle. It can be seen that for 72.7% of the total cycle duration the inlet gas temperatures to the SCR catalyst was below its activation threshold of 250 °C. Although the cycle data is derived from drayage vehicle operation, it is representative of heavy-duty goods movement operations in the Los Angeles region of California. Figure 2 shows the vehicle speed-time trace for the local port drayage test cycle.

**Table 5 Chassis Cycle Metrics for Local Operation**

| **Local Cycle** | |
|---|---|
| Average Vehicle Speed | 9.33 |
| Average Engine Torque (N-m) | 358 |
| Average Engine Speed (rpm) | 1066 |
| Average SCR Inlet Temperature (°C) | 192 |
| Duration of engine operation below after-treatment temperature of 250°C (sec) | 2446 |
| Percentage of engine operation below after-treatment temperature of 250°C (%) | 72.7 |

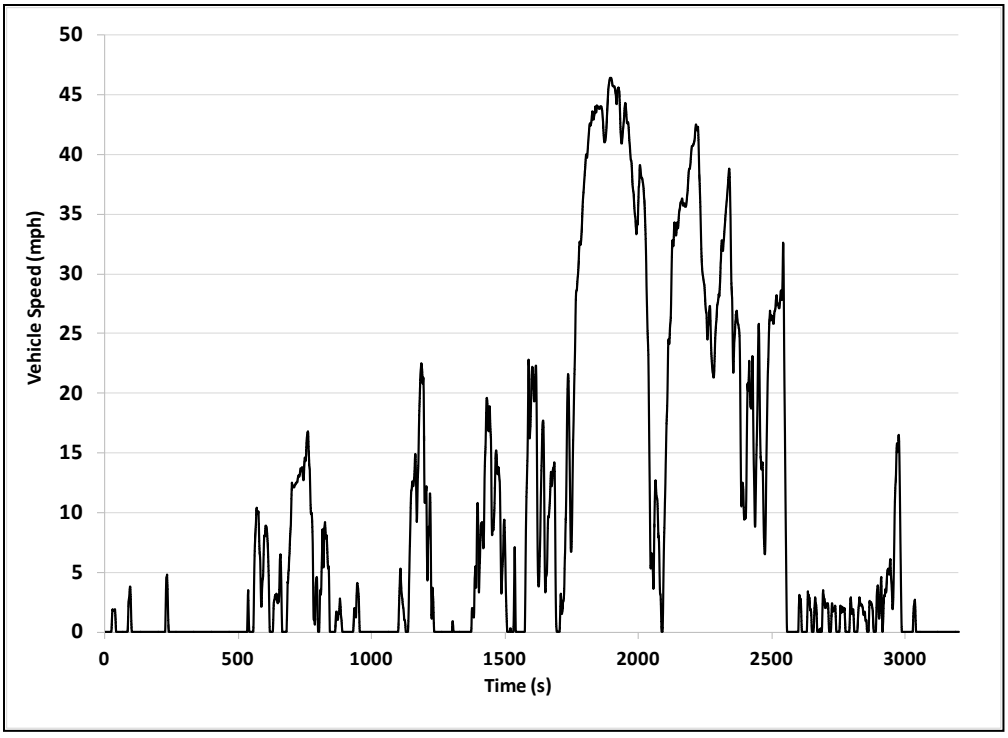


**Figure 2 Speed trace for local drayage test cycle**

#### *1.4.1.3 REGIONAL CYCLE*

The regional cycle is representative of heavy-duty goods transportation by heavy-duty vehicles to destinations that are between 20 and 120 miles away from the port and involve predominant high speed freeway operation. The vehicle operation during this cycle is characterized by high speeds and higher exhaust gas temperature conditions (Couch, 2011a). Table 6 shows the chassis dynamometer cycle metrics for the regional cycle. It can be seen that for 51.2% of the total cycle duration the inlet gas temperatures to the SCR catalyst was below its activation threshold of 250 °C. A 3,000 second high speed section of the cycle contributes to higher exhaust gas temperatures compared to the local cycle. The cycle duration is 4,452 seconds with a total distance of 27.4 miles. Figure 3 shows the vehicle speed-time trace for the regional drayage cycle.

**Table 6 Chassis cycle metrics for regional operation**

| **Regional Cycle** | |
|---|---|
| Average Vehicle Speed | 22 |
| Average Engine Torque (N-m) | 530 |
| Average Engine Speed (rpm) | 1224 |
| Average SCR Inlet Temperature (°C) | 234 |
| Duration of engine operation below after-treatment temperature of 250°C (sec) | 2283 |
| Percentage of engine operation below after-treatment temperature of 250°C (%) | 51.2 |

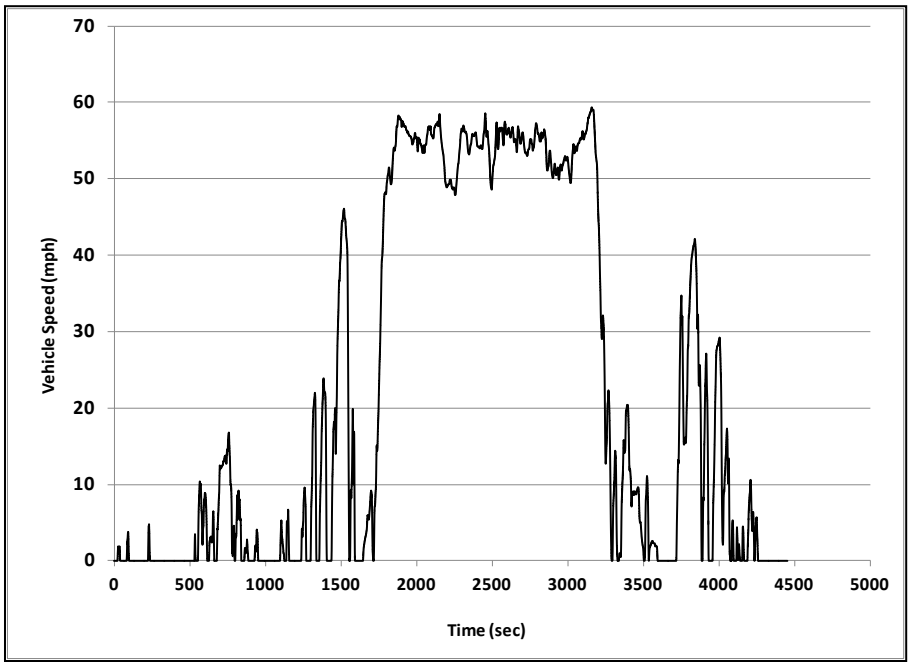


**Figure 3 Speed trace for regional drayage test cycle**

### *1.4.2 HEAVY-DUTY URBAN DYNAMOMETER DRIVING SCHEDULE (HD-UDDS)*

The UDDS cycle simulates the freeway and non-freeway operation of a heavy-duty vehicle. The HD-UDDS and the heavy-duty federal test procedure (FTP) cycle used for engine certification were derived from the same data set. The cycle duration is 1,060 seconds with a maximum speed of 58 mph. Figure 4 shows the speed-time trace for the HD-UDDS driving cycle. The vehicle is exercised over 5.5 miles over the entire test cycle. The HD-UDDS cycle is similar in load characteristics to that of the FTP transient engine dynamometer test procedure since both cycles were developed from the same data set. However, the chassis dynamometer HD-UDDS driving cycle is not a substitute for FTP engine dynamometer test procedure.

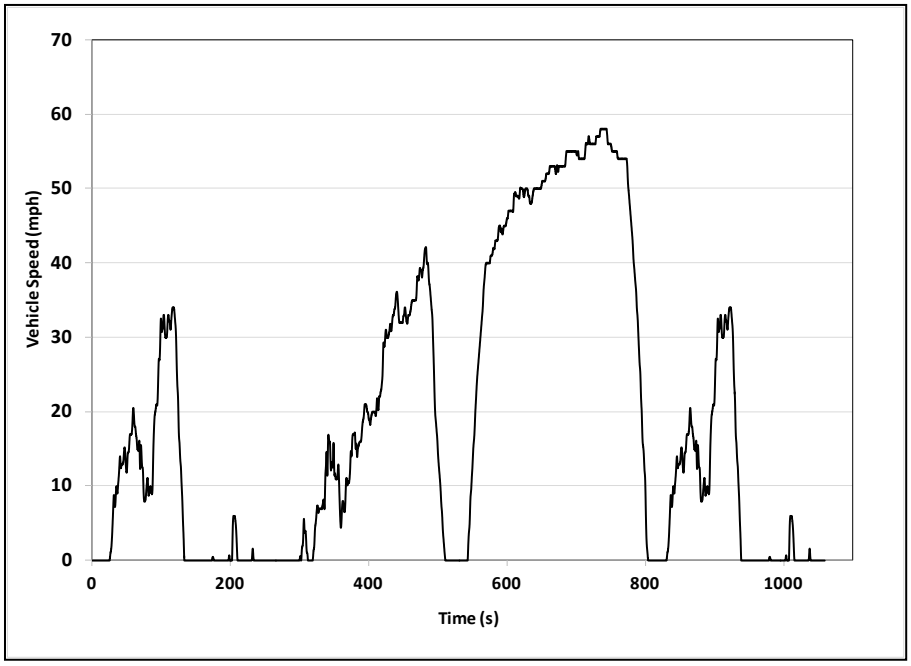


**Figure 4 Speed trace for UDDS driving cycle**

### *1.4.3 ORANGE COUNTY TRANSIT AUTHORITY (OCTA) TRANSIT BUS DRIVING CYCLE*

The OCTA driving cycle was developed by WVU to represent the typical driving characteristics for the urban bus population in Los Angeles, California. The driving cycle is 1,950 seconds in duration and represents a total driving distance of 6.5 miles.

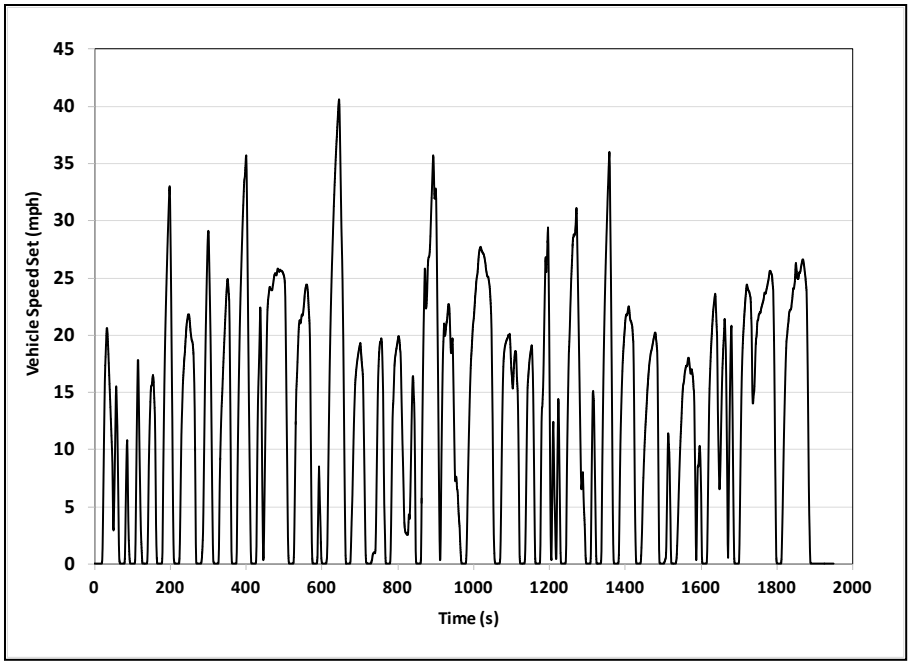


**Figure 5 Speed trace for OCTA transit bus driving cycle**

### *1.4.4 CENTRAL BUSINESS DISTRICT (CBD) CYCLE*

The CBD cycle is the prescribed chassis dynamometer test cycle under the SAE J1376 fuel economy measurement test for trucks and buses. The cycle consists of a series of idle, acceleration, and deceleration speed-time trace. The CBD cycle is a 560 seconds long cycle representing a distance of 2.06 miles. The short duration of the CBD test would contribute to inadequate mass loading of PM filters and therefore result in PM mass below the detection limits of the gravimetric system. To alleviate this concern a double length version of this cycle was used during this study. Figure 6 shows the vehicle speed-time trace of the double length CBD driving cycle.

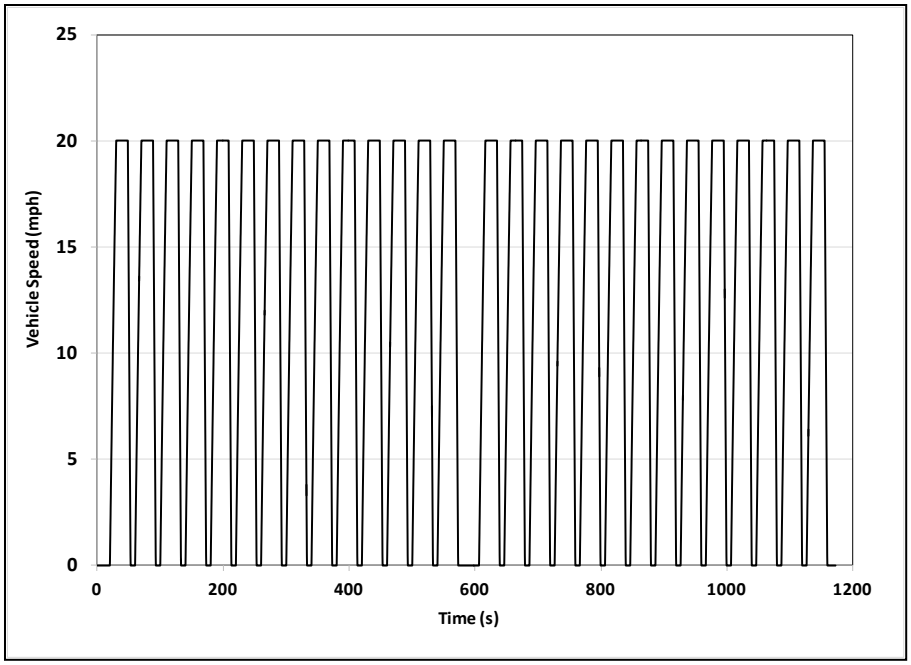


**Figure 6 Speed trace for CBD driving cycle**

### *1.4.5 SCAQMD REFUSE TRUCK CYCLE*

The SCAQMD refuse truck cycle is a modified version of the William H. Martin refuse truck cycle previously developed by WVU and consists of the refuse truck operation cycle (SCAQMD-RTC) and the refuse truck compaction operation cycle (SCAQMD-RCC). The SCAQMD-RTC consists of two modes, namely: transportation mode, and the curbside pick-up mode. The transportation mode is representative of vehicle operation from the depot to the community, and the curbside pick-up is representative of vehicle operation associated with the collection of garbage. The curbside pick-up mode is representative of multiple short idle times with frequent stop-and-go operation. The cycle is characterized by frequent accelerations and decelerations. The frequent stop-and-go operation could lead to lower catalytic activity and higher mass tailpipe emissions rates. The SCAQMD-RTC has been developed to combine one mode of transportation and three repeats of the curbside pick-up mode. The duration of the SCAQMD-RTC is 2,117 seconds, representing a distance of 4.3 miles. Figure 7 shows the vehicle speed-time trace for the SCAQMD-RTC cycle.

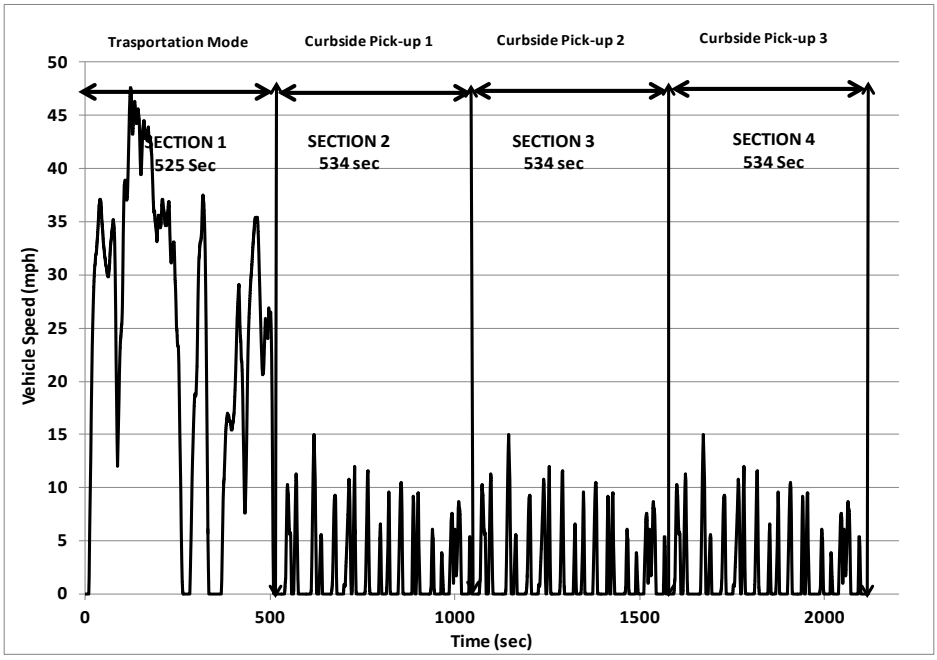


**Figure 7 Speed trace for AQMD refuse truck driving cycle**

The SCAQMD-RCC represents the compaction operation of a refuse truck. Engine load information was obtained from the engine control unit (ECU) during compaction operation, in order to develop a representative chassis cycle to represent the compaction operation on the chassis dynamometer. The compaction cycle involved the operation of the vehicle at steady-state speed of 30 mph with an intermittent axle loading of 80 horsepower (hp) and 20 hp applied to simulate the auxiliary loading of the compaction system. The duration of the compaction cycle is 880 seconds and representing an equivalent distance travelled of 6.8 miles. Figure 8 shows the vehicle speed-time trace and axle power loading of the refuse truck compaction cycle.

Since the compaction operation does not accrue any driving miles in real-world, the emissions from the compaction cycle will be represented on a time-specific basis. Further, in order to represent the distance-specific emissions of the refuse truck operation as a whole, the total mass of emissions from the compaction cycle will be integrated as shown in the equation below.

$$Refuse\ truck\ Distance\ specific\ emissions\ \left(\frac{g}{mile}\right) = \frac{Total\ mass\ of\ emissions\ of\ SCAQMDRTC + equivalent\ mass\ of\ emissions\ of\ \ SCAQMDRTCC}{(Distance\ of\ SCAQMDRTC)}$$

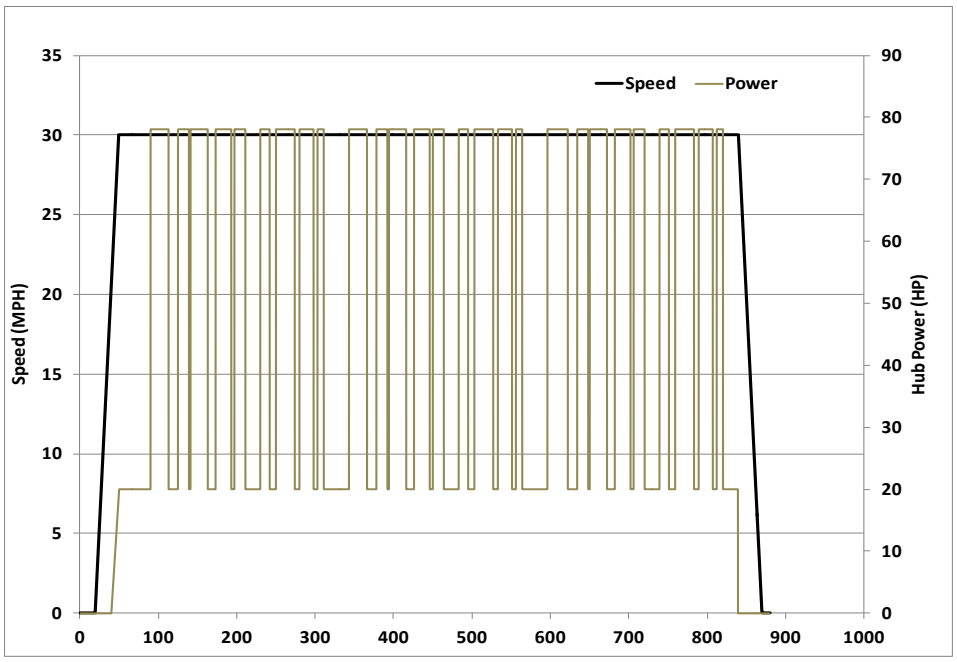


**Figure 8 Speed trace for AQMD refuse truck compaction cycle**

# 2 - EMISSIONS TESTING PROCEDURE

WVU performed this study using a transportable heavy-duty chassis dynamometer and the transportable emissions measurement system (TEMS) stationed at Ralphs Grocery facility at Riverside, CA. All emissions measurement procedures were conducted in accordance to the regulations prescribed in 40 CFR Part 1065. In addition WVU follows in-house chassis dynamometer procedure to screen, condition, and test the vehicle. This section details the chassis dynamometer and emissions test procedure adopted for this study.

## 2.1 VEHICLE SELECTION

Engine family and certification emissions number were primary criteria for vehicle selection in each technology category. The heavy-duty certification sheets for OEM engine families were accessed through the ARB database to verify the NOx certification value of an engine before recruiting the vehicle for chassis dynamometer testing. The ARB database for engine certification sheets is available at http://www.arb.ca.gov/msprog/onroad/cert/cert.php#6.

## 2.2 ENGINE ECU AND DPF SCREENING

WVU performed preliminary ECU screening at the fleet location to identify potential engine sensor or emissions control device failures prior to taking possession of the test vehicle. The ECU screening was performed using the Nexiq Prolink heavy-duty diagnostic tool to scan active and inactive engine codes. A vehicle was not recruited if any active engine code were found.

Natural-gas engines were screened with another level of detailed ECU screening performed by Cummins Cal Pacific. A representative from Cummins Cal Pacific performed a complete on-board diagnostic test to identify any active or pending fault codes reported by the on-board diagnostics (OBD).

The test for DPF failure was accomplished by testing for soot deposits in the tailpipe. A damaged particulate filter will result in visible soot deposits in the tailpipe. Other types of filter failures or emergency status messages such as “DPF full” status will be captured by the vehicle OBD system and thereby triggering a malfunction illumination light (MIL). It is to be noted that during the selection process WVU did not encounter any vehicles with active engine fault codes and imminent engine de-rate condition. Few vehicles showed messages related to DPF full status, which were automatically cleared during freeway cruise operation or through a parked DPF regeneration procedure.

## 2.3 VEHICLE INSTRUMENTATION

The test vehicles were instrumented with sensors at upstream and downstream of the each after-treatment system to record pressures, temperatures, and NOx emissions. Prior to instrumentation of the

vehicle, WVU performed a preliminary ECU data logging to discern the parameters publicly broadcasted over the CAN (i.e. J1939) by the OEM. Sensors were instrumented only to collect parameters that were not publicly broadcasted by the OEM through the ECU CAN. Table 7 lists the different parameters that were measured at different positions along the exhaust stream.

Mexa 720 raw NOx sensors (zirconium-oxide type sensors) were placed before and after the SCR to determine real-time SCR NOx reduction efficiencies. Pegasor Particle Sensors (PPS) were placed upstream and downstream of the DPF to assess the real-time filtration efficiency of the DPF. In the case of the natural gas engine the two PPS sensors were used to investigate the differences in particle emissions before and after the TWC.

One of the primary objectives of this study was to characterize ammonia emissions from stoichiometric natural gas engines. WVU instrumented all stoichiometric natural gas engines with commercially available Bosch Universal Exhaust Gas Oxygen (UEGO) sensors before and after the TWC to record the changes in operating air-fuel ratio of the engine. The data from the UEGO sensors can be used to better understand conditions favoring production of ammonia from TWC's. Further, the Mexa 720 NOx sensor was operated in oxygen mode to measure the exhaust oxygen content before and after the TWC.

**Table 7 List of Instrumentation and Sensing Positions**

| Parameter | Sensor | Position |
|---|---|---|
| Temperature | Thermocouple | 1) Pre DPF, Post DPF and Post SCR for Diesel<br>2) Pre TWC and Post TWC for stoichiometric natural gas |
| Pressure | Validyne differential pressure transducer | 1) Pre DPF, Post DPF and Post SCR for Diesel<br>2) Pre TWC and Post TWC for stoichiometric natural gas |
| NOx | MEXA 720 | Pre SCR and Post SCR |
| Oxygen | MEXA 720 and Bosch UEGO sensor | Pre TWC and Post TWC |
| PM efficiency | Pegasor | 1) Pre DPF, Post DPF and Post SCR for Diesel<br>2) Pre TWC and Post TWC for stoichiometric natural gas |
| Fuel Flow | Fuel scale | Gravimetric diesel fuel consumption for diesel and HPDI engines only. |

## 2.4 LABORATORY SET-UP

### *2.4.1 TRANSPORTABLE HEAVY-DUTY CHASSIS DYNAMOMETER*

The chassis dynamometer test bed consists of rollers, flywheel assembly, eddy current power absorbers, differentials, hub adapter, torque and speed transducer built onto a tandem axle semi-trailer.

The chassis dynamometer is unique in design as loading of the test vehicle axle is accomplished through direct coupling of the drive axle with the flywheel and power absorbing systems. Hub adapters replace the outer tires of the drive axle, in order to directly connect the laboratory load simulation system to the vehicle drive axle.

The load simulation system consists of eddy current power absorbers and a flywheel assembly to simulate road load power and vehicle inertia respectively. The chassis dynamometer is capable of simulating vehicle weight of up to 70,000 lbs. Figure 9 shows a test vehicle installed on WVU's transportable heavy-duty chassis dynamometer.


**Figure 9 WVU heavy-duty transportable chassis dynamometer. 1) Flywheel assembly; 2) Hub adapters**

### *2.4.2 TRANSPORTABLE EMISSIONS MEASUREMENT SYSTEM*

The housing for the new Transportable Emissions Measurement System (TEMS) is a reconstructed 9.1m (thirty-foot) long cargo container which houses a high efficiency particulate filter (HEPA) primary dilution unit, two primary full-flow dilution tunnels, a subsonic venturi, a secondary particulate matter sampling system, a gaseous emissions analytical bench instrumentation system, a computer-based data acquisition system and control system, a heating, ventilating and air conditioning (HVAC) system, and chassis dynamometer control systems. Figure 10 shows the schematic of the transportable laboratory container. The two primary dilution tunnels inside the container, of 0.46 m (18 inches) inner diameter and 6.1 m (20 feet) long, were designed to provide dedicated measurement capability for both low PM emissions ("clean") vehicles (with the upper tunnel referred as the "clean tunnel"), as well as traditional diesel-fueled vehicles with high PM levels (lower tunnel referred as "dirty tunnel"). This provision

reduces tunnel history effects between test programs of differing exhaust emission composition. A stainless steel plenum box houses two HEPA filters for filtering primary dilution air, as well as twin dual-wall exhaust transfer inlet tubes dedicated as exhaust inlets for the upper and lower tunnels. The HEPA plenum is connected into the main dilution tunnels, which are selectively connected to the subsonic venturi via stainless elbow sections. The air compressor and two vacuum pumps are installed inside a noise isolating overhead. An air tank stores compressed air and provides shop air to the zero air generator (a device that removes PM and THC) for instrumentation use. A PM sampling box for the secondary dilution tunnels is located alongside the primary tunnels, downstream of tunnels' sample zones. The secondary PM dilution tunnel of either the dirty or clean tunnel is connected to the PM sampling box for PM measurement during the test. Figure 11 shows the TEMS container on the transportation Landoll 435 trailer while performing real-world emissions testing.

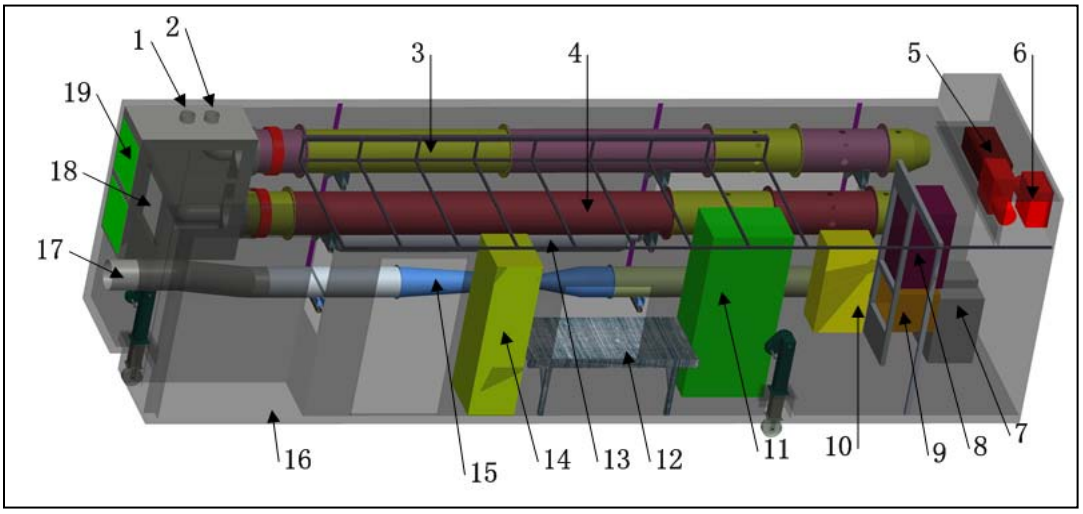


**Figure 10 Schematic of the WVU TEMS**

1- Exhaust inlet of dirty tunnel; 2- Exhaust inlet of clean tunnel; 3- Clean tunnel; 4- Dirty tunnel; 5- Air compressor; 6- Vacuum pumps; 7- Oven; 8- PM sampling box; 9- Glove box; 10- Zero air generator; 11- MEXA-7200D motor exhaust gas analyzer; 12- Computer table; 13- Air tank; 14- DAQ rack; 15- Subsonic venturi; 16- Air conditioner deck; 17- Outlet to blower; 18- Ventilation fan; 19- HEPA filters


**Figure 11 WVU TEMS performing real-world emissions testing**

### *2.4.3 CVS SAMPLING SYSTEM AND REGULATED GASEUOUS MEASUREMENTS*

The WVU TEMS is equipped with two full scale Constant Volume Sampling (CVS) dilution tunnels (clean and dirty) designed to perform emissions measurement as per procedures set forth in 40 CFR Part 1065. The laboratories CVS flow control is achieved through a subsonic venturi (SSV) and a variable speed blower. To ensure the accuracy and repeatability of SSV flow rate measurement, a straight section of Schedule 5 pipe, ten feet in length, was flanged and attached to each end of the subsonic venturi to minimize the flow wakes, or eddies, or flow circulation which might be induced by pipe bends or coarse inside walls. This particular SSV was calibrated with a reference SSV from 400 scfm to 4,000 scfm following the procedure defined in 40 CFR Part 1065.340. The flow rate of the SSV is calculated, in real time, using the equations in 40 CFR Part 1065.640 and 40 CFR Part 1065.642. HEPA filtered ambient air is used as the dilution air in the CVS. Ambient humidity and dew point are continuously monitored to calculate instantaneous NOx correction factors. Figure 12 shows the schematic of the TEMS container and experimental setup for the gaseous and PM sampling methodology adopted for this study.

The TEMS is equipped with the Horiba MEXA 7200D exhaust gas analyzers to serve as the primary gaseous emissions measurement system. The MEXA 7200D is capable of measuring all regulated emission species including THC, CO, $CO_2$, NOx and methane through a non-methane cutter equipped secondary hydrocarbon channel. The unit can be fitted with various analyzer modules, and the current configuration consists of an AIA-721A CO analyzer, an AIA-722 CO/$CO_2$ analyzer and a CLA-720 “cold” NOx analyzer part of the cold sample stream, the FIA-725A THC analyzer, and CLA-720MA NOx analyzer part of the heated sample stream.

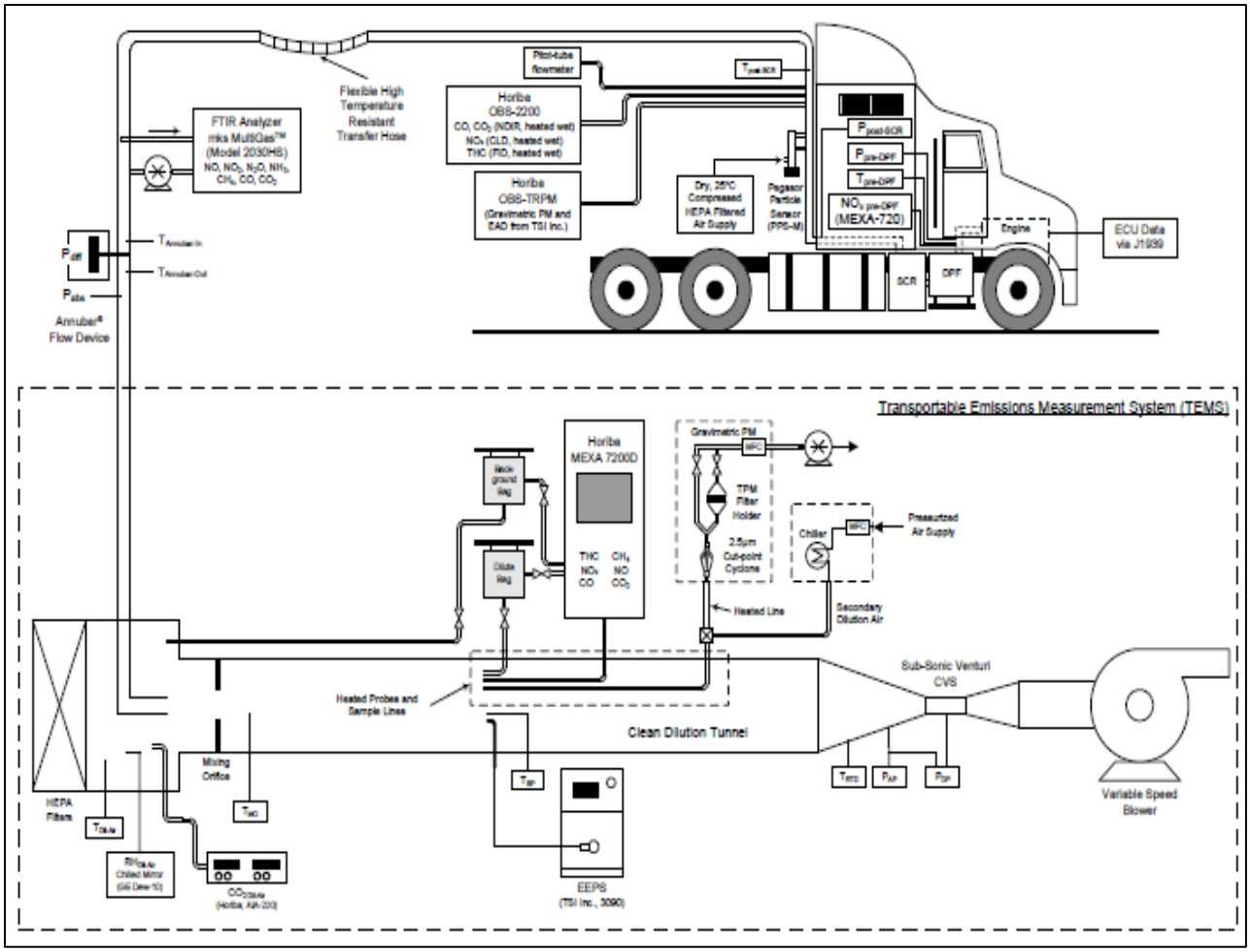


**Figure 12 Schematic of CVS sampling setup for gaseous and PM sampling systems**

### *2.4.4 PM SAMPLING AND MEASUREMENT SYSTEM*

The TEMS houses the PM sampling system designed according to procedures set forth in 40 CFR Part 1065. The PM sampling system houses separate sampling systems for the clean and dirty tunnel, in order to reduce sampling system background contamination. Figure 13 shows the view of the temperature controlled PM sampling system with independent sample streams for clean and dirty CVS tunnels. Dilution air conditioning is achieved through filtering with HEPA filters, drying using a chiller and temperature control using heated lines. WVU follows a barcode based media tracking methodology to maintain records of sample check out from Morgantown, use in field and check in back at the clean room facility at Morgantown. All sample media are fixed with a unique barcode identification that is used to track the filter weights and associated test ID.

**Figure 13 40 CFR Part 1065 compliant PM sampling system on-board the WVU TEMS**

Measurement system of pre-weighing and post weighing the PM sample filters are performed in Morgantown, WV. The WVU facility houses a class 1000 clean room, with controlled environment for accurate weighing of the filters. The measurement system is operated with in-house developed software to calibrate the scales, perform measurements, and also to monitor the filters history. Figure 14 shows the view of the inside of the Class 1,000 clean room, with Sartorius microbalance and WVU filter weighing software. The measurement scale has a minimum detection limit of 10 micrograms and with a resolution of 0.1 microgram.

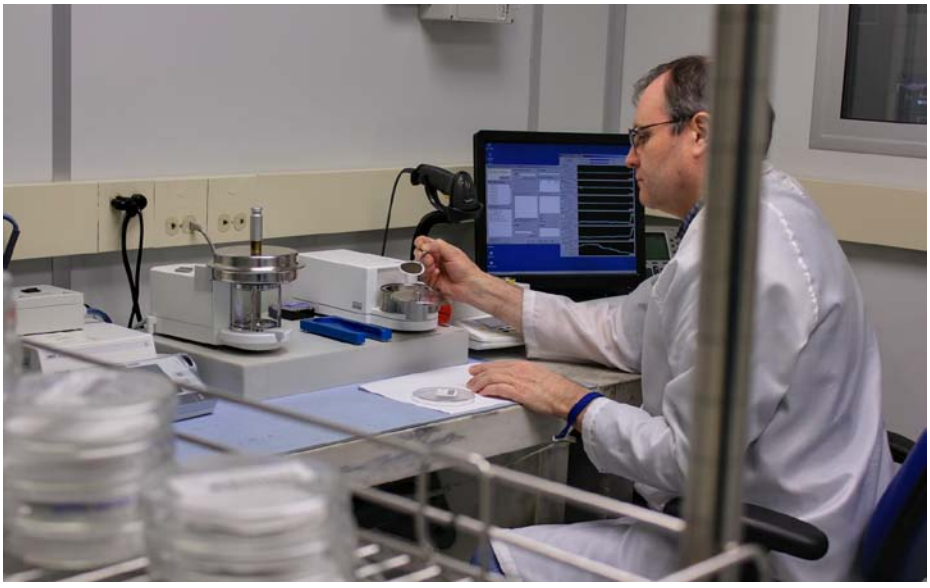

**Figure 14 WVU staff performing gravimetric filter weighing at the WVU clean room facility in Morgantown, WV**

### *2.4.5 AMMONIA AND NITROUS OXIDE MEASUREMENT SYSTEM*

An MKS Instruments MultiGas™ 2030-HS Fourier Transform Infrared Spectroscopy (FTIR) system was used for continuous high resolution measurements of $NH_3$, $N_2O$ and $NO_2$. The MultiGas™ 2030-HS is capable of quantifying up to 20 gasses that include the above mentioned compounds as well as BTEX compounds at a 5Hz data rate. Based upon published literature WVU developed a dedicated ammonia sampling and sample conditioning system aimed at minimizing possible sampling artifacts and losses caused by adsorption/desorption, memory and chemical reaction effects as well as water solubility of ammonia.

In order to address sampling losses and measurement artifacts the system is set up to sample raw exhaust directly from the exhaust stack as proposed by other studies. To prevent ammonia from dissolving in $H_2O$ and subsequently lead to irreversible sample losses, all the sample lines and sample conditioning components are maintained above dew point temperatures and controlled to about 190 °C by means of Proportional Integral Derivative (PID) controllers (Ardanese 2008). Regular stainless steel sample lines were determined to be inadequate due to possible chemical reactions between $NH_3$ and the sample line surface at elevated temperature environments, hence special 316L Silcosteel® material base sample lines were chosen.

Per WVU's established standard operating protocols, the FTIR analyzer cell and sampling conditioning components are continuously purged with dry zero air before and in-between consecutive test cycles to ensure the removal of adsorbed ammonia from the previous test run. Due to the FTIR's sensitivity to pressure fluctuations within the sample cell, the instrument is operated under slight vacuum with the sampling pump located downstream of the sample cell and a feedback activated solenoid valve upstream of the cell in order to maintain constant pressures within the sample cell.

### *2.4.6 REAL-TIME, IN-LINE PARTICULATE MATTER MEASUREMENT SYSTEM*

A real-time, in-line particle sensor from Pegasor Ltd. (i.e. *Pegasor Particle Sensor* - PPS), capable of performing continuous measurements directly in the exhaust stack and providing a real-time signal with a resolution of up to 100Hz for particle number (PN) quantification was employed. The PPS is a diffusion-charging type instrument which has been shown to exhibit a response proportional to particle surface area, and therefore, can be calibrated for either particle number or mass concentration measurements. Two PPS sensors were installed upstream and downstream of the DFP for diesel engines and TWC for natural gas engines to investigate the impact of the after-treatment system on tailpipe PM emissions. Figure 15 shows the image of the PPS used to track instantaneous DPF efficiency for this study.

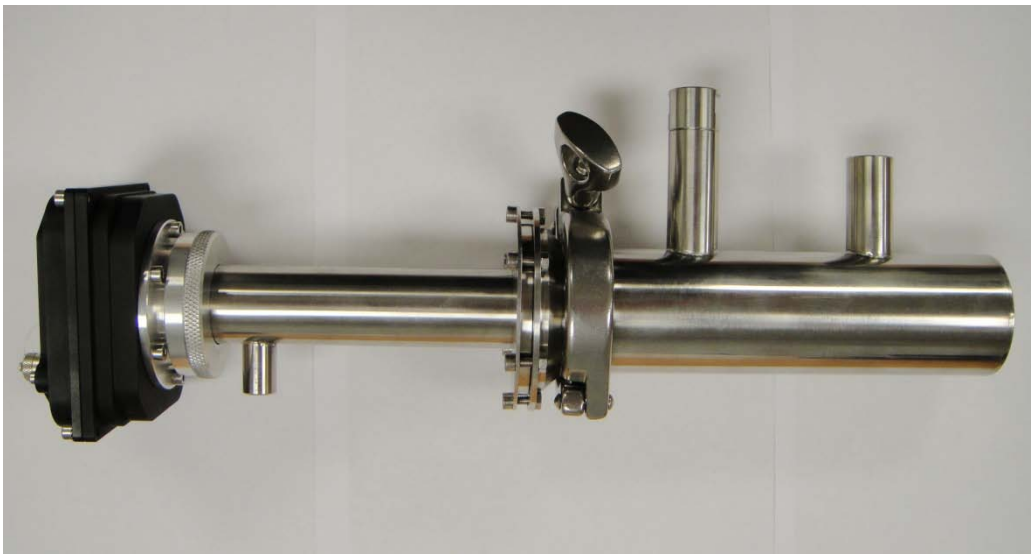

**Figure 15 Pegasor particle sensor for tailpipe PM emissions**

Further WVU employed the Engine Exhaust Particle Sizer (EEPS TSI Model 3090) to characterize the particle size distributions and number concentrations in real-time in the CVS dilution tunnel.

### *2.4.7 CYCLONIC PARTICLE CLASSIFIER*

Sampling of unregulated emissions included gravimetric analysis of particulate matter in size fractions of 10 µm, 2.5 µm, and 1 µm. This was accomplished by using cyclone classifiers (URG 16.7 lpm cyclone). A cyclone classifier makes use of vertical flow inside a cylindrical or conical chamber to separate particles depending on the flow rate. A double vortex flow is induced in the conical body of the cyclone by introducing the sample tangentially at the top where flow spirals down along the wall, which then reverses and spirals through inner core to exit the chamber. Particles with sufficient inertia impact on the cyclone wall as they cannot follow the streamlines of the flow exiting the chamber. The various size fractions of PM were sampled directly from the primary dilution, as the tunnel was built to a single stage PM sampling specification. The samples were collected on a 47mm Teflon coated glass fiber filters (T60A20). The flow through the cyclone was controlled using mass flow controllers.

A sample for unregulated speciation of elemental carbon/organic carbon (EC/OC) was collected on pre-fired quartz filters downstream of 2.5 µm cut-point cyclone.

## 2.5 LABORATORY CHECKS

Initial laboratory set-up procedures include complete measurement system verification followed by calibration. All required system verifications are performed as per requirements stated in 40 CFR, Part 1065, Subpart D. The measurement container is equipped with the Horiba MEXA 7200D Motor Exhaust

Gas Analyzer, which is capable of automatically performing the required analyzer verification tests. The verification procedure and pass criteria of the tests were in accordance to the provisions described in 40 CFR, Part 1065, Subpart D. Table 8 lists the complete set of analyzer verification checks performed on field prior to the commencement of the testing. Table 9 lists the complete set of leak checks performed on the gaseous and PM measurement systems.

**Table 8 Gaseous analyzer verification checks**

| Analyzer Checks | Pass Criteria |
|---|---|
| THC1 Hang-up | |
| THC2 Hang-up | |
| CO(L), $CO_2$ Interference Check | Within ±1% |
| THC, $O_2$ Interference Check | Within ± 2% |
| $CO_2$ Quench $NO_x1$ | Within ±1% |
| $CO_2$ Quench $NO_x2$ | Within ±1% |
| $H_2O$ Quench $NO_x1$ | Within ±1% |
| $H_2O$ Quench $NO_x2$ | Within ±1% |
| Non-Methane Cutter Efficiency | $PFCH_4$>0.85 and $PFC_2H_6$<0.02 |

**Table 9 Gaseous and PM measurement system verification checks**

| Leak Checks | Pass Criteria |
|---|---|
| Leak and Delay Time Check (all analyzers) | Within ± 5% over 30 sec interval |
| PM System 1 Leak Check | |
| PM System 2 Leak Check | |

## 2.6 CHASSIS DYNAMOMETER TEST PROCEDURE

### *2.6.1 VEHICLE SETUP*

Before mounting the vehicle on the chassis dynamometer the flywheel combination for the simulated inertial test weight was determined and locked in place to simulate the inertial load of the vehicle. Table 10 shows the flywheel settings used for the different vehicle vocations under this study. The outer rear wheel on the drive axle is removed and fitted with hub adapters which are later connected to the face plate. The vehicle was backed onto the dynamometer and the vehicle drive axle which drives the flywheel assembly and power absorbers were connected through a hub adapter. The vehicle was leveled with the drive axle and the tires were checked for any distortion as it would add to the vehicle loading. The vehicle exhaust was now connected to the dilution tunnel via insulated transfer tubes. The vehicle was chained down to the dynamometer bed as a safety measure.

**Table 10 Flywheel inertial for different vehicle vocation**

| Vehicle Vocation | Inertial Setting (lbs) |
|---|---|
| Transit Bus | 34,500 |
| Goods Movement | 65,000 |
| Refuse Truck | 56,000 |

The vehicle was made to run at a high speed after being mounted on the dynamometer to warm the lubricating oil in the differentials. This was done to reduce additional load on the vehicle due to highly viscous oil. During warming up of the differentials the gas analyzers were zero-spanned with blower operating at set-point.

### *2.6.2 VEHICLE COASTDOWN PROCEDURE*

A coast-down operation of the vehicle is performed to evaluate the system loses in the dynamometer. The coast-down operation involves driving the vehicle to accelerate to 50mph and when initiated by the control computer letting the vehicle to coast to a stop with no external assistance such as braking or gear shifts. The computer performs a series of coast-down test to evaluate the frictional loses if any in the dynamometer system. The coast-down operation is performed based on SAE J1263 recommended practice of road load determination. The coast-down program matches time taken in theoretical on road coast-down of a vehicle with the time taken for coast-down of a similar vehicle on the dynamometer. The theoretical on-road coast-down times are based on assumed vehicle aerodynamic drag coefficient, measured vehicle frontal area, tire rolling resistance friction coefficient, vehicle inertia and density of air. The tire rolling resistance friction coefficient and density of air was kept constant at 0.0071 and 1.202 $kg/m^3$, respectively. Table 11 shows the drag coefficients used for the different vocation vehicles in this study. Since the total drag force is a function of the frontal area, frontal area of each vehicle will be measured as an input to the coast down program of the transportable chassis dynamometer. A lesser coast-down time on the dynamometer indicates less resistance from the dynamometer components and hence necessary power absorber braking is needed and a greater time on the dynamometer indicates more frictional resistance from the dynamometer components hence assistance from motor is needed to overcome the additional load due to friction of dynamometer components. With the completion of the coast-down tests the vehicle is ready for chassis dynamometer testing.

**Table 11 Coast down drag coefficients settings for different vehicle vocation**

| Vehicle Vocation | Aerodynamic Drag Coefficient (Cd) |
|---|---|
| Goods movement | 0.75 |
| Refuse truck | 0.79 |
| Transit Bus | 0.80 |

### *2.6.3 VEHICLE TEST PROCEDURE*

Once the coast down procedure is completed, the vehicle is ready for chassis dynamometer testing on the prescribed driving cycles. Table 12 shows the test cycle matrix used for different vocation vehicles.

**Table 12 Test cycle matrix**

| | UDDS | OCTA | 2X CBD | AQMD Refuse Truck/Compaction | Drayage Port Cycles* |
|---|---|---|---|---|---|
| **Natural gas with TWC** | | | | | |
| Transit Bus | X | X | X | | |
| Refuse Truck | X | | | X | |
| Goods Movement Truck | X | | | | X |
| **Dual Fuel (NG/ULSD) HPDI** | | | | | |
| Goods Movement Truck | X | | | | X |
| **HD Diesel >0.20 gm/bhp-hr NOx W/O SCR** | | | | | |
| Goods Movement Truck | X | | | | X |
| Refuse Truck | X | | | X | |
| **HD Diesel <0.20 gm/bhp-hr NOx With SCR** | | | | | |
| Goods Movement Truck | X | | | | X |
| Refuse Truck | X | | | X | |
| **HD Diesel 1.2 gm/bhp-hr NOx** | | | | | |
| Goods Movement Truck | X | | | | X |

**** Drayage Port cycle: near-dock, local, and regional***

WVU typically perform three hot start repeats of a driving cycle to establish a coefficient of variation (COV) of less than 2% on distance specific $CO_2$ emissions to classify a test as valid. However, other metrics such as repeatability of distance travelled, axle work done and engine work calculated from ECU were used to assess repeatability and consistency in test procedures, particularly for diesel test engines that have multiple after-treatment systems with changing control strategies that might result in COV values greater than 2%. .

WVU used the signal from the Pegasor particle sensor, DPF temperatures and ECU broadcast to identify the onset of regeneration events for a DPF-equipped engine. The testing laboratories and SCAQMD decided that triggering of a regeneration event using ECU software would not be representative of real-world emissions as PM mass emissions rate could be higher from a clean filter. As such, although soot loading and regeneration events were monitored, in the event of DPF regeneration, associated data was not included as a valid hot start.

In the case of vehicles equipped with SCR technology, a preliminary conditioning cycle was performed to eliminate the influence of the history effects of the after-treatment system. Due to the

extended duration of the drayage port cycles, it was decided to use the last 4.8 miles of the near dock, 3.4 miles of the regional, and 8.04 miles of the local cycle as the conditioning cycle. The data from the conditioning cycles will not be presented in this report.

### *2.6.4 IN-USE CROSS COUNTRY TEST PROCEDURE*

The test route used in this study was about 2,450 miles beginning in Morgantown, WV and ending in Riverside, CA. The test route provided a range of environmental conditions, where the ambient temperature ranged between 3 to 37 °C and the relative humidity ranged between 10 to 79%. It also provided different driving conditions based on the topographical elevation and traffic density of the region along the test route, namely Appalachian Mountains in the East, Great Plains of the Mid-West, high altitude of the Rocky Mountains, arid desert between Rockies and Pacific Mountain systems, and the Pacific Mountains in the West. The test route was traversed over a period of 6 days involving only day-time driving.

The experimental setup for the cross country study is similar to the schematic shown in Figure 12. The data collection during the cross country study was split into multiple short segments to restrict data size and perform a robust QA/QC on the collected data.

Each day comprised of a representative driving schedule of a long haul truck operator. The total vehicle weight for the setup was 67,000 pounds. The test vehicle was the same vehicle listed in Table 2 under category VII as a goods movement vehicle and tested by both WVU and UCR . Figure 16 shows the route used for the study with markers indicating the data collection stops during the test campaign.

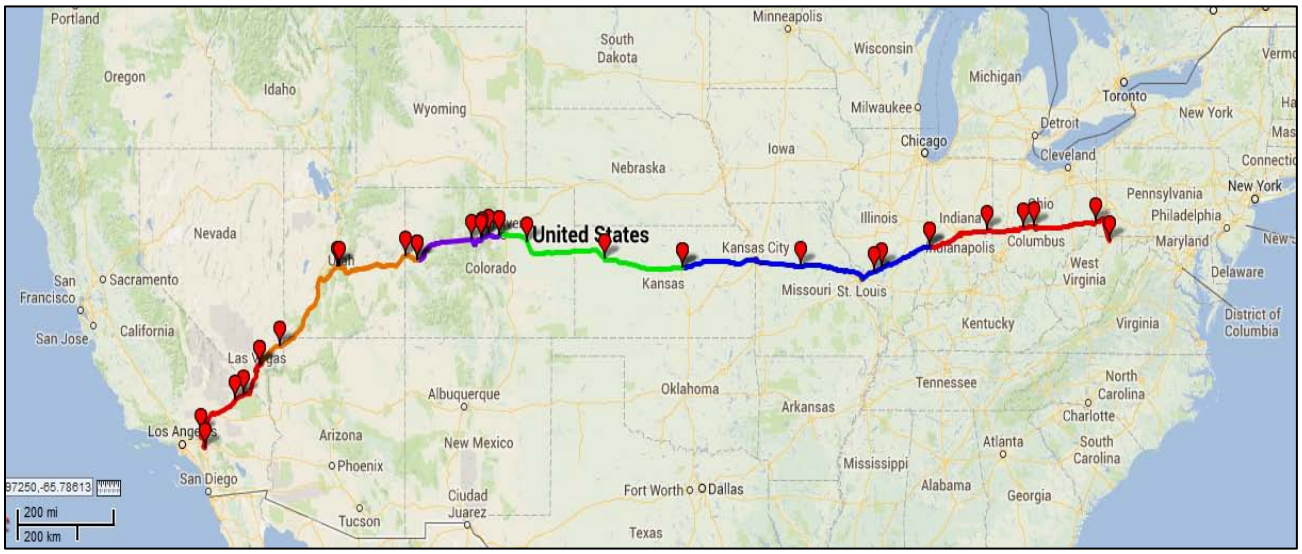


**Figure 16 Entire Test Route with Stop Indicators**

## 2.7 EMISSIONS CALCULATIONS

All emissions calculations were performed using equations provided in 40 CFR Part 1065.650. As part of this study WVU performed NTE analysis of the chassis data to investigate the in-use compliance of the vehicle while operating on real-world driving cycles. For this purpose the WVU post processing tool used only the temperature exclusion related to after-treatment temperature being over 250 °C as the only exclusion criteria.

Engine work was calculated from the ECU broadcast. NTE analysis requires a lug curve of the respective engine to identify the NTE boundaries. WVU used the six points of the lug curve broadcasted by the ECU to develop a complete curve using linear interpolation. For some vehicle WVU obtained lug curves from the OEM to corroborate the ECU broadcast.

Chassis dynamometer emissions are represented primarily as distance specific units of “grams/mile”. Brake-specific emissions were provided based on the integrity of the ECU broadcasted. All test-to-test variability was assessed from the distance specific emissions.

The fuel rate was calculated from both gravimetric measurements and iterative carbon balance detailed in 40 CFR Part 1065.655.

Pollutants measured using the FTIR from the raw exhaust stream were calculated separately using the exhaust flow measured with the Annubar® device.

A Diesel Gallon Equivalent (DGE) of natural gas value of 6.312 lbs (2.863 Kg) was used to convert mass of natural gas consumed to equivalent diesel volume consumed (www.cleanvehicle.org/linked/GGE_DGE_Background_Document.pdf, 2012).

# 3 - RESULTS AND DISCUSSIONS

This section presents emissions results from 14 heavy-duty vehicles from 3 different vocations tested on a heavy-duty chassis dynamometer. The results are organized as individual technology discussions followed by comparison of the emissions profile from different technologies under the same vocation. In addition, the result of the in-use cross-county evaluation of the MY 2011 heavy-duty Mack diesel vehicle equipped with DPF and SCR is also presented in this section. Fuel consumption for stoichiometric natural gas will be derived through exhaust carbon balance and also represented as diesel gallon equivalent (DGE) units for comparison with diesel vehicles. Fuel consumption for dual-fuel vehicles will be derived by assuming 100% natural gas substitution.

## 3.1 STOICHIOMETRIC NATURAL GAS ENGINES

One transit, one refuse, and three drayage goods movement vehicles powered by stoichiometric engines were tested in this study. The results of the chassis dynamometer test of these vehicles are discussed below.

### *3.1.1 TRANSIT BUS*

Figure 17 shows the distance-specific emissions of regulated pollutants from the stoichiometric CNG heavy-duty transit bus. The bus was exercised over the UDDS, OCTA, and the double length CBD (2X CBD) cycles. Average distance-specific NOx emissions of triplicate hot starts measured over the UDDS, OCTA, and the 2X CBD cycles were 0.761 g/mi, 0.730 g/mi, and 0.645 g/mi, respectively. CO emissions were measured to be an average of 19.22 g/mi over the UDDS, 19.91 over the OCTA and 14.41 g/mi over the 2X CBD cycle.

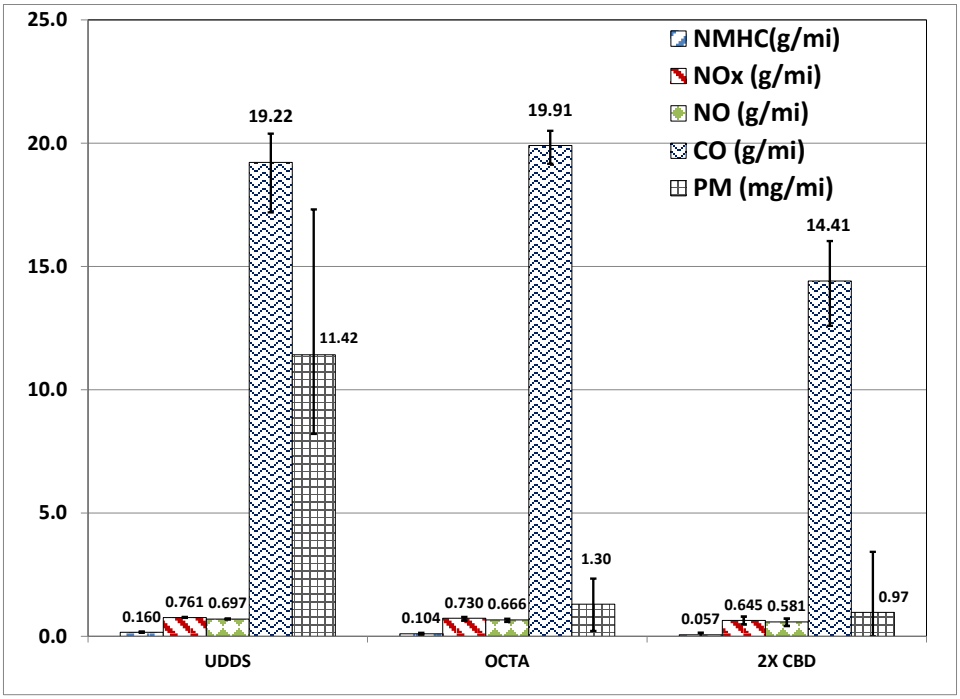


**Figure 17 Distance-specific regulated emissions results of natural gas transit bus**

PM emissions from the transit bus were 11.42 mg/mi, 1.30 mg/mi, and 0.97 mg/mi over the UDDS, OCTA and 2xCBD cycles, respectively. PM mass emission rate were characterized by high measurement variability due to relatively clean combustion of natural gas fuel. Previous studies have shown that the bulk of the PM emissions could be attributed to lubrication oil combustion contributing to metallic and elemental emissions from the tailpipe (Thiruvengadam, 2013). High exhaust temperatures in the order of 450 to 500°C resulted in minimal NMHC emissions, thereby contributing to minimal organic carbon emissions from the tailpipe.

Figure 18 shows the brake-specific NOx emissions for the entire period the transit bus was tested over UDDS, OCTA, and the 2XCBD cycles and for test periods the after-treatment temperature was greater than 250°C. The figure also shows the percentage of the test period for which the after-treatment temperature was above its nominal operating temperature as defined in the in-use compliance test procedure for heavy-duty vehicles (USEPA, 2004). It is to be noted that the figure shown below cannot be considered as a comparison to certification limits as heavy-duty engines are certified on an engine dynamometer over the FTP cycle. The in-use compliance protocol requires engines to be within 1.25 times the standard under the Not-to-exceed (NTE) operating regions of the engine. Also, the engine should suffice multiple operating conditions in addition to the NTE load points for in-use compliance consideration. Therefore the brake-specific emissions shown in Figure 18 are indicative of engine emissions outside the bounds of FTP cycle.

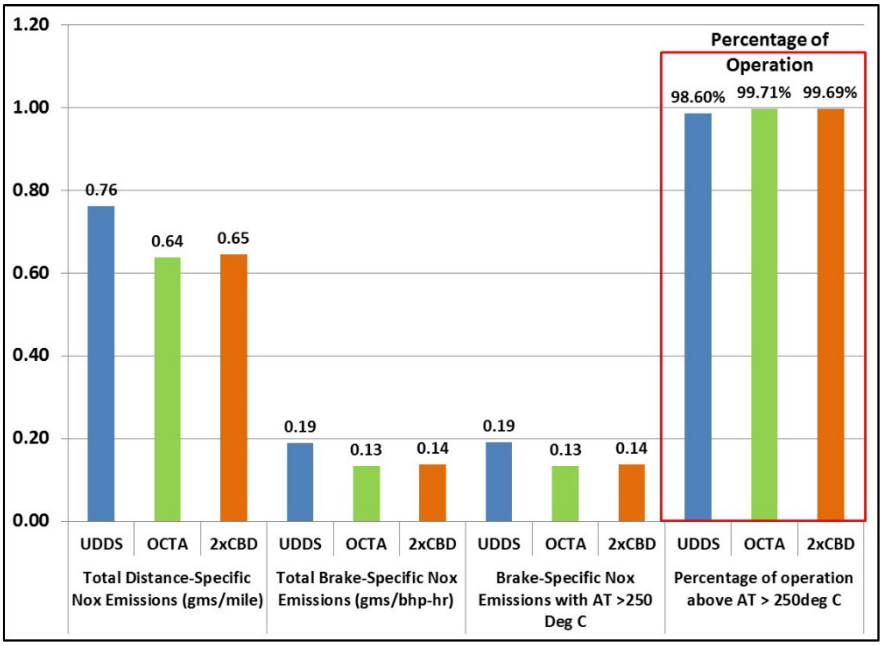


**Figure 18 Brake-specific NOx emissions and after-treatment activity for natural gas transit bus**

Brake-specific NOx emissions from the transit bus were measured to be 0.19, 0.13, and 0.14 g/bhp-hr over the UDDS, OCTA, and 2xCBD, respectively. The TWC technology in stoichiometric engines is not plagued by any temperature requirements as a SCR system in diesel engines due to the stoichiometric fueling strategy. As such, TWC temperature is independent of driving cycle and predominantly greater than 250°C. NOx emission reduction with a TWC is more a function of air-fuel ratio than exhaust temperature, however sustained high exhaust temperatures are favorable for greater NMHC reductions.

Figure 19 shows the distance-specific $CO_2$ emissions from the transit bus. The $CO_2$ emission over the UDDS cycle was measured to be 1,853 g/mi with a COV of 1.1%. The $CO_2$ emissions from the OCTA and 2xCBD cycles were 2,442 and 2,305 g/mi with a COV of 0.3% and 1.9% respectively. Although the COV statistic can be used as an indicator of test repeatability, it is to be noted that $CO_2$ emissions are dependent on feedback control from the oxygen sensors of the stoichiometric engines. Therefore, the response of oxygen sensor under transient operating conditions can result in differences in emission rates of $CO_2$. Hence, differences in transient characteristics of a driving cycle may contribute to differences in the vehicle fueling pattern.

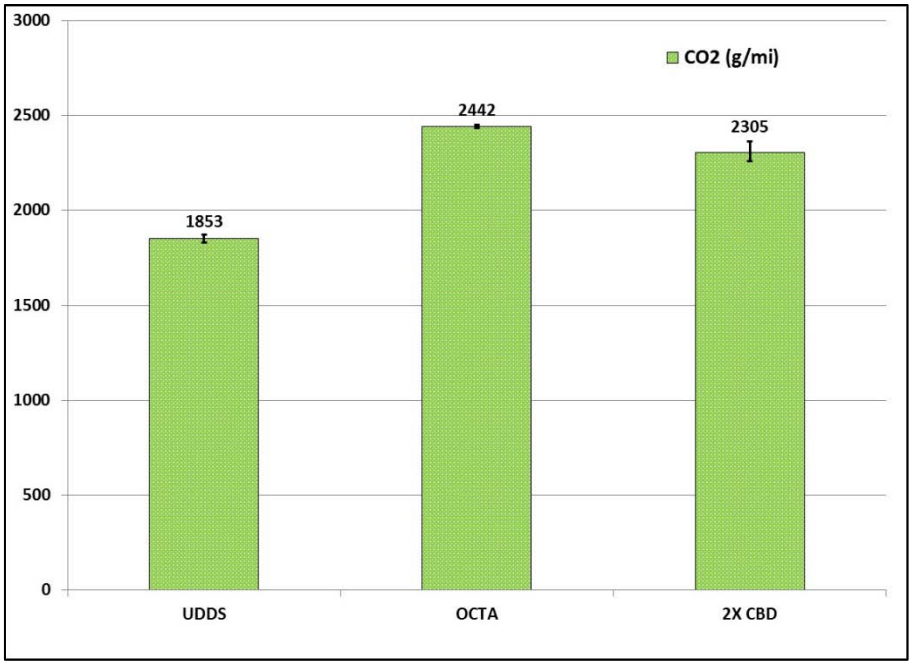


**Figure 19 Distance-specific carbon dioxide emissions from natural gas transit bus**

Figure 20 shows the distance-specific fuel consumption of natural gas calculated through exhaust carbon balance and converted to DGE units. The distance-specific fuel consumption of the transit bus was measured to be 0.68, 0.89, and 0.84 kg of natural gas/mi over the UDDS, OCTA, and 2xCBD driving cycles, respectively. The DGE fuel consumptions for the transit bus was calculated to be 4.19, 3.21, and 3.41 gal/mi over the UDDS, OCTA, and 2xCBD cycles, respectively.

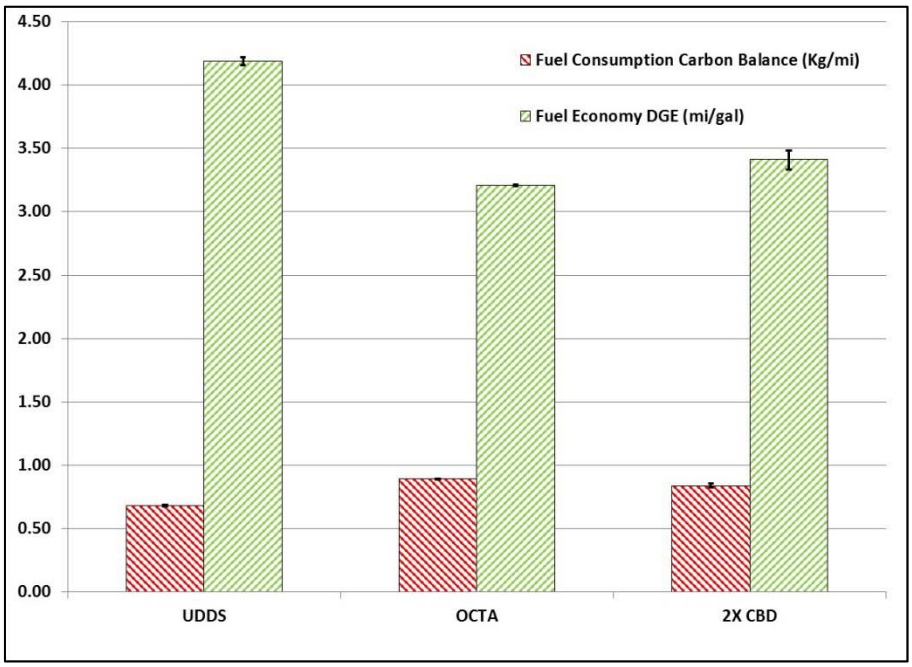


**Figure 20 Distance-specific natural gas fuel consumption and DGE fuel consumption from natural gas transit bus**

### *3.1.2 REFUSE TRUCK*

Figure 21 shows the distance-specific regulated emissions from the natural gas refuse truck over the UDDS, AQMD refuse truck cycle, and the AQMD refuse truck cycle with compaction operation included. Since actual compaction operation cannot be performed using the test truck, the AQMD compaction cycle is used to simulate the compaction operation. The average NOx emissions of triplicate hot starts measured over the UDDS, refuse truck cycle, and the refuse truck cycle with compaction are 0.338 g/mi, 0.784 g/mi, and 0.879 g/mi, respectively. Higher NOx emissions over the refuse truck cycle could be due to higher transient activity used to simulate curbside pick-up operation. Curbside pick-up activity is characterized by short, and high power demands. This could lead to an unsteady control of air-fuel ratio deviating from the optimal stoichiometric setting thereby contributing to higher NOx emissions.

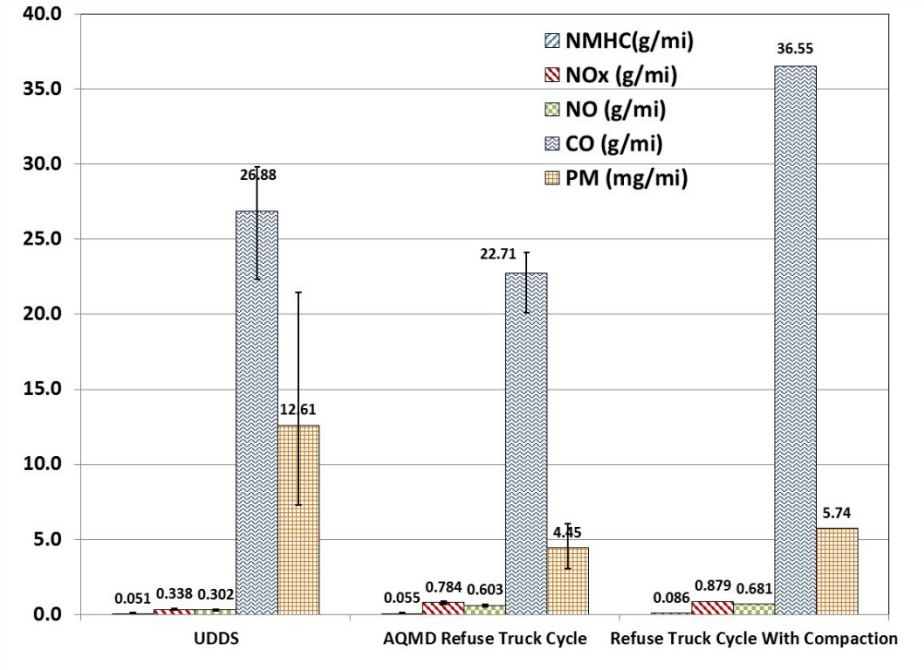


**Figure 21 Distance-specific regulated emissions results of natural gas refuse trucks**

Figure 22 shows the brake-specific NOx emissions of the refuse truck and the percentage of the test period for which the after-treatment temperature was above 250°C. Brake-specific NOx emissions measured over the UDDS and AQMD refuse truck cycles were 0.06 and 0.11 g/bhp-hr, respectively. The combined refuse truck cycle with the compaction operation resulted in a brake-specific NOx emission of 0.08 g/bhp-hr. The TWC experienced temperatures greater than 250°C for more than 99% of the vehicle operation regardless of driving cycle. High exhaust temperatures contribute to sustained catalytic activity and hence lower NMHC emissions.

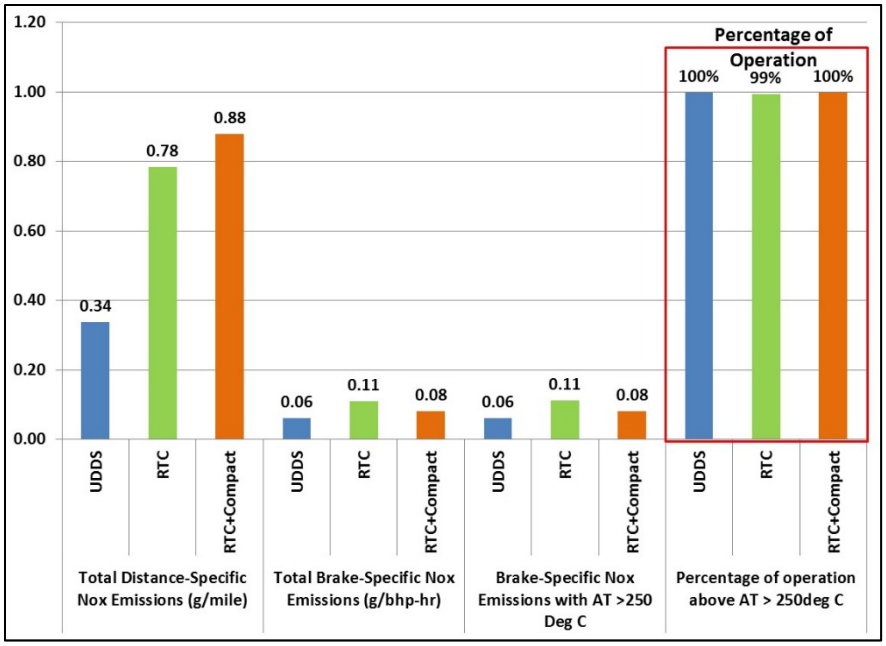


**Figure 22 Brake-specific NOx emissions and after-treatment activity for natural gas refuse truck**

Figure 23 shows the distance-specific $CO_2$ emissions from the natural gas refuse truck. Average $CO_2$ emissions over the UDDS, refuse truck cycle, and the combined refuse truck cycle were measured to be 2,365 g/mi, 3,766 g/mi, and 2,261 g/mi, respectively.

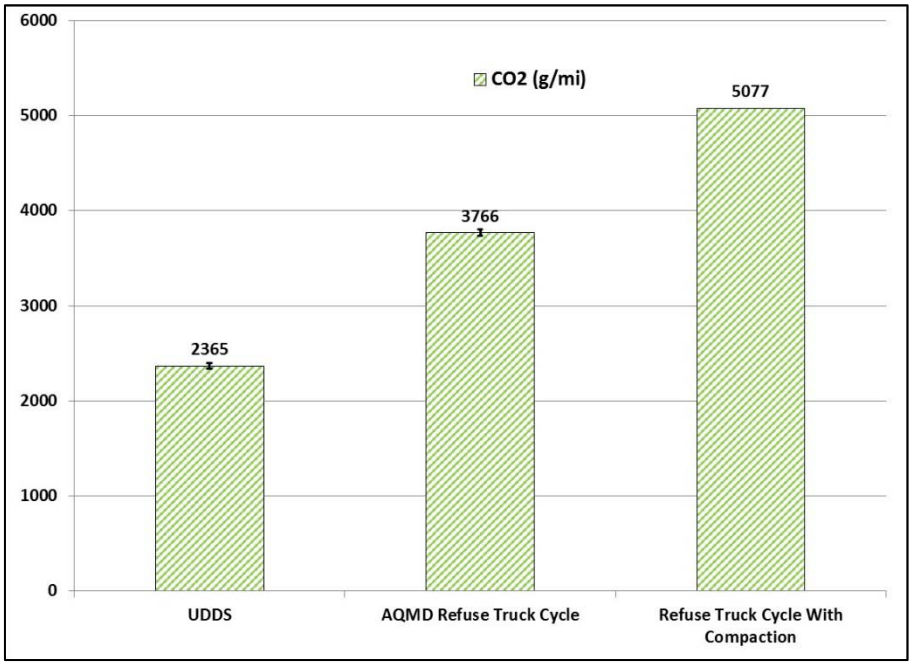


**Figure 23 Distance-specific carbon dioxide emissions from natural gas refuse truck**

Figure 24 shows the natural gas fuel consumption and the DGE fuel consumption of the natural gas refuse truck. On a DGE basis, the average fuel consumption of the refuse truck was relatively similar

(COV of 2.4%) for all driving cycles. The calculated DGE fuel consumption were 3.31 mi/gal, 3.21 mi/gal, and 3.41 mi/gal over the UDDS, refuse truck cycle, and the combined refuse truck cycle, respectively.

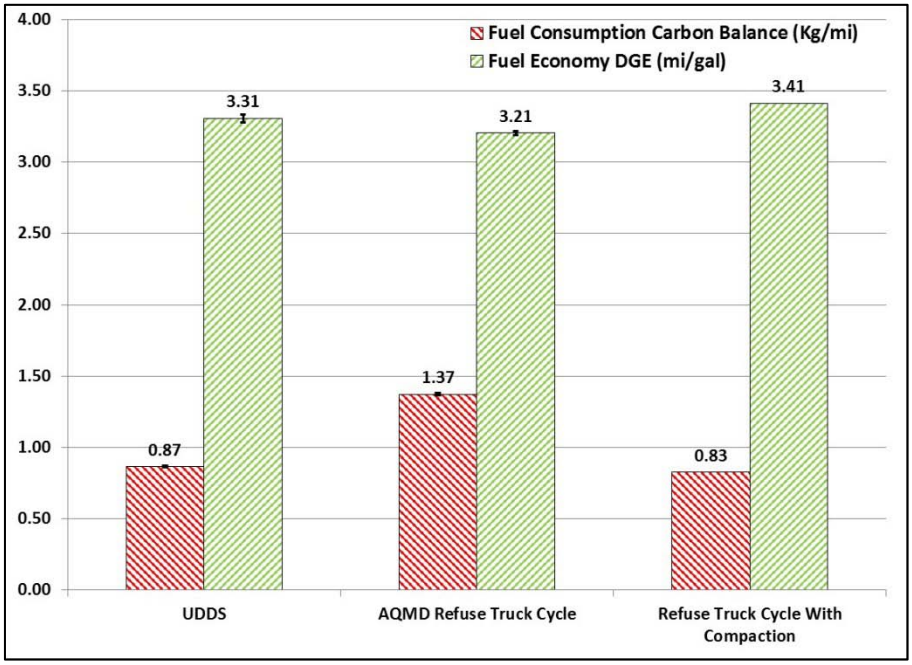


**Figure 24 Distance-specific natural gas fuel consumption and DGE fuel consumption from natural gas refuse trucks**

### *3.1.3 GOODS MOVEMENT*

Figure 25 shows the distance-specific regulated emissions results for the three natural gas fueled goods movement vehicles. Three test vehicles were chosen with different mileages in order to observe any effects of engine deterioration on emissions. Vehicle 1 was the newest with 192 miles, Vehicle 2 had 45,563 miles, and Vehicle 3 had 63,256 miles accumulated.

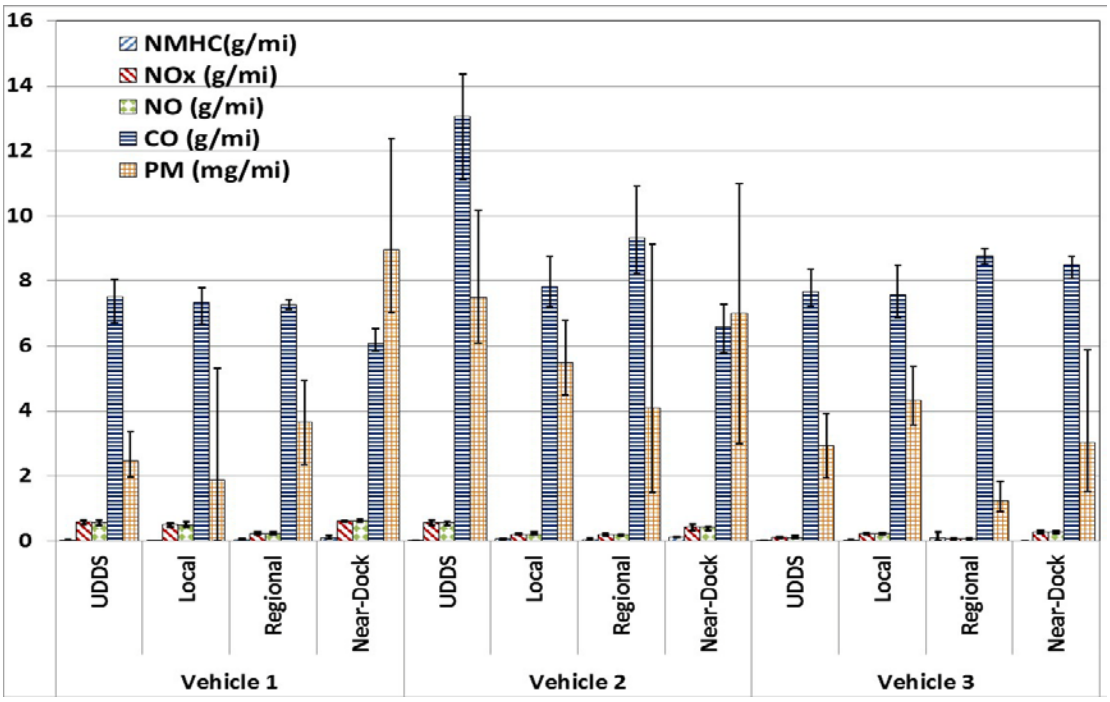


**Figure 25 Distance-specific regulated emissions results from three natural gas fueled goods movement vehicles**

Table 13 lists the distance-specific emissions results for the three natural gas fueled goods movement vehicles. Results showed Vehicle 3 (highest mileage) to be lowest in emissions of NOx and CO. Although Vehicle 1 has the least mileage among the three vehicles, results showed it produced the highest emissions of NOx and CO. High emissions of NOx and CO from Vehicle 1 can be associated with the de-greening phase of the TWC. All new catalytic surfaces undergo a period of ageing in which their catalytic activities gradually increase to achieve stability in emissions reduction. This period of ageing can be associated with higher emissions rate than during aged activity. It is also consequently seen that Vehicle 3 with an aged catalytic system produced the lowest emission of NOx and CO.

**Table 13 Distance-specific regulated emissions rate from natural gas goods movement vehicles**

| | | NMHC(g/mi) | NOx (g/mi) | NO (g/mi) | CO (g/mi) | PM (mg/mi) |
|---|---|---|---|---|---|---|
| **Vehicle 1** | UDDS | 0.03 | 0.59 | 0.58 | 7.53 | 2.47 |
| | Local | 0.00 | 0.51 | 0.50 | 7.34 | 1.87 |
| | Regional | 0.06 | 0.24 | 0.24 | 7.26 | 3.65 |
| | Near-Dock | 0.11 | 0.61 | 0.61 | 6.07 | 8.96 |
| | | | | | | |
| **Vehicle 2** | UDDS | 0.03 | 0.57 | 0.56 | 13.06 | 7.50 |
| | Local | 0.07 | 0.22 | 0.21 | 7.82 | 5.49 |
| | Regional | 0.06 | 0.20 | 0.19 | 9.32 | 4.10 |
| | Near-Dock | 0.13 | 0.43 | 0.44 | 6.60 | 6.99 |
| | | | | | | |
| **Vehicle 3** | UDDS | 0.02 | 0.11 | 0.11 | 7.67 | 2.94 |
| | Local | 0.03 | 0.24 | 0.24 | 7.58 | 4.32 |
| | Regional | 0.11 | 0.08 | 0.08 | 8.76 | 1.24 |
| | Near-Dock | bdl | 0.29 | 0.29 | 8.51 | 3.03 |

NOx and CO emissions from a stoichiometric engine can be dependent on both TWC activity and the air-fuel ratio control established through a closed loop oxygen sensor. In many cases the response of the oxygen sensor might induce significant differences in emissions rates. Oxygen sensors with low response rate can provide sluggish feedback to the ECU, which could in turn result in longer periods of lean or rich operation. Longer period of lean operation will result in higher NOx and CO emissions.

Figure 26 shows the brake-specific emissions and the percentage of the test period for which the TWC temperature was above 250°C. The TWC temperature was above 250°C almost 100% of the test period over all driving cycles. Although comparison of brake specific emissions from chassis dynamometer testing to FTP engine dynamometer standards is generally not appropriate, it is appropriate here because the three tested vehicles exhibit low NOx emissions for real-world operation. Specifically, Figure 26 showed that the brake-specific emissions of all three vehicles over all the 4 driving cycles were significantly below the US-EPA 2010 FTP standard of 0.20 g/bhp-hr. This is due to the fact that the TWC activity is not temperature dependent and the stoichiometric fueling strategy is designed to primarily reduce NOx emissions. The stoichiometric fueling strategy and the TWC activity is efficient regardless of engine load and operating conditions as observed in the low speed drayage cycles such as near-dock and local.

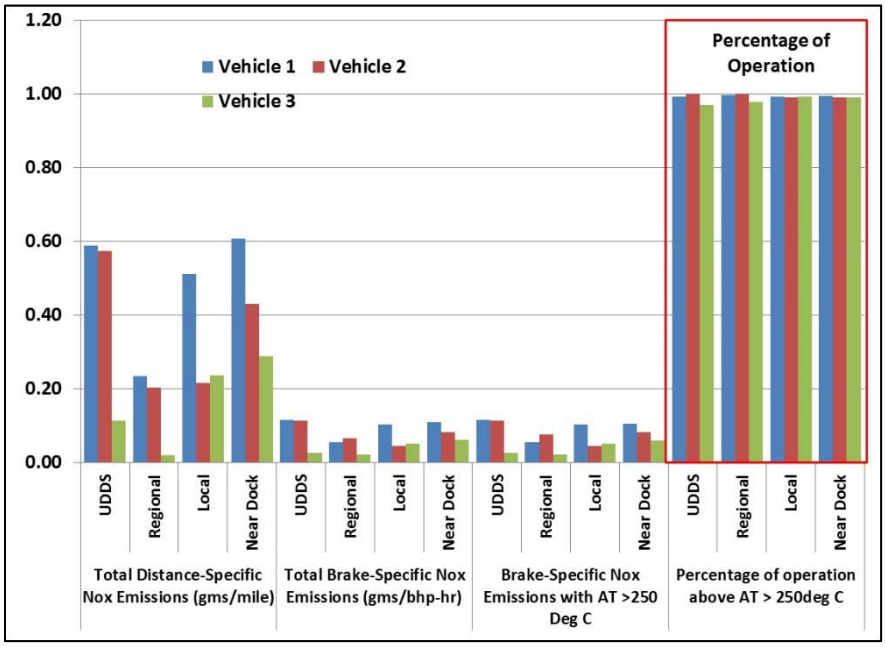


**Figure 26 Brake-specific NOx emissions and after-treatment activity for natural gas goods movement trucks**

Figure 27 shows the distance-specific $CO_2$ emissions from the three natural gas fueled trucks over the UDDS and the 3 drayage port cycles. $CO_2$ emissions are a direct indication of fuel consumption and inversely indicative of fuel economy. Figure 28 shows the distance-specific fuel economy and fuel

consumption of the three goods movement vehicles in DGE and mass of natural gas metrics, respectively. The results show that the lowest $CO_2$ emissions and highest fuel economy were observed during vehicle operation over the regional drayage cycle. Regional type operation is characterized by extended freeway cruise and longer steady-state high speed vehicle operation. It is common for the OEM to adopt a slightly leaner fueling strategy during extended cruise mode operation to achieve better fuel economy and hence lower $CO_2$ emissions. On the contrary the near-dock cycle, characterized by extended idling and creep mode operation with higher duration of low speed transients resulted in the highest $CO_2$ emissions and lowest fuel economy. Higher power demand during transient activities result in frequent rich mode fueling contributing to higher CO emissions and lower fuel economy.

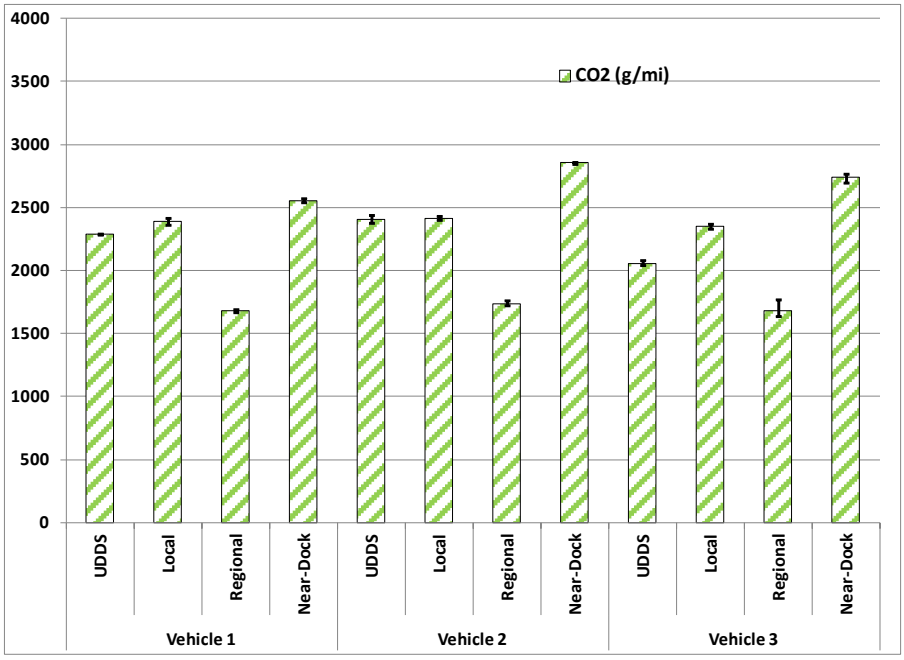


**Figure 27 Distance-specific carbon dioxide emissions from natural gas goods movement vehicles**

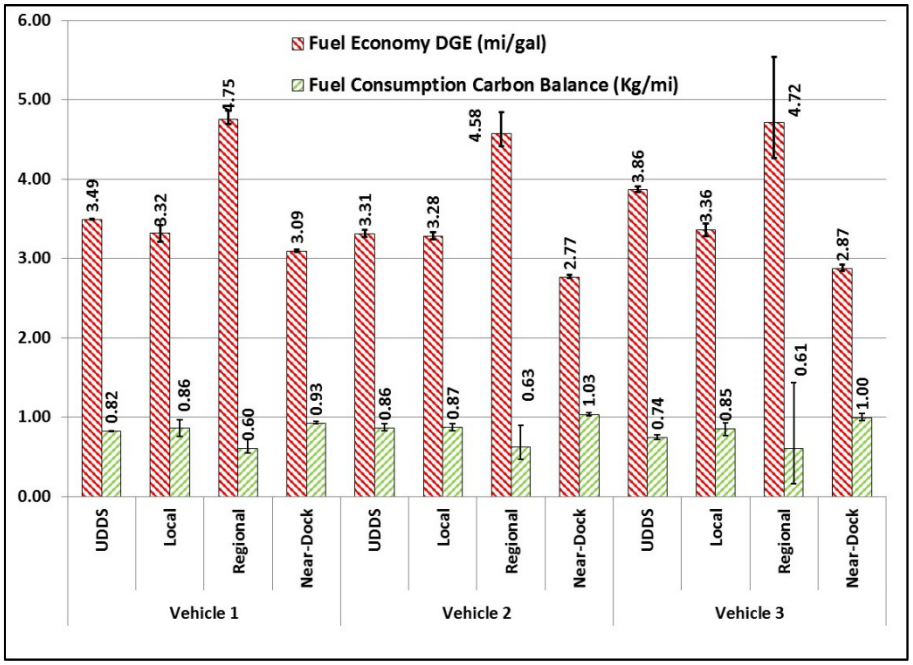


**Figure 28 Distance-specific natural gas fuel consumption and DGE fuel economy from natural gas goods movement trucks**

## 3.2 DIESEL ENGINES

Four refuse vehicles, eight goods movement vehicles and one school bus powered by diesel engines were tested in this study. As shown in Table 1, eight of the vehicles were tested by UCR, while the remaining five consisting of two refuse and three goods movement vehicles were tested by both WVU and UCR. The results of the two refuse and three goods movement diesel vehicles tested by WVU are discussed below.

### *3.2.1 REFUSE TRUCKS*

During the vehicle procurement phase of the study, it was found that no refuse truck with a GVWR rating of 60,000 lbs and powered by a diesel engine certified above 0.20 g/bhp-hr (Category VII in Table 1) is still being operated in Southern California. Hence, it was decided to test a refuse truck powered by the same engine technology as in Category VII but with GVWR rating of 33,000 lb. Therefore, the refuse vehicle in Category VII was tested at a test weight of 33,000 lb, while the refuse vehicle in Category VIII was tested at 56,000 lb. Due to this difference in test weights, distance-specific emissions comparison between the two refuse vehicle categories cannot be performed. Therefore the chart below is merely a representation of the results and not for emissions comparison.

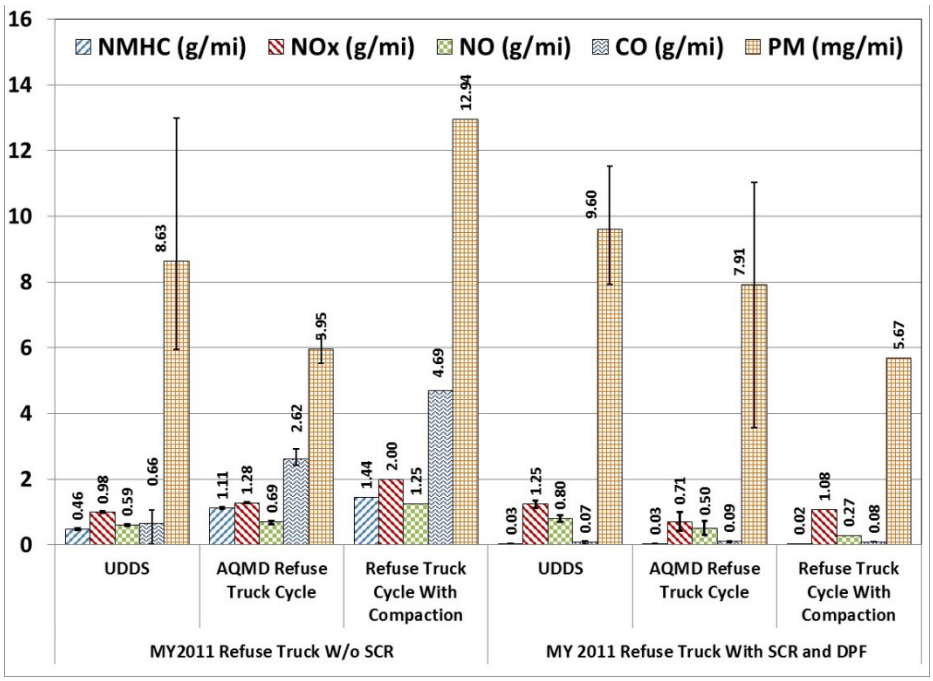


**Figure 29 Distance-specific regulated emissions results of USEPA 2010 compliant diesel refuse trucks**

Figure 29 shows the distance-specific emissions results from the two diesel refuse trucks. The NOx emissions from the Category VII refuse truck over the UDDS, refuse truck cycle, and the refuse truck cycle with compaction were measured to be 0.98 g/mi, 1.28 g/mi, and 0.94 g/mi, respectively. The engine technology part of this category utilizes high EGR rates to achieve low engine out NOx. The NO/NOx ratio for this high EGR engine technology was observed to be 0.60, 0.54, and 0.65 over the UDDS, refuse truck, and the refuse truck with compaction cycle, respectively. Although this engine was fitted with a post turbocharger fuel injector for active regeneration of DPF, high $NO_2$ concentrations would be a characteristic of such high EGR rate engines so as to passively control soot loading rates on the DPF. NMHC emissions from this vehicle were observed to be significantly high. Hydrocarbon emissions from current technology diesel engines are commonly observed to be below detection limits. The higher hydrocarbon emissions observed from this vehicle suggests lower combustion efficiency due to high in-cylinder EGR to control NOx emissions. PM emissions over the UDDS cycle showed high variability (COV of 44%) with an average of 8.6 mg/mi. The variability in the PM measurement could be due to changes in soot loading of DPF contributing to changes in filtration efficiency. It is to be noted that prior to the beginning of the UDDS cycles, the after-treatment system triggered an active regeneration event. As result a drop in filtration efficiency due to a regenerated filter and subsequent soot loading can contribute to changes in PM mass emissions. PM emissions from the refuse truck cycle were measured to be an average of 6 mg/mi with a COV of 10%.

NOx emissions from the category VIII refuse truck (with SCR) were measured to be 1.25 g/mi, 0.71 g/mi, and 0.50 g/mi over the UDDS, AQMD refuse truck cycle, and refuse truck cycle with compaction respectively. The NO/NOx ratio for this engine was measured to be 0.64, 0.71, and 0.53 over the UDDS, AQMD refuse truck cycle, and the refuse truck cycle with compaction, respectively. The NMHC emissions from this vehicle were close to the detection limits of the emissions measurement system. PM emissions from this vehicle were measured to be 9.6 mg/mi, 7.9 mg/mi, and 4.2 mg/mi over the UDDS, AQMD refuse truck cycle, and the refuse truck with compaction cycle, respectively. Variability in PM mass in this case could be attributed to measurement error associated with measuring very low PM mass collection over the gravimetric filter.

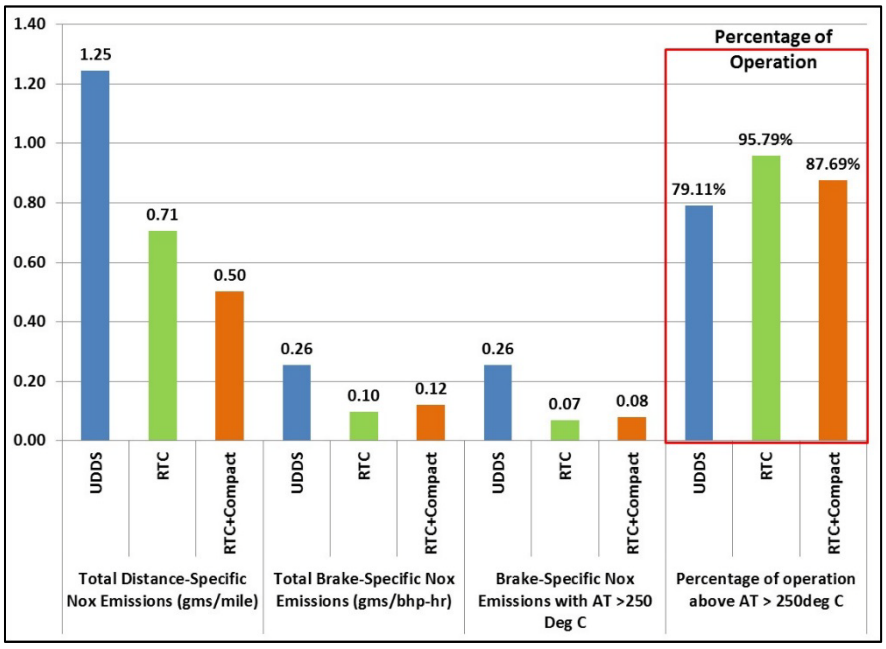


**Figure 30 Brake-specific NOx emissions and after-treatment activity of SCR diesel refuse truck**

Figure 30 shows the brake-specific NOx emissions and percentage of the test period for which the SCR temperature was above 250°C. The results showed that the SCR temperature was above 250°C for 79%, 95.7%, and 87.6% of test period over the UDDS, refuse truck cycle, and the refuse truck cycle with compaction, respectively. The brake-specific NOx emissions over the UDDS, refuse truck cycle, and the refuse truck compaction cycle were 0.26 g/bhp-hr, 0.10 g/bhp-hr, and 0.12 g/bhp-hr for the entire test period, respectively. It is to be noted that the SCR refuse truck was powered by an 8.3 liter, 300HP Cummins engine. A smaller engine powering a 60,000-lb vehicle required sustained operation of the engine at higher loads and as a result higher exhaust temperature. The engine also frequently triggered SCR thermal management to increase exhaust temperatures to the SCR activity range of between 200 to 250°C. A combination of SCR thermal management strategy and downsized engine and after-treatment system contributed to a greater percent of SCR activity and consequently lower NOx emissions.

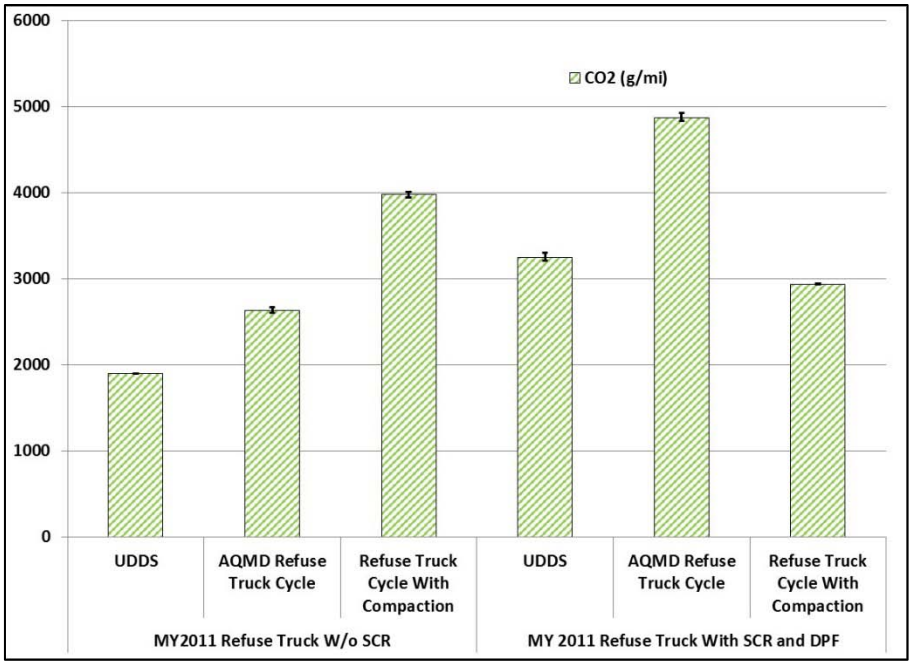


**Figure 31 Distance-specific $CO_2$ emissions results of diesel refuse trucks**

Figure 31 shows the distance-specific $CO_2$ emissions from the two diesel refuse trucks. Highest $CO_2$ emissions were observed during the refuse truck cycle. Frequent short accelerations and extended idle contribute to higher $CO_2$ emissions over the refuse truck operation.

Figure 32 shows the fuel consumption profile of the two diesel refuse trucks. The results showed the refuse truck cycle to be the least fuel efficient operation due to extended idle and frequent acceleration events. Also, in the case of the SCR refuse truck, thermal management activity and predominant operation of the engine at higher load conditions contributed to a fuel economy of 2.19 mi/gal.

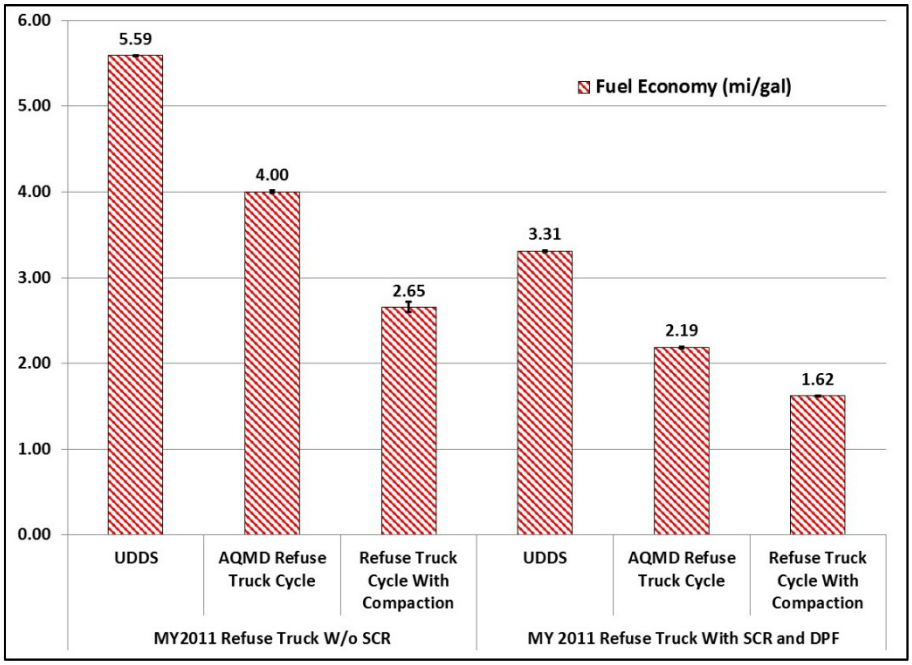


**Figure 32 Fuel economy results of diesel refuse trucks**

### *3.2.2 GOODS MOVEMENT*

The US-EPA 2010 compliant engines certified over 0.20 g/bhp-hr without a SCR after-treatment system were developed by Navistar. The engine employed a combination of high EGR rates, optimized engine and transmission and a DPF to achieve desired NOx and PM. The engine is designed for operating at lower engine speed, which is conducive for optimum fuel economy and lower soot loading rate in DPF. This strategy required drivers to operate the vehicle at higher gears during most transient operation. This type of operating is in contrast to regular driving practice which will require frequent downshift and upshift from the operator during vehicle transients. This type of operation enabled the truck to operate in a narrow engine speed window of between 1,300 rpm and 1,600 rpm. The ECU provided a dead pedal (no throttle response) for any gear change operation above 1,600 rpm. Since the engine uses high EGR rates to achieve lower NOx, fuel penalty and higher soot loading rates are setbacks of this strategy. Therefore an engine lugging type operation could be forced by the OEM to continuously operate the power train in an efficient bandwidth of fuel economy and lower soot loading.

Table 14 presents the distance-specific emissions rates of regulated pollutants from diesel vehicles powered by engines in Categories IV, VII and VIII in Table 1.

**Table 14 Lists the average distance-specific emissions from diesel fueled goods movement trucks**

| MY 2009 Diesel W/ DPF | | | | | | |
|---|---|---|---|---|---|---|
| | **NMHC (g/mi)** | **NOx (g/mi)** | **NO (g/mi)** | **CO (g/mi)** | **CO2 (g/mi)** | **PM (mg/mi)** |
| **UDDS** | 0.03 | 8.77 | 5.57 | 0.60 | 2756.7 | 8.40 |
| **Local** | 0.05 | 9.33 | 6.61 | 0.22 | 2979.3 | 5.98 |
| **Regional** | 0.01 | 5.86 | 3.82 | 0.10 | 2069.7 | 3.24 |
| **Near-dock** | 0.12 | 9.50 | 7.01 | 0.57 | 3175.7 | 8.17 |
| **MY 2011 Diesel with DPF only** | | | | | | |
| | **NMHC (g/mi)** | **NOx (g/mi)** | **NO (g/mi)** | **CO (g/mi)** | **CO2 (g/mi)** | **PM (mg/mi)** |
| **UDDS** | 0.12 | 5.51 | 3.18 | 4.54 | 2114.7 | 3.81 |
| **Local** | 0.08 | 5.49 | 3.75 | 2.75 | 1994.0 | 7.90 |
| **Regional** | 0.07 | 3.89 | 2.39 | 1.27 | 1506.3 | 5.61 |
| **Near-dock** | 0.22 | 6.86 | 5.09 | 3.60 | 2107.0 | 11.71 |
| **MY 2011 Diesel w/SCR and DPF** | | | | | | |
| | **NMHC (g/mi)** | **NOx (g/mi)** | **NO (g/mi)** | **CO (g/mi)** | **CO2 (g/mi)** | **PM (mg/mi)** |
| **UDDS** | 0.00 | 1.98 | 1.62 | 0.22 | 2421.6 | 9.71 |
| **Local** | -0.02 | 5.89 | 5.09 | 0.75 | 2493.3 | 9.68 |
| **Regional** | -0.02 | 1.31 | 1.15 | 0.17 | 1873.0 | 2.17 |
| **Near-dock** | 0.01 | 9.04 | 7.92 | 0.85 | 2745.3 | 5.73 |

Figure 33 shows the distance-specific criteria emissions from the vehicles in Table 13 over UDDS and the drayage port cycles. Over the UDDS cycle, the category IV, VII, and VIII vehicles emitted 8.77 g/mi, 5.51 g/mi, and 1.98 g/mi of NOx emissions, respectively. Highest NOx emissions measured from the vehicle in Category IV is due to the vehicle being powered by an engine certified to a less stringent standard than engines in Categories VII and VIII. NOx emissions from the SCR equipped diesel engine (Category VIII) was 64% lower than that of a high EGR non SCR diesel engine (Category VII) over the UDDS cycle. Also, it is interesting to note that the highest CO emissions were observed from the category VII vehicle with a high EGR strategy. Similar to the refuse truck in the same category, the CO emissions from this engine technology is significantly higher in comparison to other diesel engines. This can be attributed to lower in-cylinder combustion efficiency due to the high EGR strategy.

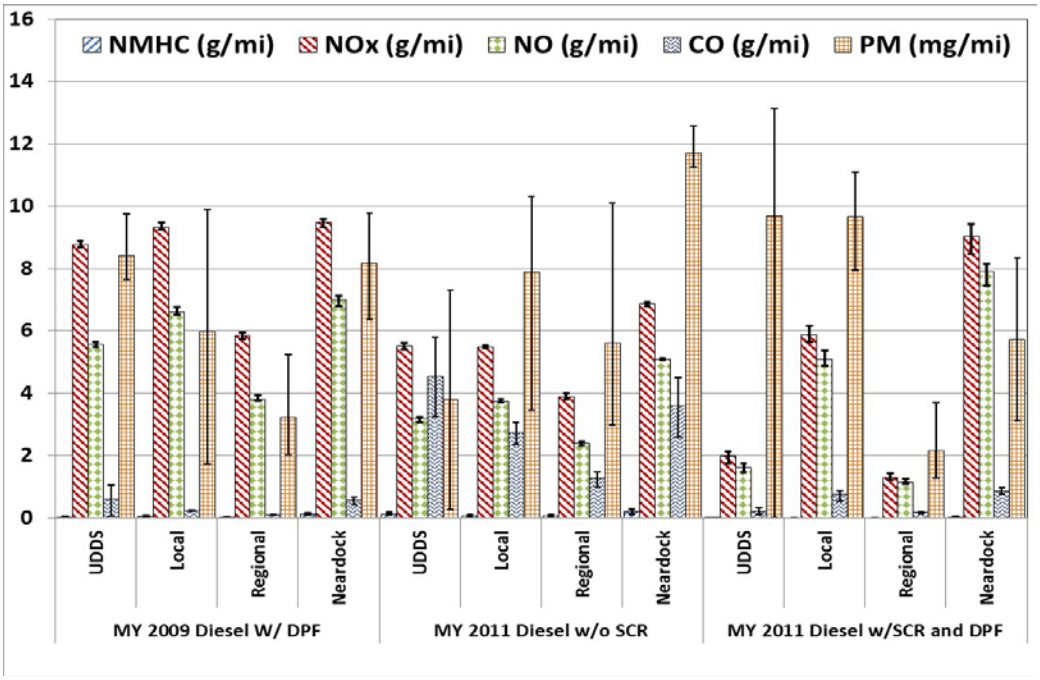


**Figure 33 Distance-specific regulated emissions results of USEPA 2010 compliant diesel goods movement trucks**

Additionally, Figure 33 shows that SCR operation is critical to lower NOx emissions during port drayage operation. Of the three drayage driving cycles used, the near-dock and local are characterized by extended idling, creep, and low load operations. Regional cycle produced the lowest NOx emissions from all diesel engines with an average distance-specific NOx emission of 5.86 g/mi, 3.89 g/mi, and 1.31 g/mi from Category IV, VII, and VIII vehicles, respectively.

Because the SCR was not triggered during near-dock cycle, the average distance-specific NOx emission from the SCR-equipped diesel vehicle (Category VIII) was measured to be 9.04 g/mi, which is fairly comparable to NOx emission of 9.50 g/mi from the non-SCR equipped diesel vehicle (Category IV). With partial SCR activity during the local drayage cycle, the distance-specific NOx emission from the same SCR-euipped vehicle in Category VIII was measured to be 5.89 g/mi.

The NO/NOx ratios from vehicles in Categories VII and VIII were observed to be 0.58 and 0.81, respectively. The higher NO/NOx ratio from the SCR equipped diesel vehicle shows lower $NO_2$ emissions from the tailpipe. This can be attributed to the passive regeneration strategy that consumes most of the $NO_2$ emissions for soot light-off.

PM emissions from all DPF equipped vehicles showed high variability. The Category VII high EGR technology vehicle regenerated actively during multiple runs. However, the data represented in the charts are only that from non-regeneration test runs.

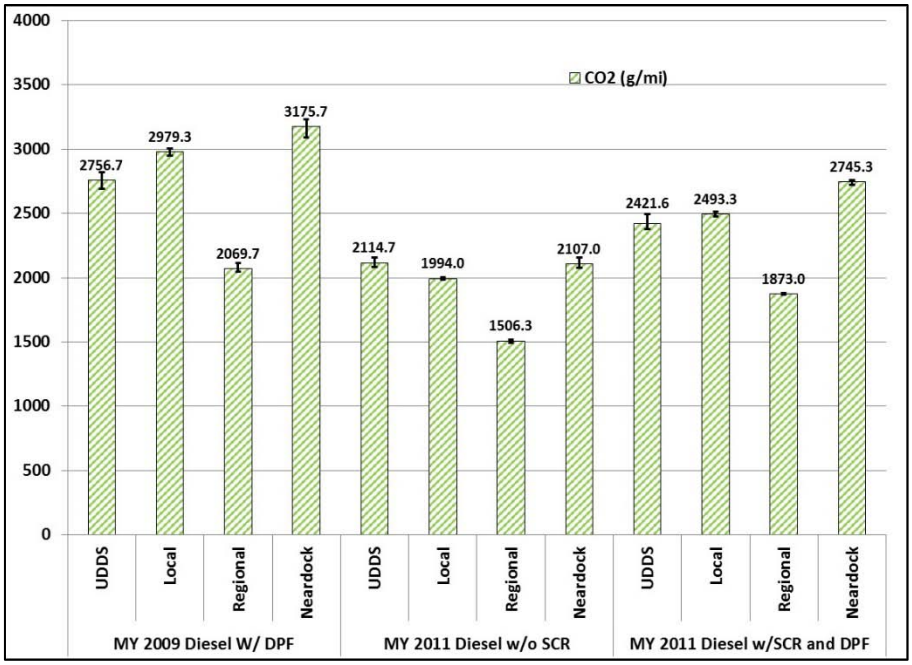


**Figure 34 Distance-specific $CO_2$ emissions results of diesel goods movement vehicles**

Figure 34 shows the distance-specific $CO_2$ emissions from the diesel fueled goods movement vehicle from the three technology categories. The lowest $CO_2$ emissions were observed from the high EGR category VII vehicle. This can be attributed to the lugging type operation forced by the manufacturer to enable operation at optimum fuel consumption. The $CO_2$ emissions of the high EGR engine was 12% lower than that of the SCR equipped diesel over the UDDS driving cycle. Similarly, the high EGR US-EPA 2010 compliant engine operated at 30% better fuel economy when compared to the MY 2009 engine.

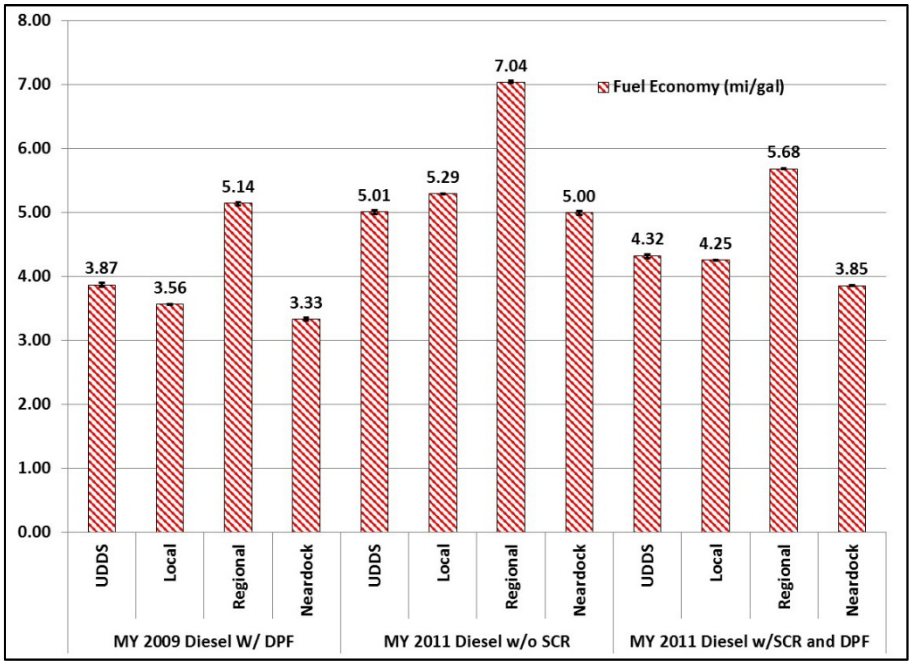


**Figure 35 Fuel economy results from diesel goods movement vehicles**

The fuel economy results shown in Figure 35 reveal that vehicles subjected to the newer emissions standard are operating with better fuel economy than those subject toa less stringent emission standard.. In the case of SCR equipped diesel, the SCR after-treatment system can be calibrated to assist a fuel economy based engine calibration. This trend can be observed from the fuel economy values from the regional cycle, wherein the SCR equipped diesel vehicle operated at 5.68 mi/gal. This means that during SCR activity periods, engine operation can be tuned to better fuel economy and higher engine out NOx while an optimized SCR after-treatment system will assist in lowering NOx emissions to remain within compliance. Over the UDDS cycle the SCR equipped diesel engine operated at 12% better fuel economy than the MY 2009 engine. In the case of the high EGR engine the better fuel economy over the regional cycle can be attributed to the sustained freeway operation with minimum transients combined with lugging type operation required by the engine.

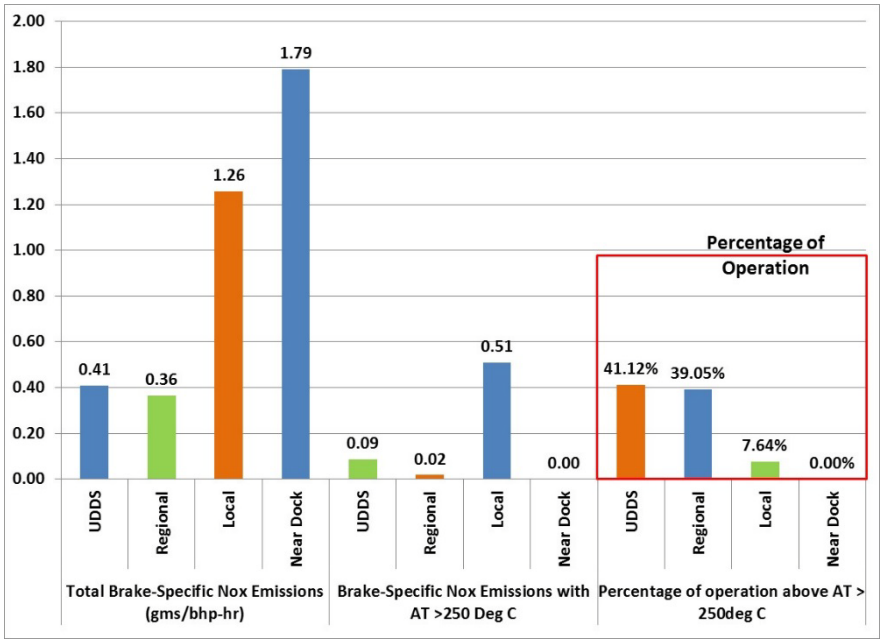


**Figure 36 Brake-specific NOx emissions and percentage SCR activity of SCR equipped diesel goods movement vehicle**

Figure 36 shows the results of brake-specific NOx emissions from the Category VIII vehicle measured over the UDDS and port drayage cycles and percentage of the test period for which the SCR temperature was above 250°C. Brake-specific NOx emissions over the UDDS, regional, local, and near-dock cycle were measured to be 0.41 g/bhp-hr, 0.36 g/bhp-hr, 1.26 g/bhp-hr, and 1.79 g/bhp-hr, respectively. The percentages of test period for which the SCR temperature was above 250°C reveal poor SCR activity over all types of drayage operation. The near-dock drayage operation resulted in exhaust temperatures that were not adequate to trigger SCR activity. Similarly, exhaust temperatures over the local and regional cycles were more than 60% of the time below the threshold limit of 250°C. It is interesting to note that although exhaust temperatures were below threshold during most parts of the drayage driving cycles, the manufacturer's strategy did not trigger any SCR thermal management activity. This could be attributed to the fact that manufacturers are not subject to meet the 0.20 g/bhp-hr on real-world engine operation and thermal management could be active only during select regions of the engines lug curve.

### 3.3 HPDI

Three MY 2009 and one MY 2011 goods movement vehicles powered by HPDI engines were in this study. The results of the chassis dynamometer test of these vehicles are discussed below.

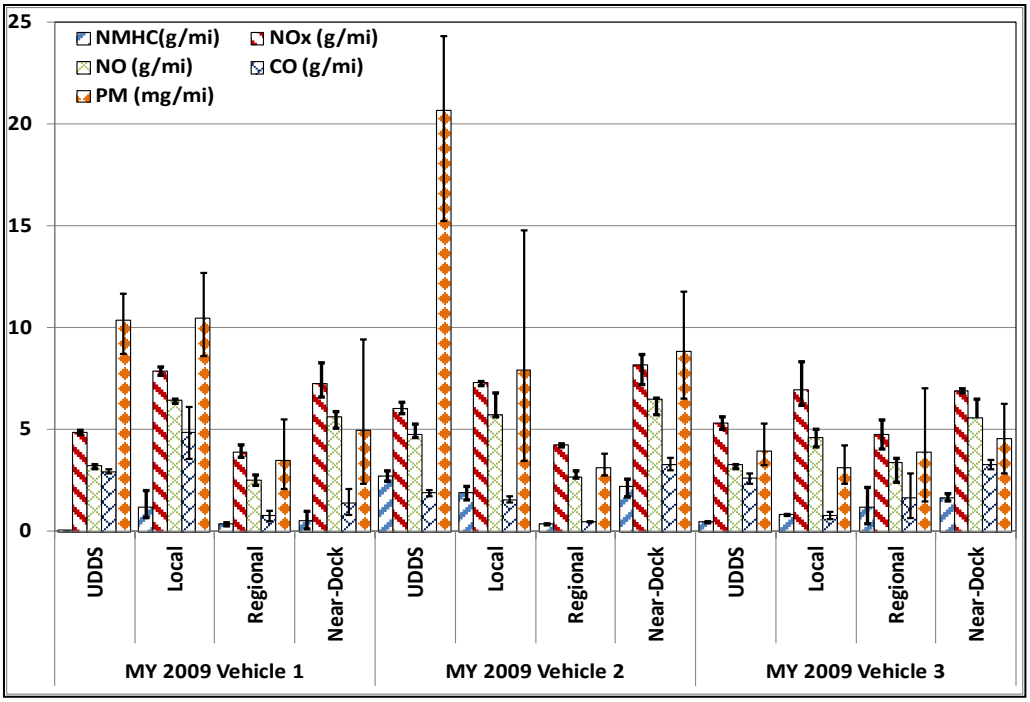


**Figure 37 Distance-specific regulated emissions results of MY 2009 dual-fuel HPDI goods movement trucks**

Figure 37 shows the distance-specific regulated emissions of three MY 2009 HPDI goods movement trucks tested over the UDDS and the three drayage port cycles. The results show an average distance-specific NOx emission from the three vehicles over the UDDS cycle to be 5.40 g/mi with an 11% COV between vehicles. PM emissions rate showed the highest variation between vehicles. Average distance-specific PM emissions from the three vehicles over the UDDS cycle were measured to be 11.68 mg/mi with a 72% COV between vehicles. Highest PM emissions were observed from Vehicle 2 with an average distance-specific PM emission of 20.70 mg/mi over the UDDS cycle. Vehicle 2 exhibited regeneration events both during the UDDS and the local cycle. The subsequent loss in filtration efficiencies associated with the DPF regeneration contributed to higher PM mass emissions from this vehicle. Vehicle 1 had a DPF full status message prior to recruiting the vehicle, following which a full parked regeneration was intimated to clear any active status messages before chassis dynamometer testing. Vehicle 1 also exhibited significantly higher PM emissions compared to Vehicle 3 following active regeneration events. Vehicle 3 exhibited the lowest PM emissions rate with an average distance-specific emission of 3.95 mg/mi, 3.12 mg/mi, 3.90 mg/mi, and 4.57 mg/mi over the UDDS, local, regional, and near-dock cycle respectively. The variations in PM emissions could suggest changes in the diesel pilot injection rate thereby contributing to differences in PM loading in the DPF. Gravimetric fuel mass measured for diesel fuel shows that the lowest diesel fuel consumption was observed for Vehicle 3 with an average of 0.43 kg consumed over the length of the UDDS cycle, in comparison to 0.73 and 0.82 consumed by Vehicles 1 and 2 respectively. Vehicles with the two highest diesel fuel consumption produced highest soot loading

rate in the DPF and the resulting regeneration events contributed to the highest PM emissions. Table 14 lists the average distance-specific regulated emissions of the three MY 2009 HPDI goods movement trucks.

**Table 15 Regulated emission results of three HPDI goods movement vehicles**

| | MY 2009 Vehicle 1 | | | | |
|---|---|---|---|---|---|
| | NMHC(g/mi) | NOx (g/mi) | NO (g/mi) | CO (g/mi) | PM (mg/mi) |
| **UDDS** | 0.00 | 4.87 | 3.22 | 2.95 | 10.40 |
| **Local** | 1.21 | 7.89 | 6.44 | 4.88 | 10.48 |
| **Regional** | 0.35 | 3.88 | 2.53 | 0.81 | 3.50 |
| **Near-Dock** | 0.50 | 7.25 | 5.63 | 1.42 | 4.98 |
| | **MY 2009 Vehicle 2** | | | | |
| **UDDS** | 2.75 | 6.02 | 4.79 | 1.91 | 20.70 |
| **Local** | 1.93 | 7.30 | 5.72 | 1.55 | 7.93 |
| **Regional** | 0.39 | 4.26 | 2.67 | 0.46 | 3.16 |
| **Near-Dock** | 2.23 | 8.18 | 6.52 | 3.31 | 8.83 |
| | **MY 2009 Vehicle 3** | | | | |
| **UDDS** | 0.46 | 5.33 | 3.28 | 2.64 | 3.95 |
| **Local** | 0.82 | 6.97 | 4.62 | 0.79 | 3.12 |
| **Regional** | 1.20 | 4.78 | 3.38 | 1.64 | 3.90 |
| **Near-Dock** | 1.65 | 6.93 | 5.59 | 3.26 | 4.57 |
| | **Average for three vehicles** | | | | |
| **UDDS** | 1.07 | 5.40 | 3.76 | 2.50 | 11.68 |
| **Local** | 1.32 | 7.39 | 5.59 | 2.41 | 7.18 |
| **Regional** | 0.65 | 4.31 | 2.86 | 0.97 | 3.52 |
| **Near-Dock** | 1.46 | 7.45 | 5.91 | 2.66 | 6.13 |

Results from the HPDI vehicles show a significant progress towards a cleaner technology when compared to legacy dual-fuel engines that were plagued by high CO, NMHC, and NOx emissions. The low CO and NMHC emissions observed from these vehicles suggest efficient in-cylinder combustion with the presence of a DPF to trap the soot generated from the diesel pilot injection. Since the base engine of the HPDI platform is a MY 2009 Cummins diesel engine, the combination of EGR and dual-fuel operation has enabled the certification of 1.2 g/bhp-hr engine at 0.80 g/bhp-hr.

Figure 38 shows the $CO_2$ emissions profile of the three MY 2009 HPDI dual-fuel trucks. The carbon balance fuel consumption that was calculated from the $CO_2$ emissions assumed 100% natural gas substitution rate. Vehicle 2 exhibited the highest $CO_2$ emissions in comparison to the other vehicles. This could be attributed to a higher fueling rate of both natural gas and diesel compared to the other two vehicles. Figure 39 shows the fuel consumption and fuel economy profile of the three HPDI goods movement trucks tested over the UDDS and three drayage cycles.

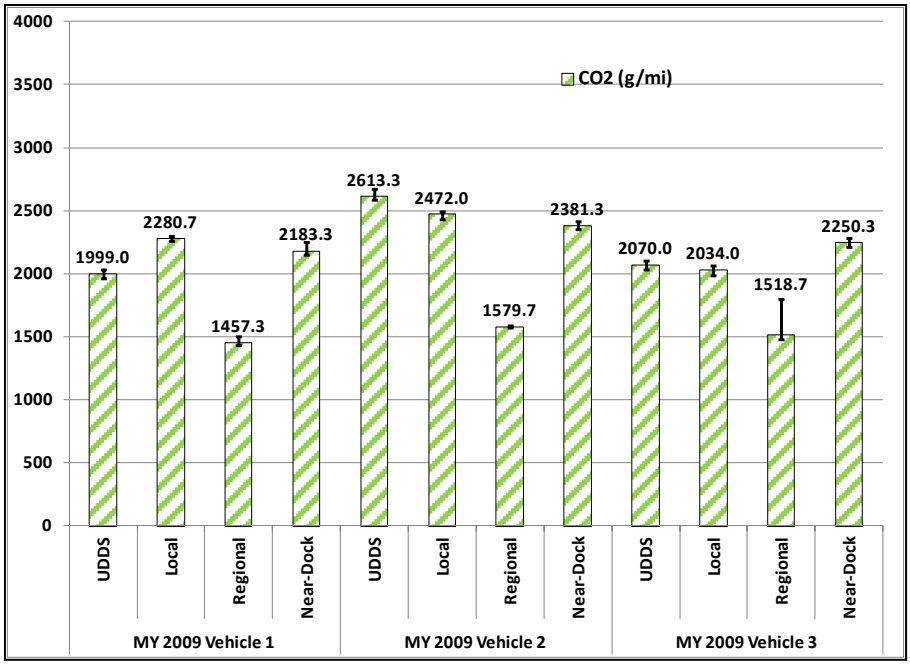


**Figure 38 Distance-specific $CO_2$ emissions from MY 2009 dual-fuel goods movement trucks**

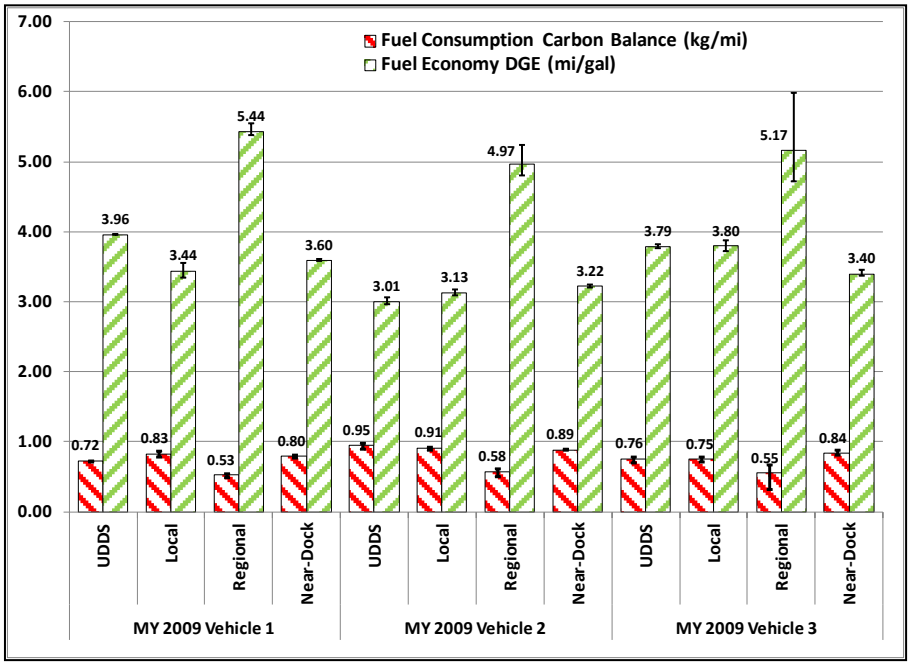


**Figure 39 Distance-specific fuel consumption and fuel economy results of MY 2009 HPDI trucks**

Figure 40 shows the distance-specific regulated emissions results from the US-EPA 2010 compliant HPDI truck. Distance-specific NOx emissions from this truck was measured to be 0.74 gm/mi, 0.65 gm/mi, 0.47 gm/mi, and 0.87 gm/mi over the UDDS, local, regional, and near-dock cycle, respectively. The truck exhibited significantly lower NOx emissions on all cycles compared to 2010 compliant diesel

vehicles. The combination of dual-fuel operation and SCR after-treatment package contributes to overall lower distance-specific emissions than comparable diesel engines. Emissions of other regulated pollutants are also lower in magnitude than comparable diesel engines.

While comparing HPDI and the stoichiometric natural gas engine platform, the HPDI platform offers similar performance and mileage range as diesel engines. Although the stoichiometric platform is economical in its after-treatment package the shorter mileage range restricts its use as a goods movement to local city type drayage operation.

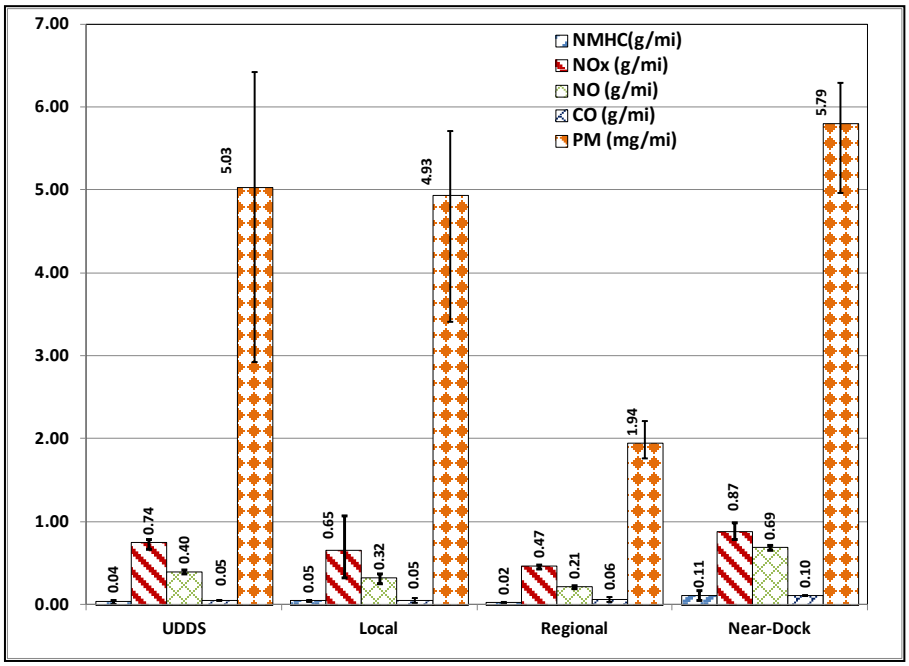


**Figure 40 Distance-specific emission results of MY 2011 dual-fuel HPDI goods movement truck**

### 3.4 EMISSIONS COMPARISON BETWEEN DIESEL AND NATURAL GAS

This section compares NOx emissions profile between diesel, natural gas and HPDI technology. The results in this section are aimed at illustrating the effect of engine exhaust temperature on the NOx emissions from the different technology. Therefore this section will compare data only from TWC equipped natural gas engine and engines equipped with SCR aftertreatment system.

Figure 41 shows the distance-specific and brake-specific NOx emissions from diesel, natural gas, and dual-fuel goods movement vehicles. Figure 41 also shows the brake-specific NOx emissions and the percentage of the test period for which the aftertreatment temperature was above 250°C. The results clearly illustrate the effect of exhaust temperature on the activity of the SCR system in a diesel engine. Diesel vehicles equipped with SCR exhibited the highest distance-specific emissions compared to both the TWC equipped and dual-fuel natural gas vehicle.

A natural gas vehicle with TWC exhibits superior NOx reduction over all driving cycles. This can be attributed to the fact that, NOx reductions with the TWC are dependent on operating air-fuel ratio rather than exhaust temperatures. Exhaust temperatures from stoichiometric natural gas engines are greater than 250$^{o}$C for over 99% of the cycle duration. Although the TWC NOx reduction is more air-fuel ratio dependent than temperature, high exhaust temperature also contributes to significant reductions in non-methane hydrocarbons and CO emissions. The results from creep and idle mode operation in the drayage cycle, show that, unlike SCR aftertreatment systems, TWC NOx reduction is not affected by engine duty cycle.

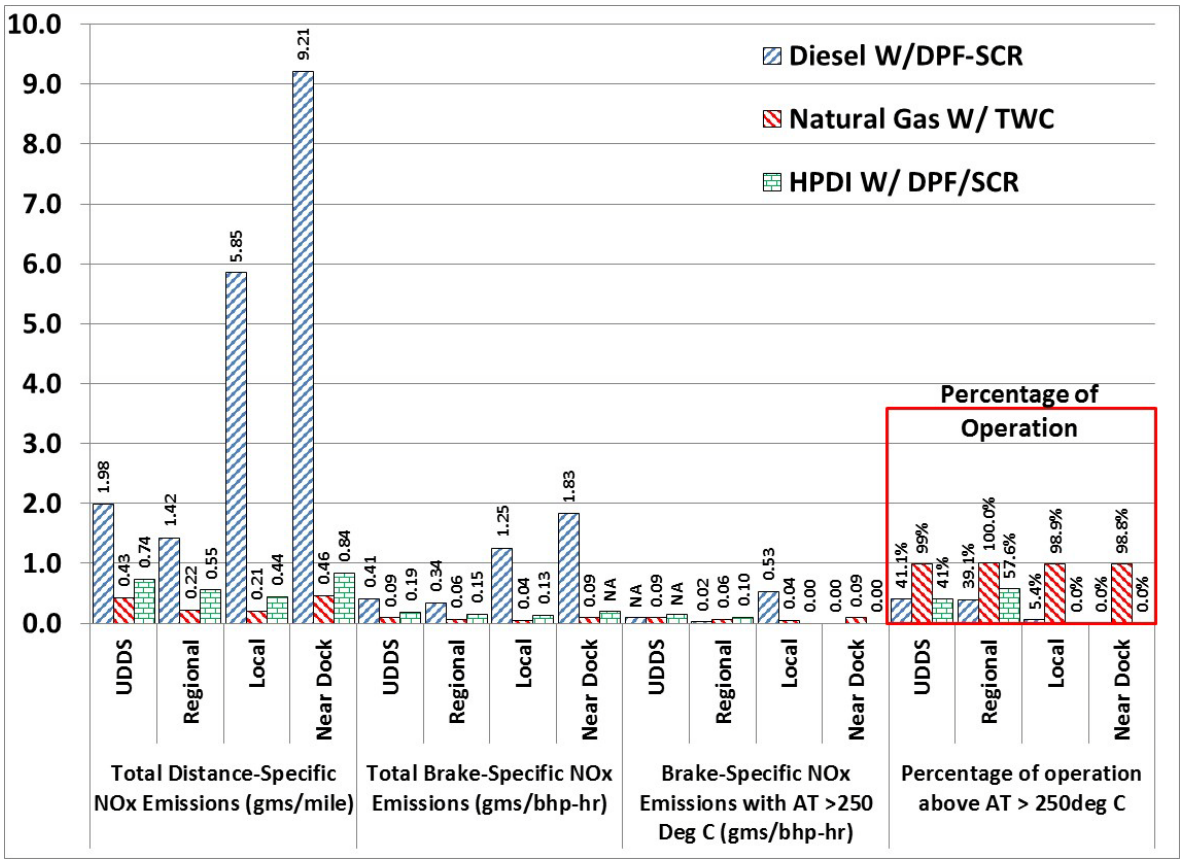


**Figure 41 Distance and brake-specific emissions comparison of NOx emissions from diesel and natural gas for the goods movement application**

The local and the near-dock cycles resulted in the least percentage of test period for which SCR temperature was above 250°C for both diesel and HPDI technology. The diesel vehicle activity operated only 5.4% over the temperature threshold over the local cycle and reported no activity over this temperature threshold over the near-dock cycles. The exhaust temperatures from the HPDI vehicles did not exceed the 250$^{o}$C temperature threshold during the near-dock and local cycles. However, the HPDI technology still reported a 90% lower NOx emissions than a SCR equipped diesel vehicle. The lower

NOx emissions from the HPDI engine can be attributed to the compressed ignition of natural gas with diesel pilot injection that generates lower in-cylinder NOx than conventional diesel fuel combustion.

The brake-specific NOx emissions of the diesel vehicle over the local and near-dock cycles were measured to be 1.25 and 1.83 g/bhp-hr, respectively. It is to be noted that OEMs are not required to comply with in-use NTE standard (1.25 time FTP standard) at exhaust temperatures below 250°C. Since the local and near-dock cycle resulted in vehicle operation less than this threshold more than 95% of the time, the SCR inactivity contributes to high NOx emissions. However, during the short test period for which SCR temperature was above 250°C, diesel vehicle reports a brake-specific NOx emission of 0.53 and 0.08 g /bhp-hr measured over local and near-dock cycles, respectively. The HPDI vehicle regardless of SCR activity exhibits a significant lowering of NOx emissions over both the local and drayage cycle.

The regional drayage cycle is the most aggressive of the three with respect to engine load and vehicle speed and consequently results in the highest percentage of test period for which aftertreatment temperature was over 250°C. Diesel vehicles equipped with SCR exhibited NOx emissions that are at least 75% lower over the regional cycle than local cycle or near-dock cycles, however the SCR activity was reported only for 39% of the entire duration. The brake-specific NOx emission measured over regional cycle during which the SCR temperature was above 250°C was 0.06 g/bhp-hr.

Both the TWC equipped natural gas and the dual-fuel HPDI vehicles exhibit an order of magnitude lower NOx emissions than the diesel technology, further suggesting the low emissions capability of the natural gas platform over cycles that are not conducive for SCR activity.

The results show that both the dual-fuel HPDI and the natural gas with TWC are better suited than a diesel with SCR at period for which aftertreatment temperature is less than 250°C. The superior activity of the TWC and the lower engine out NOx emissions of the dual-fuel technology reduces the influence of engine load on NOx emissions characteristics and hence realizing an overall reduction in real-world NOx emissions.

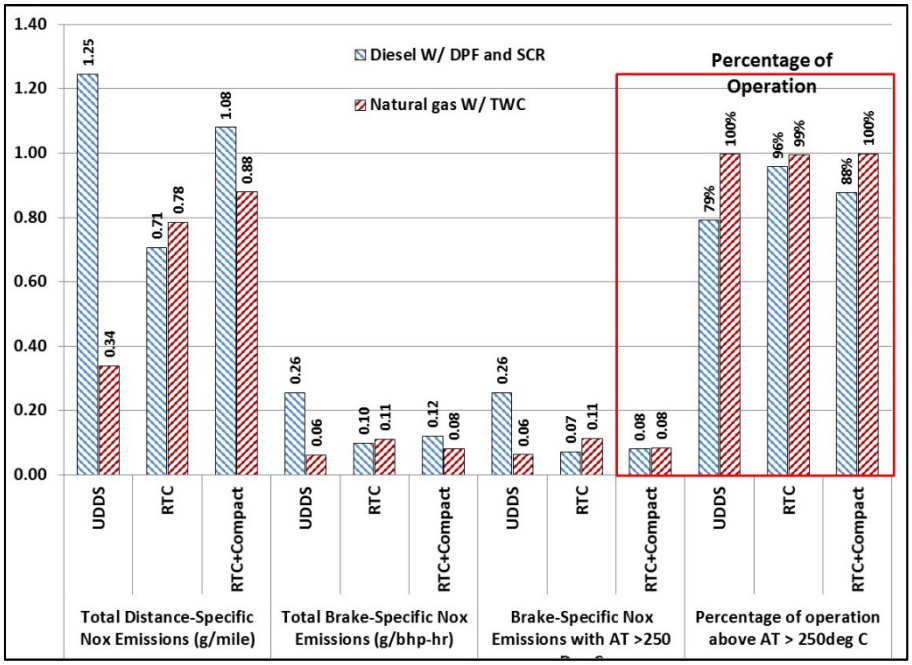


**Figure 42 Distance and brake-specific emissions comparison of NOx emissions from diesel and natural gas for the refuse truck application**

Figure 42 shows the NOx emissions comparison between diesel with SCR and natural gas with TWC for the refuse truck application. The results from the UDDS cycle show natural gas refuse truck to emit 76% lower NOx emissions than diesel refuse truck. The refuse truck cycle showed the natural gas and diesel vehicle to emit a similar NOx emissions characteristics. The exhaust temperature characteristics show that the diesel refuse truck operated 79% of the UDDS cycle above 250$^{o}$C, while it operated for 96% of the refuse truck cycle duration above the temperature threshold. This suggests the possibility of thermal management being employed for extended SCR activity during the frequent stop-and-go activity of the refuse truck cycle.

### *3.4.1 COLD START NOX EMISSIONS*

The study conducted cold start emissions test using the HD-UDDS driving cycle for all vehicles. All vehicles were exercised over the HD-UDDS driving cycle following an overnight soak. The results of the cold start test may not be representative of an engine dynamometer conditioned cold start. Instead this test procedure would be more representative of a real-world cold start emissions rate that would be dependent on the last test cycle that was performed prior to the over-night soak. Particularly, the SCR cold start could be biased with a lower cold start NOx emissions due to an aggressive cycle such as the regional being performed prior to the overnight soak.

Figure 43 shows the distance-specific and brake-specific NOx emissions from a cold start HD-UDDS test from stoichiometric natural gas, HPDI and diesel goods movement vehicles. The

stoichiometric natural gas vehicles exhibited the lowest NOx emissions during cold start operation. This can be attributed to the lower thermal inertia of the TWC system and the higher exhaust energy of stoichiometric engine exhaust. The results show that the NOx emissions from the stoichiometric natural gas engine is 62% lower than an SCR equipped diesel during a cold start HD-UDDS operation. Also, the HPDI engine equipped with an SCR showed a 26% lower cold start NOx emissions compared to a diesel vehicle equipped with SCR. The USEPA 2010 diesel engine equipped with only a DPF showed 5 times greater NOx emissions than a stoichiometric natural gas engine and 1.3 times greater NOx emissions than a diesel engine equipped with SCR.

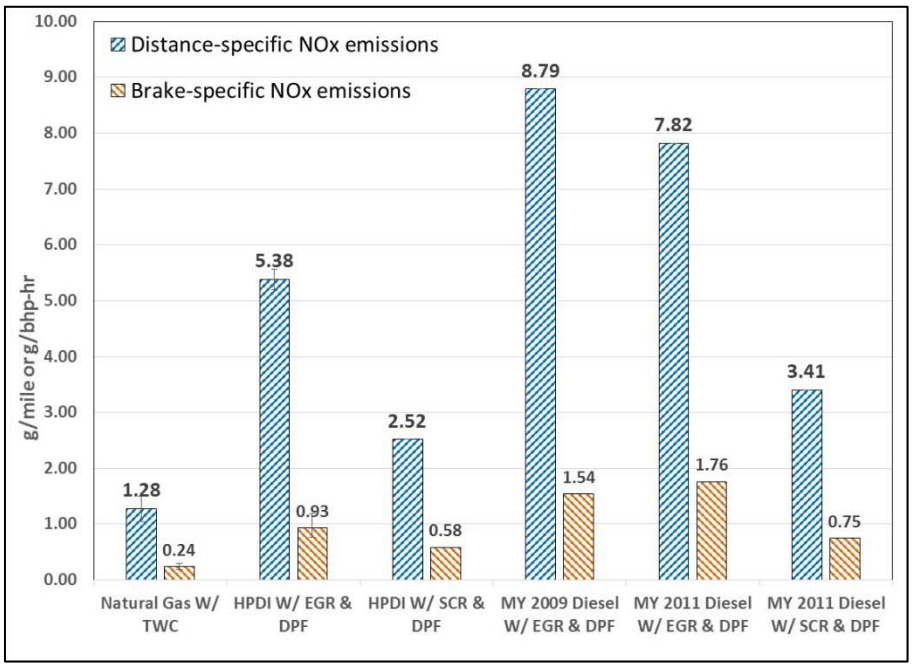


**Figure 43 Comparison of cold start HD-UDDS NOX emissions**

### *3.4.2 GREENHOUSE GAS EMISSIONS COMPARISON*

Figure 44 shows the greenhouse gas emission rates and the global warming potential (GWP) comparison between natural gas with TWC, HPDI with DPF and SCR, and USEPA 2010 emissions compliant diesels. The GWP calculations used the intergovernmental panel on climate change (IPCC) values of 25 times $CO_2$ equivalent for methane and 298 times $CO_2$ equivalent for nitrous oxide as given the IPCC fourth assessment report (IPCC, 2007).

Natural gas is a lower carbon fuel than diesel fuel, and as such, the distance-specific $CO_2$ emissions from a stoichiometric natural gas engine was observed to be 7% lower than a diesel vehicle equipped with SCR. Also the HPDI engine operating with lean-burn strategy resulted in 11% lower distance-specific $CO_2$ emissions than comparable diesel vehicle.

The bulk of the GWP from stoichiometric natural gas vehicles is contributed by methane emissions. It is to be noted that the magnitude of methane emissions is lower compared to legacy lean-burn natural gas engines. Considering the HPDI engine, majority of the GWP is contributed by nitrous oxide and methane emissions. The emissions of nitrous oxide could be related to incomplete SCR reactions due to a lower exhaust temperature conditions.

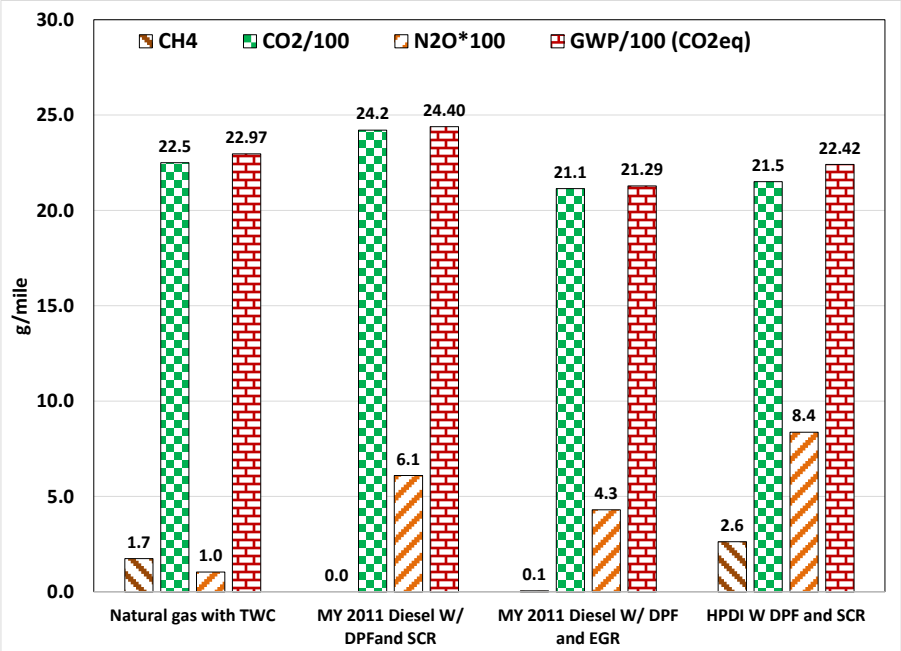


**Figure 44 Comparison of greenhouse gas emission of goods movement vehicles**

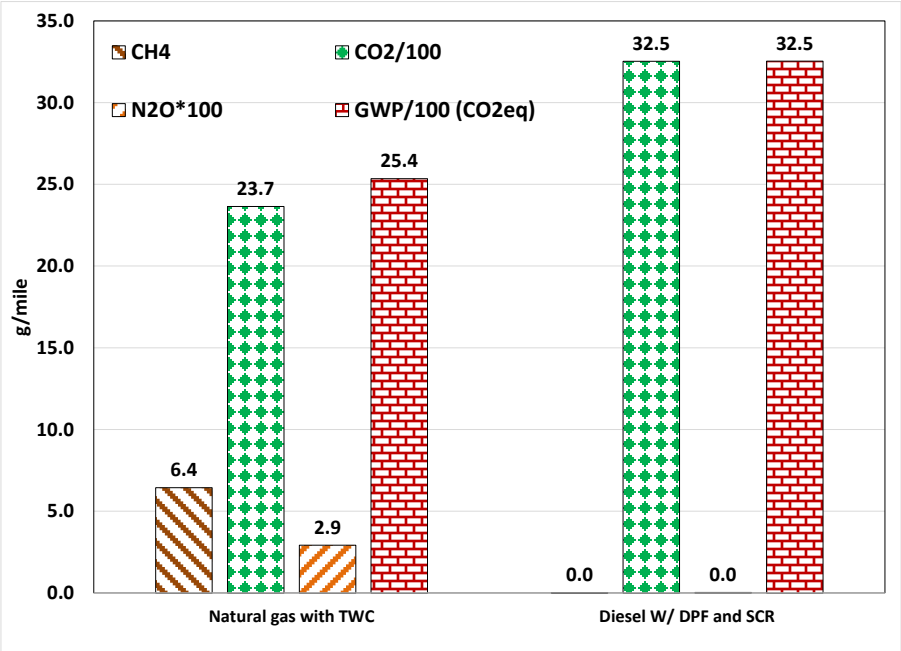


**Figure 45 Comparison of greenhouse gas emissions of refuse trucks**

Figure 45 shows the comparison GHG emission and GWP between a diesel refuse truck and natural gas refuse truck. The GWP of the natural ga refuse truck with tWC is 22% lower than the diesel equipped with DPF and SCR. The difference in GWP is primarily due to the differences in fuel carbon. The methane emissions from natural gas refuse truck did not contribute to significant fractions of the total GWP.

### 3.5 NO, $NO_2$ AND $NO_2$/NOX RATIO

PM and NOx after-treatment systems have been linked to increased tailpipe $NO_2$ emissions. A study by Rexeis and Hausberger predicted the $NO_2$/NOx ratio of newer diesel vehicles to increase relative to older diesel vehicles due to the use of catalytic after-treatment systems (Rexeis and Hausberger, 2009). Although tailpipe $NO_2$ is not regulated by the USEPA, California regulates the $NO_2$ emissions for retrofit systems to not exceed 15% of baseline NOx in the tailpipe (CCR, Title 13, Division 3).

Both PM and NOx after-treatment systems require higher $NO_2$ concentrations for their optimal operation. Passively regenerating DPFs require higher $NO_2$ concentrations in the exhaust for lowering soot light-off temperatures. SCR after-treatment systems require a stoichiometric ratio of NO and $NO_2$ for initiating fast SCR NOx reactions (Johnson, 2009). Table 16 lists the distance-specific NO and NO2 split of the tailpipe NOx emissions rate with the observed ratio of $NO_2$ to NOx emissions.

**Table 16 NO, $NO_2$ and $NO_2$/NOx ratio of heavy-duty vehicles in goods movement application**

| | UDDS | | | Near-Dock | | | Local | | | Regional | | |
|---|---|---|---|---|---|---|---|---|---|---|---|---|
| | NO | NO2 | Ratio (NO2 /NOX ) | NO | NO2 | Ratio (NO2 /NOX ) | NO | NO2 | Ratio (NO2/ NOX) | NO | NO2 | Ratio (NO2/ NOX) |
| Diesel W/ DPF and SCR | 1.62 | 0.36 | 18% | 7.92 | 1.12 | 12% | 5.09 | 0.80 | 14% | 1.31 | 0.16 | 11% |
| Diesel only DPF W/o SCR | 5.51 | 2.33 | 30% | 5.09 | 1.77 | 26% | 3.75 | 1.75 | 32% | 2.39 | 1.50 | 39% |
| 1.2 g NOx Diesel W/ DPF | 5.57 | 3.20 | 36% | 7.01 | 2.49 | 26% | 6.61 | 2.72 | 29% | 3.82 | 2.05 | 35% |
| HPDI W/ DPF and SCR | 0.40 | 0.35 | 47% | 0.69 | 0.19 | 21% | 0.32 | 0.33 | 51% | 0.21 | 0.26 | 55% |
| Stoichiometric Natural Gas | 0.43 | 0.01 | 2% | 0.44 | 0.00 | 0% | 0.32 | 0.01 | 3% | 0.17 | 0.00 | 0% |

Figure 46 shows the results of the $NO_2$/NOx ratio from diesel and natural gas vehicles operating in the goods movement application. The results from the diesel vehicles show that the diesel with SCR resulted in a $NO_2$/NOx ratio close to half that observed from diesel vehicles with DPF. This could be attributed to the fact that SCR aids in reduction of $NO_2$ generated by the oxidation catalyst through its selective catalyst reactions. Both the MY 2009 and MY 2011 diesel vehicles with only DPF report a

similar $NO_2$/NOx ratio in the exhaust. The dual-fuel HPDI vehicle with SCR reported the highest tailpipe $NO_2$/NOx ratio over all the driving cycles. Higher $NO_2$ emissions observed from these engines could be a result of incomplete SCR reactions leading to excessive $NO_2$ slip through the catalyst. Natural gas engines with TWC report less than 2% of total NOx to be $NO_2$. Stoichiometric fueling results in an oxygen lean exhaust, that is not conducive for catalytic $NO_2$ formation.

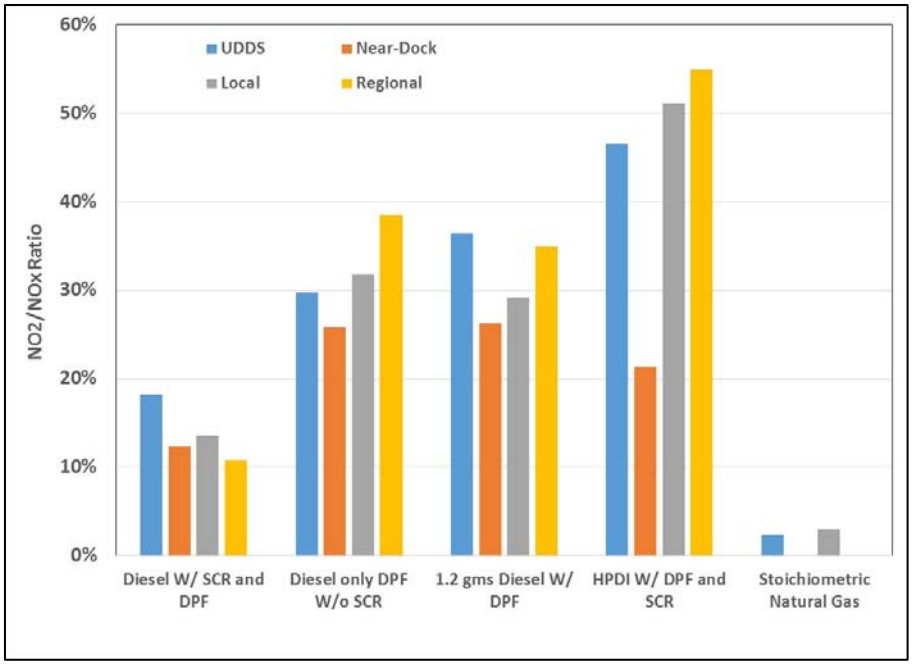


**Figure 46 $NO_2$/NOx ratio of diesel and natural gas goods movement vehicles**

Table 17 shows the distance-specific NO/$NO_2$ split and the $NO_2$/NOX ratio from diesel and natural gas refuse trucks. The results show that the refuse truck equipped with SCR emitted higher $NO_2$ during the refuse truck cycle compared to the UDDS.

**Table 17 NO/$NO_2$ split of heavy-duty vehicles in refuse truck application**

| | UDDS | | | AQMD Refuse Truck | | |
|---|---|---|---|---|---|---|
| | NO | NO2 | NO2/NOX Ratio | NO | NO2 | NO2/NOX Ratio |
| Diesel W/ SCR | 0.80 | 0.45 | 36% | 0.27 | 0.23 | 47% |
| Stoichiometric Natural Gas | 0.34 | 0.04 | 11% | 0.88 | 0.20 | 19% |

### 3.6 CROSS-LABORATORY CORRELATION

Five diesel vehicles were tested by both UCR and WVU for cross-laboratory comparison. Although six laboratories are required for a statistically significant comparison, the data obtained from this study still allow a comparison of values from two independent laboratories and create a measure of confidence in the accuracy of the data since the two laboratories would presumably not have the same bias in the data

sets. Three port vehicles and two refuse haulers were jointly tested and data for brake-specific $CO_2$ ($bsCO_2$), engine work, reference torque and emissions were compared between WVU and UCR to ensure the quality of the data. The three port vehicles represented emission levels between 1.2 g/bhp-hr and less than 0.2 g/bhp-hr NOx, while the refuse trucks representing USEPA 2010 emissions compliance with one certified at greater than 0.2 g/bhp-hr and another certified less than 0.2 g/bhp-hr.

This cross-laboratory correlation task serves as a quality check for the emissions data that were collected independently by each laboratory. This correlation attempts to compare the emissions testing procedures of both laboratories, including the chassis dynamometer loading of the test vehicle and the associated emissions measurement system. Although both WVU and UCR may adopt different procedures to conduct an emissions measurement campaign, the resulting data should be within an acceptable tolerance for real-world representativeness in each laboratory. Both UCR and WVU conducted the emissions measurement within immediate succession before returning test vehicles back into their regular revenue service. This procedure ensured the vehicle condition remained the same between WVU and UCR with no engine faults or maintenance conducted between the test intervals. Both laboratories tested the vehicle during day time conditions in Riverside CA (as WVU was located only 5 miles away from UCR with their mobile laboratory setup).

### *3.6.1 ENGINE WORK*

Engine work was calculated from ECU reported actual engine percent torque, nominal friction torque, engine speed and reference torque. Although the design of the two chassis dynamometers are vastly different, with, WVU absorbing power directly at the wheel and hub and UCR absorbing power using rollers, the work comparison averaged around 3% negative bias (-3%) where UCR's laboratory was slightly lower than WVU's with a spread of -9% to +4% on average. Both WVU and UCR show very low test to test variability with coefficient of variation (COV) less than 2% for all tests.

There were a few test vehicles with small absolute biases, but with relatively larger biases. Typically the work differences were around ±5% (5 hp), but for two port regional cycles the power difference was as high as 9 hp for the MY 2009 diesel port vehicle (vehicle#2) and 14 hp for MY 2011 diesel port vehicle (vehicle #3). Both UCR and WVU investigated their power numbers with chassis dyno wheel torque and other power metrics. The values presented are real and are not erroneous ECM signals. Interesting for both UCR and WVU most of the vehicles on the port cycles generated the same amount of work 107 bhp-hr. For UCR they were high by 13 bhp-hr for the vehicle #2 and WVU was low for the by 25 bhp-hr for the vehicle #3.

### *3.6.2 CARBON DIOXIDE*

The $bsCO_2$ is the most suitable metric for cross-laboratory comparison, since $CO_2$ is an accurate indicator of both fueling and work. Fueling of the engine is highly liner with engine work, and therefore a similar work between the two laboratories should result in a similar $bsCO_2$. This metric will provide the comparison of the emissions measurement system of the two laboratories. This comparison also normalizes chassis dynamometer setup differences to evaluate the ability to measure engine conditions. The $bsCO_2$ was very close and averaged around 5% positive bias where UCR's laboratory was slightly higher than WVU's with a spread of 0% to 10% overall. Both WVU and UCR show very low test to test variability with COV less than 3% for all tests.

### *3.6.3 OXIDES OF NITROGEN*

For SCR equipped diesel engines efficiency of NOx control is highly dependent on temperature; in fact, conversion of NOx increases exponentially with temperature. As a consequence, small temperature differences during a test will lead to different NOx emissions from one laboratory to another. The importance of temperature is evident in the test data in that the COV results for $CO_2$ can be approximately 1% and can be as high as 10% for NOx. Given this backdrop the observed differences between the two laboratories in the NOx levels for the SCR-equipped vehicles are reasonable.

The cold start NOx variability between UCR and WVU is expected due to different catalyst conditions for the testing. Differences at low emission levels for the SCR-equipped vehicles are not a significant difference, but represent an expected variability for aftertreatment systems and NOx emissions.

The Navistar engine in Vehicle #2 was 0.7 g/bhp-hr different in brake specific NOx emissions for UCR and WVU during the regional port cycle. Since both showed very good agreement for bsCO2 (0% difference) the higher NOx may be a result of higher sustained loads for the UCR test compared to the WVU test. The Navistar engine utilized an advanced NOx system to approach a 0.5 g/bhp-hr certification level. If UCR had a slightly higher load then Vehicle #2 results could be related to the DPF regeneration and $NO_2$ used in that process.

Test vehicle #4 (advanced EGR refuse vehicle) shows a significant difference in NOx emissions measured over the SCAQMDRTC cycle, and not the UDDS cycle. The two laboratories showed a NOx emission factor ranging from 0.25 g/bhp-hr to 0.29 g/bhp-hr for the UDDS cycle, but 0.28 g/bhp-hr to 1.56 g/bhp-hr for the SCAQMDRTC cycle. Figure 47 shows the accumulated NOx measured by UCR over the SCAQMDRTC cycle. NOx from 0 to 2000 seconds is reporting 0.29 g/bhp-hr (almost a perfect match with WVU), but after about 2000 seconds UCR measured NOx emission increases dramatically to

3.6 g/bhp-hr for the end of the curbside portion of the cycle and all of the compaction part of the cycle. WVU did not see the same high NOx during the compaction part of the cycle.

To further understand the NOx emissions from these higher EGR engines during partial regeneration and non-regeneration operation, WVU had instrumented the vehicle with pre DPF and post DPF tailpipe NOx sensors. These sensors are installed by WVU for internal sanity check of the measured data. Figure 48 and Figure 49 show the pre and post DPF NOx concentrations during a test in which no DPF regeneration was detected and during a test in which a partial regeneration was detected. It can be observed that the DPF in these vehicles are contributing to a significant reduction in NOx concentrations during vehicle operation. This can be attributed to the continuous passive regeneration of the catalyzed DPF to utilize $NO_2$ to light-off soot accumulation. On an average the DPF contributes to 68% reduction in engine-out NOx during normal vehicle operation. However, in some instances when passive soot light-off is insufficient, the engine strategy employs one or more different approaches to improve soot light off. The approaches included an in-cylinder increase in NOx concentration together with exhaust fuel injection. Figure 49 shows a partial active regeneration event during which a significant increase in NOx emissions is observed followed by a return to normal vehicle operation towards the end of the test.

UCR data for the refuse truck cycle could be characterized by such an event, which is beyond the control of the test laboratory and hence could have resulted in a significant difference in brake-specific NOx emissions.

Test vehicle #5 (SCR equipped refuse vehicle) showed a difference in NOx between 0.18 g/bhp-hr and 0.25 g/bhp-h on the UDDS cycle. This difference is small considering the test to test variably was high. The high variability is again related to stability of the SCR.

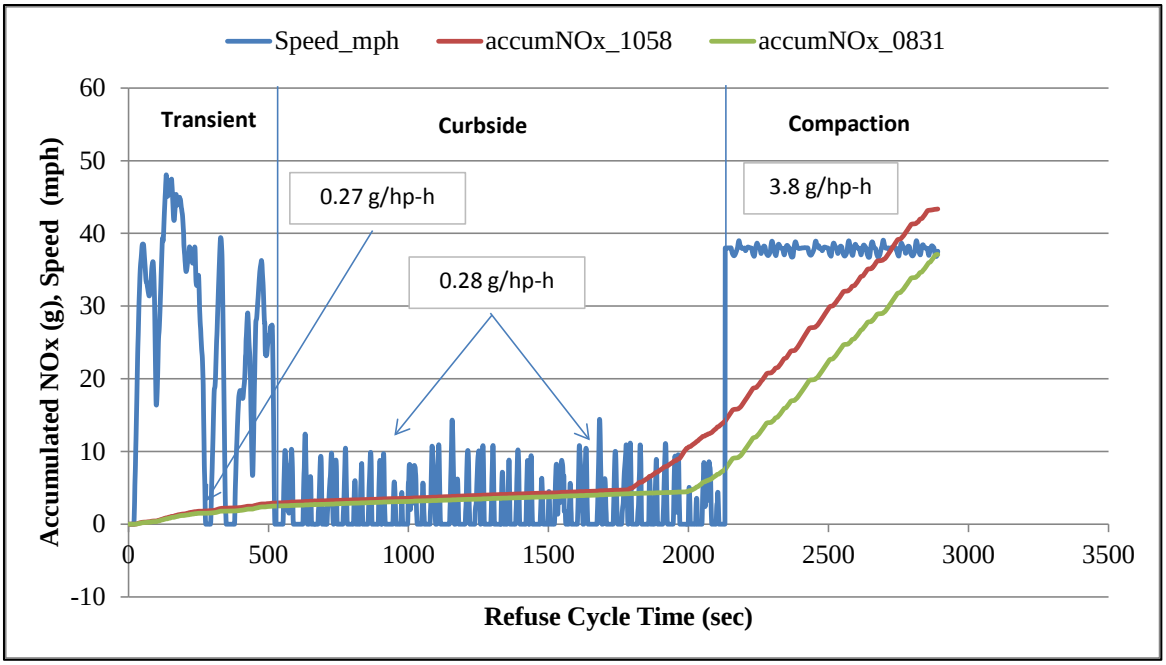


**Figure 47 Refuse hauler shared vehicle #4 (Navistar A260 2011)**

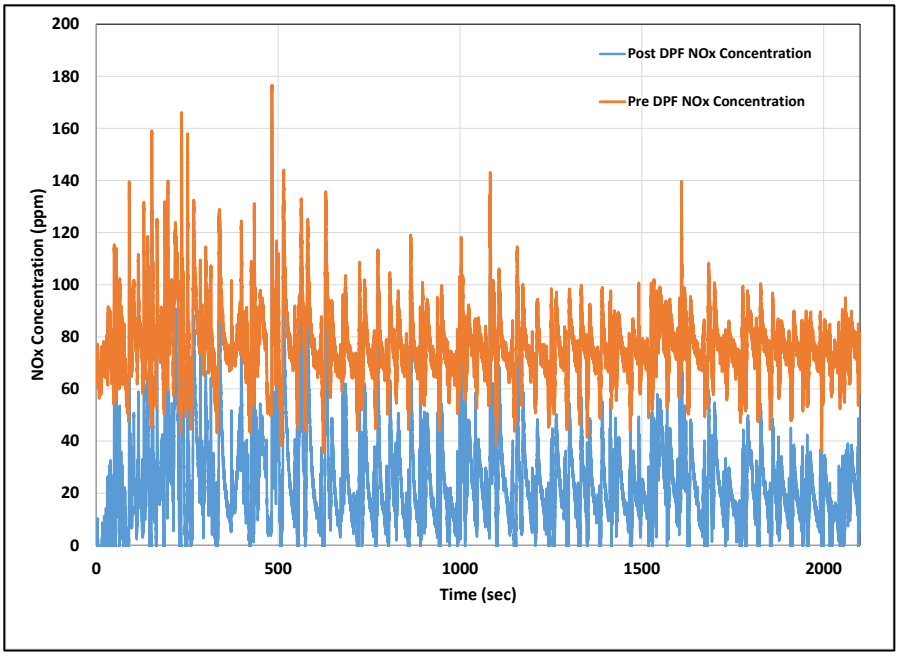


**Figure 48 Pre and Post DPF NOx concentration for a non-regeneration vehicle operation**

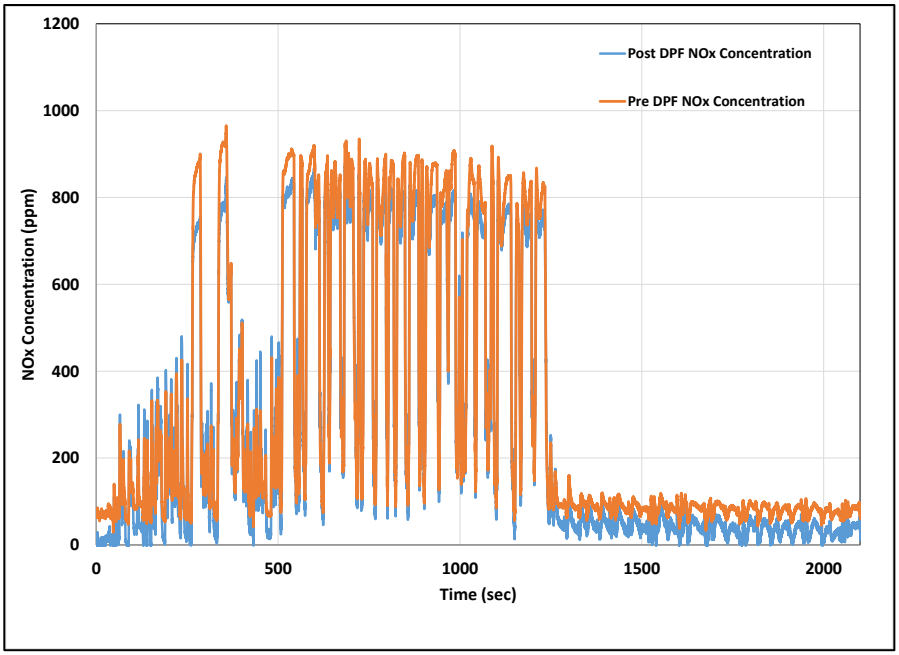


**Figure 49 Pre and Post DPF NOx during partial active regeneration during refuse truck cycle**

### *3.6.4 PARTICULATE MATTER*

The bsPM emission levels were low for both UCR and WVU and were below the PM certification value for all tests and typically around 10% of the standard (< 1 mg/bhp-h) as expected for a properly functioning DPF. The PM emissions were similar between both laboratories and no significant outliers were identified.

### *3.6.5 AMMONIA*

The bsNH3 emissions were very low where there was no statistical difference between the different vehicles. As suggested for UCR, see Section 8.6, most of the NH3 measurements were at or just above the lower detection limits of UCR's NH3 measurement method. WVU also suggested several of the vehicles showed no quantifiably NH3 emissions. The NH3 emissions were similar between both laboratories and no significant outliers were identified.

### *3.6.6 RESULTS SUMMARY*

Tables 18-22 show the UCR and WVU engine work and selected emissions for five different shared vehicles including the cycle to cycle averaged coefficient of variation (COV). The emissions comparison is on a brake specific basis and includes bsCO2, bsNOx, bsPM, and bsNH3 in g/bhp-hr. Although chassis dynamometer data is traditionally reported as distance-specific, for laboratory comparison purposes, changes in vehicle loading procedure and dynamometer setup can result in differences in distance-specific

emissions. Therefore, brake-specific emissions were chosen as metric for comparison as components such as CO2 are linear with work done by the engine.

### *3.6.7 PORT VEHICLE #1 (MACK MP8445C 2011)*

**Table 18 Port vehicle #1 comparative bsCO2, Engine Work & Emissions (g/bhp-h)**

| Results | Cycle | Engine Work bhp-h | Average Emissions g/bhp-h $CO_2$ | NOx | PM | $NH_3$ | COV Emissions [1,2] Work hp-hr | g/bhp-h $CO_2$ | NOx | PM | $NH_3$ |
|---|---|---|---|---|---|---|---|---|---|---|---|
| UCR | CS_UDDS | 29.0 | 555 | 0.40 | 0.0007 | 0.002 | | | | | |
| UCR | UDDS | 25.8 | 525 | 0.27 | 0.0003 | 0.003 | 1.2% | 0.9% | 14.9% | 0.9% | 1.1% |
| UCR | Near Dock | 26.5 | 561 | 1.80 | 0.0004 | 0.001 | 1.3% | 1.1% | 2.7% | 2.0% | 1.5% |
| UCR | Local | 40.1 | 556 | 1.10 | 0.0004 | 0.001 | 0.4% | 1.8% | 1.4% | 0.9% | 2.6% |
| UCR | Regional | 107.2 | 513 | 0.36 | 0.0011 | 0.005 | 0.9% | 0.7% | 27.6% | 4.3% | 1.0% |
| WVU | CS_UDDS | 29.0 | 506 | 0.51 | 0.0010 | 0.036 | | | | | |
| WVU | UDDS | 26.5 | 493 | 0.40 | 0.0020 | <0.003 | 1.4% | 0.6% | 8.9% | 1.8% | - |
| WVU | Near Dock | 28.3 | 544 | 1.79 | 0.0011 | <0.003 | 0.3% | 0.8% | 5.6% | 0.6% | - |
| WVU | Local | 40.8 | 532 | 1.26 | 0.0021 | <0.003 | 0.6% | 0.7% | 4.5% | 0.9% | - |
| WVU | Regional | 98.4 | 520 | 0.36 | 0.0006 | <0.003 | 0.4% | 0.4% | 7.4% | 0.4% | - |

[1] The COV is the coefficient of variation defined as one standard deviation divided by the averaged measured value. For PM and $NH_3$ the measurements were small and thus the COV was calculated as Stdev/10mg/bhp-h for PM was used and Stdev/60mg/bhp-h for $NH_3$.PM = 10 mg/bhp-h was used based on the 10 mg/bhp-h certification standard and 60 mg/bhp-h is used based on an average of 10 ppm flow weighted limit for the raw exhaust.

[2] Blank values represent only one value or no data available. For example there were only single cold start tests and thus no COV was calculated. The dashes for $NH_3$ indicate no COV was practical.

### *3.6.8 PORT VEHICLE #2 (NAVISTAR MAXX-FORCE13 2009)*

**Table 19 Port vehicle #2 comparative bsCO2, Engine Work & Emissions (g/bhp-h)**

| Results | Cycle | Engine Work bhp-h | Average Emissions g/bhp-h $CO_2$ | NOx | PM | $NH_3$ | COV Emissions [1,2] Work hp-hr | g/bhp-h $CO_2$ | NOx | PM | $NH_3$ |
|---|---|---|---|---|---|---|---|---|---|---|---|
| UCR | CS_UDDS | 29.5 | 584 | 1.69 | 0.0005 | 0.005 | | | | | |
| UCR | UDDS | 29.4 | 557 | 1.56 | 0.0002 | 0.003 | 2.8% | 1.1% | 0.4% | 0.3% | 4.6% |
| UCR | Near Dock | 23.5 | 760 | 2.16 | 0.0002 | 0.004 | 1.8% | 1.4% | 3.4% | 1.3% | 4.0% |
| UCR | Local | 41.0 | 657 | 2.00 | 0.0004 | 0.005 | 1.0% | 2.9% | 2.3% | 3.5% | 10.3% |
| UCR | Regional | 120.8 | 531 | 2.23 | 0.0001 | 0.006 | 0.6% | 0.8% | 2.0% | 1.1% | 3.1% |
| WVU | CS_UDDS | 31.8 | 591 | 1.58 | - | <0.003 | | | | | |
| WVU | UDDS | 28.8 | 591 | 1.42 | 0.0124 | <0.003 | 1.3% | 2.4% | 5.4% | 6.7% | - |
| WVU | Near Dock | 27.9 | 617 | 1.84 | 0.0016 | <0.003 | 0.3% | 2.3% | 1.6% | 0.3% | - |
| WVU | Local | 43.7 | 589 | 1.84 | 0.0008 | <0.003 | 1.2% | 0.9% | 1.4% | 0.1% | - |
| WVU | Regional | 106.7 | 528 | 1.50 | 0.0008 | <0.003 | 2.0% | 1.9% | 1.7% | 0.1% | |

[1] The COV is the coefficient of variation defined as one standard deviation divided by the averaged measured value. For PM and $NH_3$ the measurements were small and thus the COV was calculated as Stdev/10mg/bhp-h for PM was used and Stdev/60mg/bhp-h for $NH_3$.PM = 10 mg/bhp-h was used based on the 10 mg/bhp-h certification standard and 60 mg/bhp-h is used based on an average of 10 ppm flow weighted limit for the raw exhaust.

2 Blank values represent only one value or no data available. For example there were only single cold start tests and thus no COV was calculated. The dashes for NH3 indicate no COV was practical.

### *3.6.9 PORT VEHICLE #3 (NAVISTAR MAXX-FORCE12 2011)*

**Table 20 Port vehicle #3 comparative bsCO2, Engine Work & Emissions (g/bhp-h)**

| Results | Cycle | Engine Work bhp-h | Average Emissions g/bhp-h $CO_2$ | NOx | PM | $NH_3$ | COV Emissions [1,2] Work hp-hr | g/bhp-h $CO_2$ | NOx | PM | $NH_3$ |
|---|---|---|---|---|---|---|---|---|---|---|---|
| UCR | CS_UDDS | 25.6 | 564 | 1.49 | 0.0002 | 0.009 | | | | | |
| UCR | UDDS | 26.4 | 516 | 1.15 | 0.0001 | 0.004 | 1.4% | 0.9% | 5.8% | 0.7% | 2.5% |
| UCR | Near Dock | 19.1 | 749 | 1.85 | 0.0004 | 0.012 | 1.2% | 1.8% | 2.2% | 0.2% | 3.6% |
| UCR | Local | 33.2 | 636 | 1.59 | 0.0000 | 0.006 | 0.5% | 1.8% | 7.0% | 0.3% | 4.6% |
| UCR | Regional | 107.1 | 506 | 1.04 | 0.0002 | 0.009 | 0.9% | 0.3% | 3.7% | 0.5% | 1.3% |
| WVU | CS_UDDS | 23.5 | 565 | 1.83 | 0.0012 | <0.003 | | | | | |
| WVU | UDDS | 23.6 | 487 | 1.27 | 0.0009 | <0.003 | 2.1% | 1.8% | 2.0% | 0.2% | - |
| WVU | Near Dock | - | - | - | - | - | - | - | - | | - |
| WVU | Local | 34.6 | 500 | 1.38 | 0.0020 | <0.003 | 2.0% | 0.5% | 0.9% | 0.2% | - |
| WVU | Regional | 82.3 | 498 | 1.28 | 0.0019 | <0.003 | 0.6% | 0.8% | 2.6% | 0.5% | - |

[1] The COV is the coefficient of variation defined as one standard deviation divided by the averaged measured value. For PM and $NH_3$ the measurements were small and thus the COV was calculated as Stdev/10mg/bhp-h for PM was used and Stdev/60mg/bhp-h for $NH_3$.PM = 10 mg/bhp-h was used based on the 10 mg/bhp-h certification standard and 60 mg/bhp-h is used based on an average of 10 ppm flow weighted limit for the raw exhaust.

[2] Blank values represent only one value or no data available. For example there were only single cold start tests and thus no COV was calculated. The dashes for $NH_3$ indicate no COV was practical.

### *3.6.10 REFUSE VEHICLE #4 (NAVISTAR A260 2011)*

**Table 21 Refuse vehicle #4 comparative bsCO2, Engine Work & Emissions (g/bhp-h)**

| Results | Cycle | Engine Work bhp-h | Average Emissions g/bhp-h $CO_2$ | NOx | PM | $NH_3$ | COV Emissions [1,2] Work hp-hr | g/bhp-h $CO_2$ | NOx | PM | $NH_3$ |
|---|---|---|---|---|---|---|---|---|---|---|---|
| UCR | CS_UDDS | 17.5 | 608 | 0.36 | 0.0008 | 0.004 | | | | | |
| UCR | UDDS | 17.4 | 612 | 0.25 | 0.0004 | 0.007 | 2.7% | 1.0% | 1.7% | 1.5% | 4.0% |
| UCR | RTC | 26.9 | 816 | 1.56 | 0.0003 | 0.004 | 1.8% | 1.3% | 6.9% | 2.4% | 6.1% |
| WVU | CS_UDDS | 18.6 | 663 | 2.09 | - | <0.003 | | | | | |
| WVU | UDDS | 18.5 | 569 | 0.29 | 0.0026 | <0.003 | 0.9% | 0.0% | 2.7% | 0.7% | - |
| WVU | RTC | 37.4 | 556 | 0.28 | 0.0020 | <0.003 | 0.9% | 1.3% | 0.5% | 0.1% | - |

[1] The COV is the coefficient of variation defined as one standard deviation divided by the averaged measured value. For PM and $NH_3$ the measurements were small and thus the COV was calculated as Stdev/10mg/bhp-h for PM was used and Stdev/60mg/bhp-h for $NH_3$.PM = 10 mg/bhp-h was used based on the 10 mg/bhp-h certification standard and 60 mg/bhp-h is used based on an average of 10 ppm flow weighted limit for the raw exhaust.

[2] Blank values represent only one value or no data available. For example there were only single cold start tests and thus no COV was calculated. The dashes for $NH_3$ indicate no COV was practical.

### *3.6.11 REFUSE VEHICLE #5 (CUMMINS ISC 8.3 2012)*

**Table 22 Refuse vehicle #5 comparative bsCO2, Engine Work & Emissions (g/bhp-h)**

| Results | Cycle | Engine Work bhp-h | Average Emissions g/bhp-h $CO_2$ | NOx | PM | $NH_3$ | COV Emissions [1,2] Work hp-hr | g/bhp-h $CO_2$ | NOx | PM | $NH_3$ |
|---|---|---|---|---|---|---|---|---|---|---|---|
| UCR | CS-UDDs | 29.1 | 584 | 0.36 | 0.0035 | 0.023 | | | | | |
| UCR | UDDS | 26.6 | 607 | 0.18 | 0.0006 | 0.010 | 2.1% | 1.5% | 4.3% | 1.0% | 4.7% |
| UCR | RTC | 43.6 | 612 | 0.32 | 0.0003 | 0.012 | 0.6% | 0.4% | 16.6% | 0.6% | 2.9% |
| WVU | CS_UDDS | - | - | - | - | - | | | | | |
| WVU | UDDS | 26.7 | 672 | 0.25 | 0.0020 | <0.003 | 1.3% | 1.4% | 9.4% | 1.9% | - |
| WVU | RTC | 50.4 | 654 | 0.11 | 0.0013 | <0.003 | 1.8% | 1.0% | 39.0% | 4.9% | - |

[1] The COV is the coefficient of variation defined as one standard deviation divided by the averaged measured value. For PM and $NH_3$ the measurements were small and thus the COV was calculated as Stdev/10mg/bhp-h for PM was used and Stdev/60mg/bhp-h for $NH_3$.PM = 10 mg/bhp-h was used based on the 10 mg/bhp-h certification standard and 60 mg/bhp-h is used based on an average of 10 ppm flow weighted limit for the raw exhaust.

[2] Blank values represent only one value or no data available. For example there were only single cold start tests and thus no COV was calculated. The dashes for $NH_3$ indicate no COV was practical. WVU did not have a cold start test on this vehicle due to vehicle availability.

## 3.7 AMMONIA AND NITROUS OXIDE EMISSIONS

### *3.7.1 STOICHIOMETRIC NATURAL GAS VEHICLES*

Ammonia and nitrous oxide emissions were quantified real-time using the MKS HS 2030 high speed FTIR. The source of ammonia emissions from the stoichiometric natural gas engines can be attributed to the activity of the TWC in reducing NOx emissions. As one of the secondary pathways during the overall NOx reduction reaction using the CO molecules, the presence of high exhaust temperature and water vapor could initiate the formation of water gas shift-reactions that can result in the formation of ammonia in the exhaust (Defoort et al., 2003). For highly efficient NOx reductions, a TWC must operate at stoichiometric or slightly rich of stoichiometric. Hence, the engine controls of a stoichiometric engine frequently dithers the air-fuel ratio between lean and rich of stoichiometric ratio to effectively reduce NOx, CO, and hydrocarbons. As a result the production of ammonia is also a function of this dithering operation of the air-fuel ratio.

Ammonia emissions from SCR-equipped heavy-duty diesel engines can be attributed to ammonia slip through the SCR catalyst during aqueous urea dosing in the tailpipe.

$N_2O$ emissions from a TWC-equipped natural gas vehicle primarily occur during the warm-up phase of the after-treatment system. The formation of $N_2O$ can be attributed to the low temperature NOx reduction reaction involving NO and CO which react on the catalytic surface to produce $N_2O$ (Odaka et al., 1998).

Figure 50 shows the distance-specific ammonia emissions from the natural gas fueled refuse truck. The average distance-specific ammonia emissions measured over the UDDS, SCAQMD-RTC, and SCAQMD-RCC cycles were 1.17 g/mi, 1.09 g/mi, and 2.80 g/mi, respectively. $N_2O$ emissions measured over all driving cycles were close to detection limits. However the cold start UDDS cycle resulted in 0.144 g/mi of $N_2O$ emission.

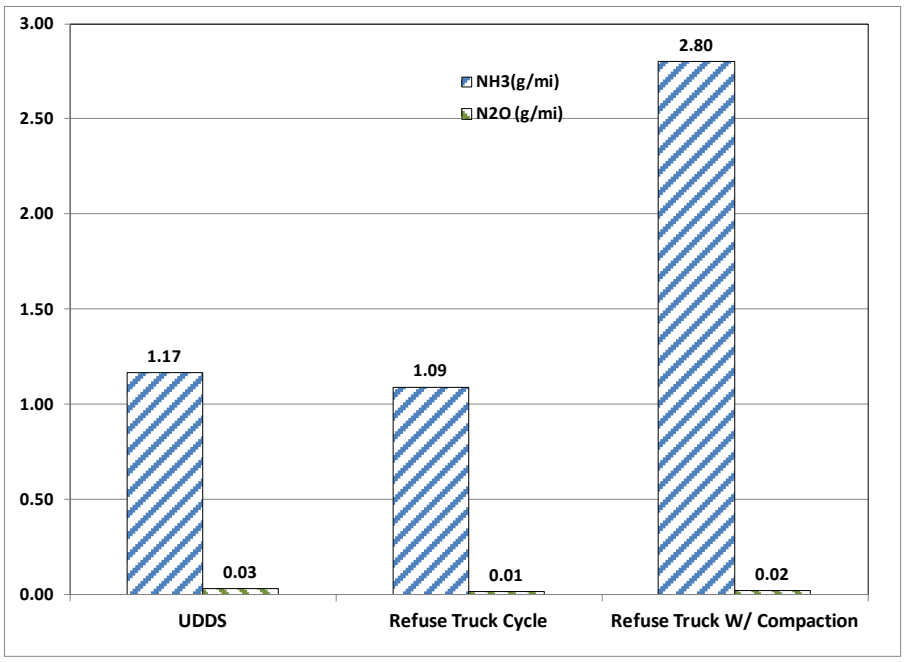


**Figure 50 Distance-specific ammonia and nitrous oxide emissions from natural gas refuse truck**

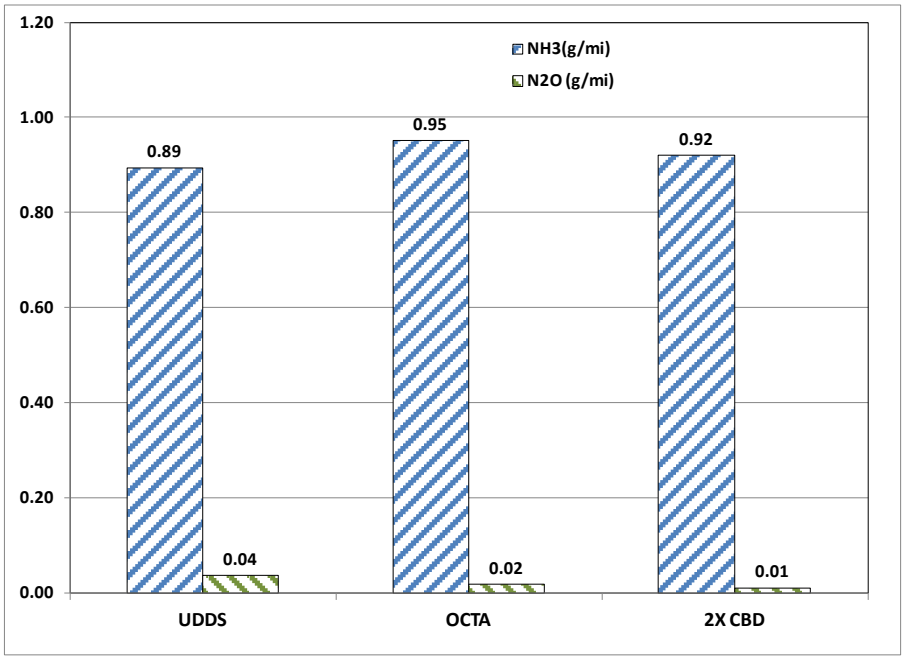


**Figure 51 Distance-specific ammonia and nitrous oxide emissions from natural gas transit bus**

Figure 51 shows the distance-specific ammonia and $N_2O$ emissions from the natural gas fueled transit bus measured over the UDDS, OCTA, and 2XCBD driving cycles. The ammonia emissions measured over UDDS, OCTA 2XCBD cycle were 0.89 g/mi, 0.95 g/mi, and 0.92 g/mi, respectively. The $N_2O$ emissions measured over all driving cycles were close to the detection limits of the instrument. However the cold start UDDS cycle of the transit bus resulted in $N_2O$ emissions of 0.29 g/mi. Similar to

refuse truck, the $N_2O$ emissions over the cold start operation is an order of magnitude higher than during hot start operations.

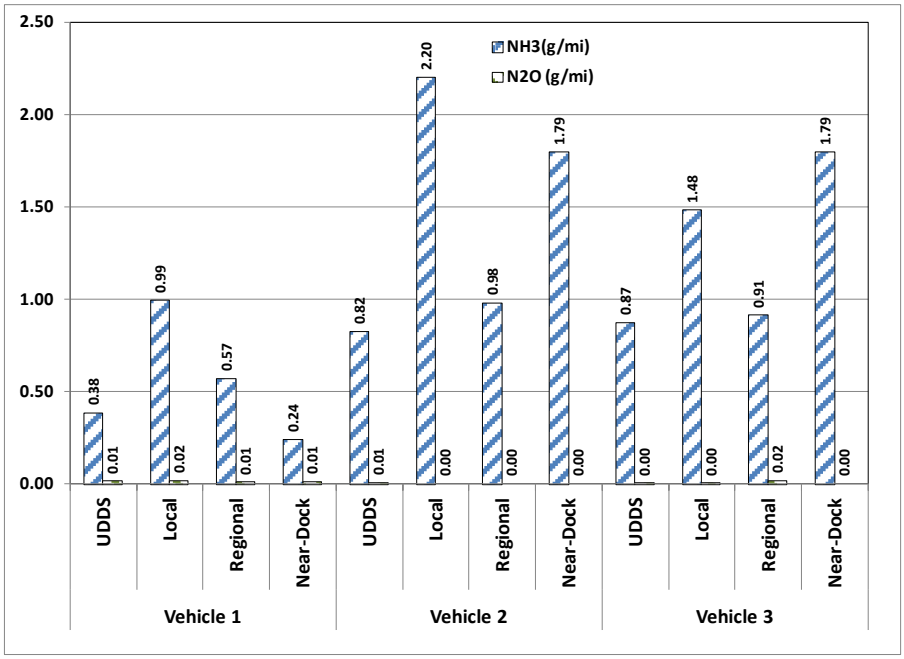


**Figure 52 Distance-specific ammonia and nitrous oxide emissions from natural gas goods movement vehicles**

Figure 52 shows the distance-specific ammonia and $N_2O$ emissions of the natural gas goods movement vehicles measured over the UDDS and port drayage cycles. The average distance-specific ammonia and $N_2O$ emissions measured over the UDDS cycle were 0.69 g/mi and 0.01 g/mi, respectively between the three vehicles. Vehicle 1 was the newest of the three vehicles with less than 200 miles and produced the lowest distance-specific ammonia emissions. This could possibly be related to a better air-fuel ratio control and the effect of a relatively new TWC. Both Vehicle 2 and Vehicle 3 with odometer mileage of 45,563 miles and 65,700 miles respectively emitted 0.82 gm/mi and 0.87 g/mi of ammonia, respectively. A similar emissions profile is also observed for the drayage port cycles, with Vehicle 1 emitting lower distance-specific ammonia emissions than Vehicle 2 and Vehicle 3.

The ammonia emissions from the natural gas vehicles can also be influenced by the feedback provided by the exhaust oxygen sensors. Stoichiometric engines employ exhaust oxygen sensors to achieve closed loop fueling and monitor stoichiometric operation. However, high exhaust temperatures and exhaust water content can age the oxygen sensor, thereby affecting the frequency of the feedback signal. Although this aging of the oxygen sensor is not detrimental to the engine operation, it can result in slight deviations to the air-fuel ratio that can adversely affect ammonia emissions.

### *3.7.2 DUAL-FUEL VEHICLES*

Figure 53 shows the distance-specific ammonia emissions from the MY 2011 dual-fuel HPDI and the MY 2008 dual-fuel HPDI vehicles. The MY 2011 dual-fuel vehicles were equipped with a DPF and SCR system, while the MY 2008 vehicles were equipped only with a DPF. Ammonia slip was detected from the SCR after-treatment system during the local, regional, and near-dock cycles. Ammonia slip from the SCR after-treatment system was detected during its warm-up phase, while stored ammonia on the substrate was being desorbed. The local, regional, and near-dock resulted in distance-specific ammonia emission of 0.20 g/mi, 0.13g/mi, and 0.24 g/mi respectively.

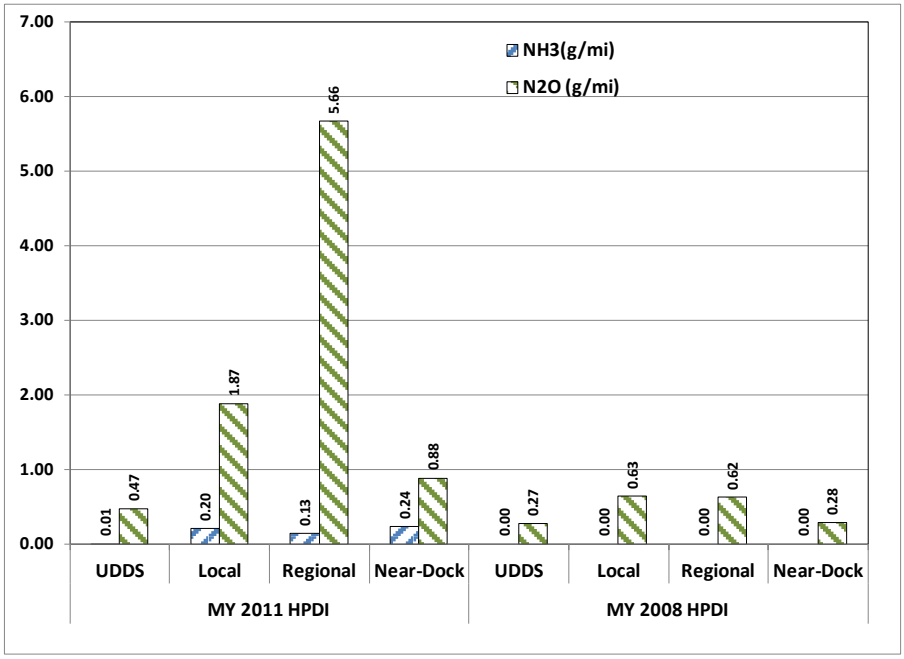


**Figure 53 Distance-specific ammonia and nitrous oxide emissions from dual-fuel HPDI goods movement vehicles**

$N_2O$ emissions from the MY 2011 dual-fuel HPDI vehicle were significantly higher than the MY 2008 vehicles. A study by Cummins has shown that the catalyzed DPF and oxidation of ammonia at high temperatures over the SCR substrate could contribute to significant concentrations of tailpipe $N_2O$ emissions (Kamasundaram et al.). The study also shows that vanadium and copper zeolite based substrates are more favorable for $N_2O$ formation. Similarly the source of $N_2O$ emissions from the MY 2011 dual-fuel HPDI could be attributed to oxidation of excess ammonia over the SCR catalyst.

### *3.7.3 DIESEL VEHICLES*

Figure 54 shows the distance-specific ammonia and $N_2O$ emissions from the MY 2009 and MY 2011 diesel vehicles with and without SCR. Ammonia emissions from SCR equipped diesel vehicles were

observed to be close to detection limits of the instrument. Ammonia emission was detected only during the regional operation of the SCR equipped diesel vehicle. $N_2O$ emissions from all model year vehicles were observed to be of the same order of magnitude. Studies have previously reported the possible contribution of catalyzed DPF and SCR towards $N_2O$ emissions. However, no significant $N_2O$ emissions were detected from any of the diesel technology vehicles.

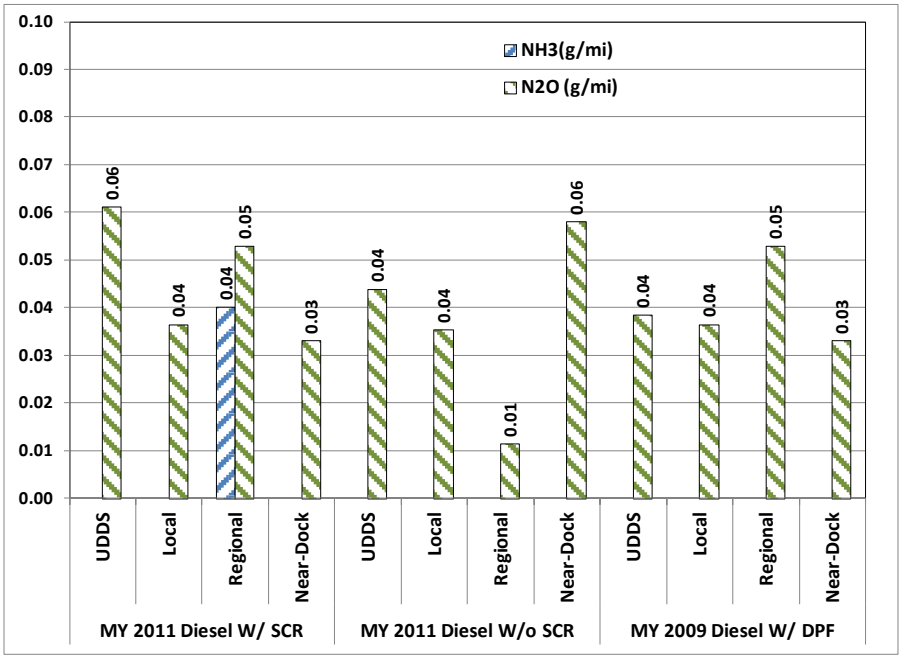


**Figure 54 Distance-specific ammonia and nitrous oxide emissions from diesel goods movement vehicles**

## 3.8 UNREGULATED EMISSIONS

### *3.8.1 BTEX EMISSIONS*

BTEX emissions were quantified through gas chromatography analysis of diluted exhaust samples collected in steel canisters. The results detail the distance-specific emissions of BTEX compounds from the different technology vehicles. Emissions results in this section are presented as uncorrected for background concentrations with tunnel background plotted separately for the different driving cycles. This method of presentation avoids the reporting of negative mass rates for certain test conditions that resulted in background concentrations higher than vehicle tailpipe concentrations.

Table 23 shows the dilution factor ratio for the different driving cycles and engine technologies. Dilution factor is defined as the ratio of average volume of dilution air to the average volume of CVS flow. The dilution factors can be used to interpret the tunnel background concentrations presented in Figures 55 through 71. The product of dilution factor and background concentration will result in the contribution of background concentration on individual pollutants to the total mass measured in the CVS sample stream.

**Table 23 List of dilution factors for different driving cycles and engine technologies**

| | | Dilution Factor = Vdil/Vmix |
|---|---|---|
| Diesel | NearDock | 0.98 |
| | Regional | 0.96 |
| | Local | 0.97 |
| | UDDS | 0.94 |
| | Refuse Truck | 0.95 |
| | Compaction | 0.94 |
| Natural Gas | NearDock | 0.98 |
| | Regional | 0.95 |
| | Local | 0.97 |
| | UDDS | 0.95 |
| | Refuse Truck | 0.96 |
| | Compaction | 0.95 |
| | OCTA | 0.96 |
| | 2xCBD | 0.96 |
| Dual-Fuel | NearDock | 0.98 |
| | Regional | 0.97 |
| | Local | 0.98 |
| | UDDS | 0.96 |

#### *3.8.1.1 STOICHIOMETRIC NATURAL GAS VEHICLES*

Dilute exhaust concentrations of BTEX compounds from both natural gas transit bus and refuse truck were observed to below the instrumentation detection limit of 10 ppbv. Hence, the results of the distance-specific emissions from the transit bus and refuse truck are not reported in this section.

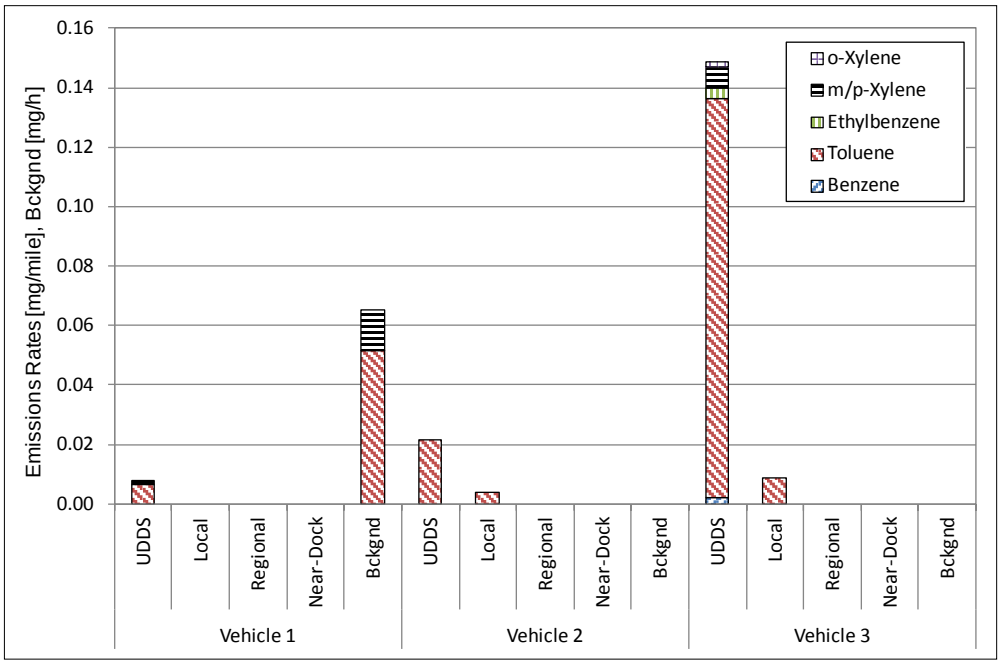


**Figure 55 Distance-specific BTEX emissions results from three natural gas fueled goods movement vehicles**

Figure 55 shows the distance-specific BTEX emissions from natural gas goods movement vehicles measured over the UDDS and the drayage driving cycles. Toluene was observed to be the only compound observed at relatively higher magnitude in comparison to other BTEX species. The highest toluene emissions were measured over the UDDS cycle from all vehicles. Vehicle 3 reported the highest toluene emissions of 0.13 mg/mi. BTEX emissions from internal combustion engines can be attributed to incomplete combustion of fuel or lubrication oil. Also, almost all oxidation catalyst has superior activity in oxidizing higher chain hydrocarbons even at low exhaust temperatures. The high exhaust temperature of stoichiometric natural gas engines provides a suitable condition for superior catalytic activity in controlling the emissions of BTEX compounds.

#### *3.8.1.2 DIESEL VEHICLES*

BTEX emissions from diesel refuse trucks with SCR were below the instrument detection limits and therefore has not been shown in the chart below. Figure 56 shows the distance-specific BTEX emissions from diesel refuse truck without SCR after-treatment system. The results show that benzene and isomers of xylene were observed at levels higher than those observed in background during vehicle operation over the refuse truck cycles. However, emissions of these compounds were not detected during the UDDS cycle. The frequent stop-and-go characteristic of the refuse truck cycle resulted in higher soot loading of the DPF and consequently contributed to frequent DPF regeneration activities. Although the study attempted to isolate tests with DPF regeneration, the vehicle could have initiated regeneration during part

of the driving cycle during which unregulated sampling was performed. Therefore the additional fueling in the exhaust to provide the energy for DPF regeneration could be attributed to the higher benzene and xylene emissions that are observed.

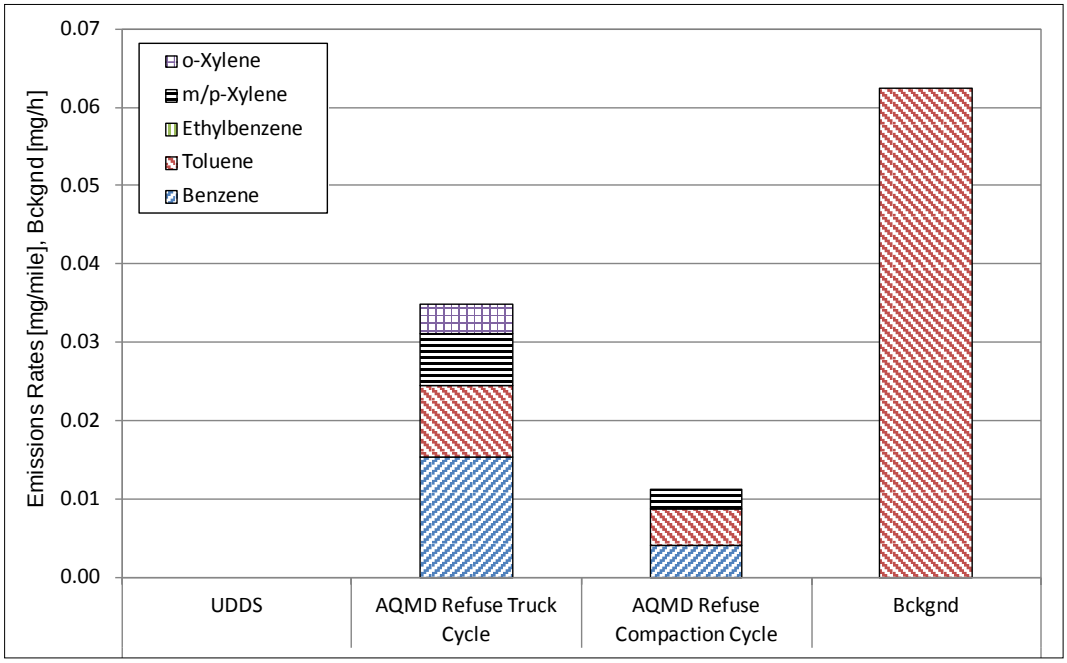


**Figure 56 Distance-specific BTEX emissions from diesel refuse truck without SCR**

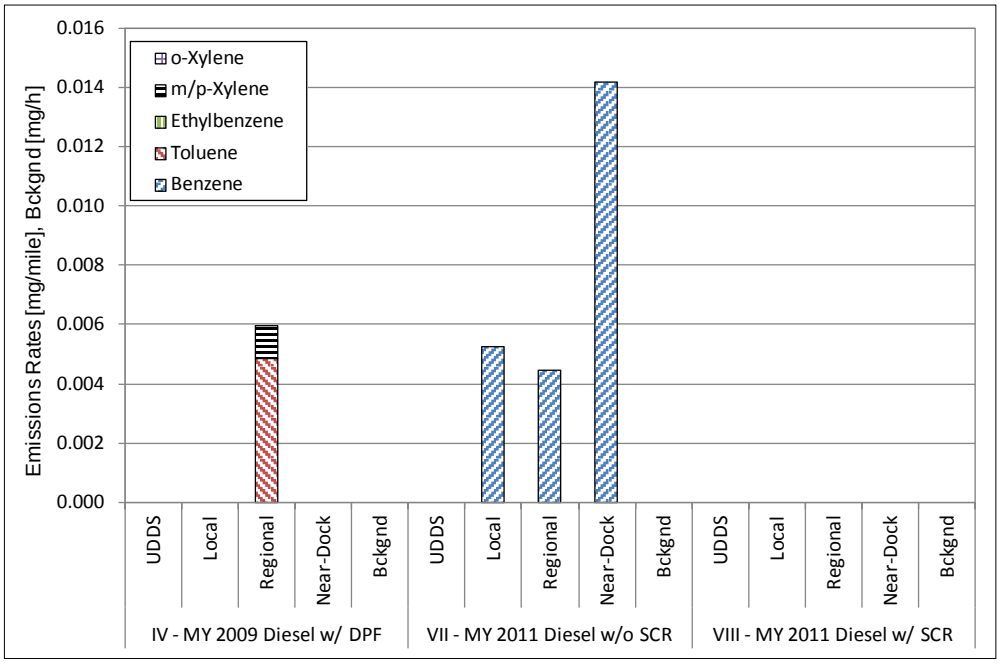


**Figure 57 Distance-specific BTEX emissions from diesel goods movement application**

Figure 57 shows the distance-specific BTEX emissions from diesel fueled vehicles operating in the goods movement vocation. BTEX emissions from diesel vehicle equipped with SCR were below

detection limits. However, emissions of benzene were observed during all the drayage driving cycle for the MY 2011 diesel vehicle without SCR. Similar to the refuse truck, these engines did result in frequent active regeneration events during which diesel fuel is admitted in to the exhaust to provide energy for soot combustion over the DPF. This method of soot regeneration can be attributed to incomplete combustion of diesel fuel and therefore higher benzene emissions.

#### *3.8.1.3 HPDI VEHICLES*

Figure 58 shows the distance-specific BTEX emissions from MY 2009 and MY 2011 dual-fuel HPDI goods movement vehicles. The results show benzene to be the major compound with levels higher than background air. Diesel fuel is the secondary fuel in the dual-fuel engines, serving the primary purpose of igniting the natural gas fuel. Therefore the quantity of diesel fuel injected is significantly less when compared to the natural gas fuel. However, lower load operation with high EGR fraction could lead to incomplete combustion of diesel fuel that could be attributed to the benzene emissions observed from these vehicles. Typically diesel oxidation catalysts are very efficient in controlling higher chain hydrocarbons at low exhaust temperatures, however the dual-fuel operation does result in lower combustion temperatures compared to traditional diesel combustion and could contribute to lower catalytic activity at lower load conditions such as idle and creep mode operation.

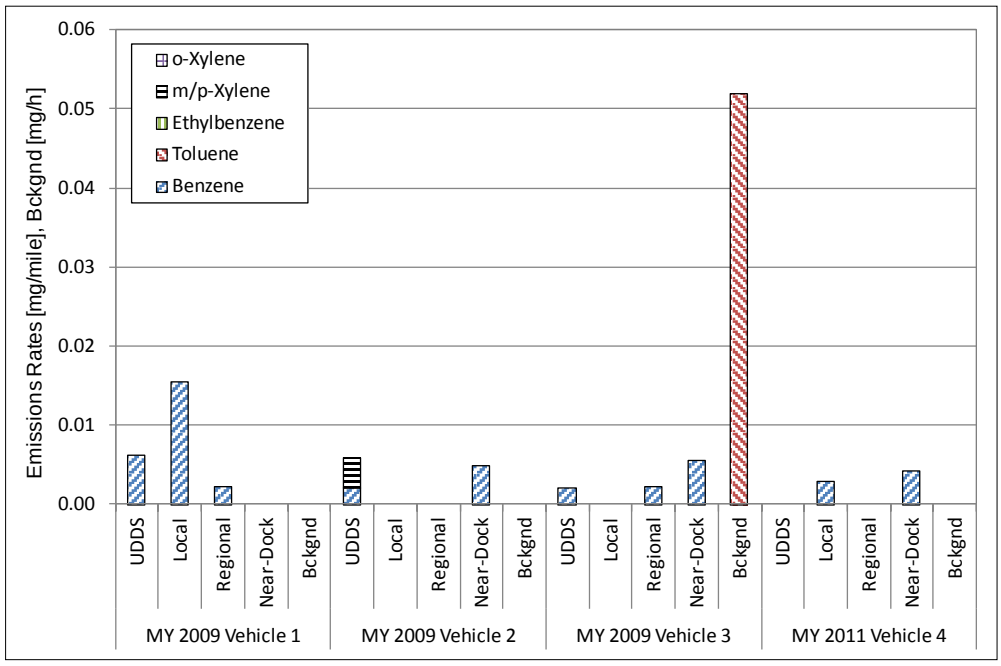


**Figure 58 Distance-specific BTEX emissions results from three MY 2009 and one MY 2011 dual-fuel HPDI goods movement vehicles**

### *3.8.2 CARBONYL EMISSIONS*

Carbonyl species are characteristic of natural gas engine exhaust. Carbonyl emissions can be attributed to the incomplete combustion of methane in a spark ignited internal combustion engine. Historically, uncontrolled lean burn natural gas engines were a significant contributor to carbonyl emissions. However, the advent of oxidation catalysts and advanced natural gas engine technology have contributed to orders of magnitude reduction in tailpipe carbonyl emissions (Thiruvengadam et al., 2011b, Okamoto et al., 2006, Yoon et al., 2014).

#### *3.8.2.1 STOICHIOMETRIC NATURAL GAS VEHICLES*

Figure 59 shows the distance-specific carbonyl emissions from the natural gas transit bus. The results show tailpipe emissions of most carbonyl species over all driving cycles to be lower than levels found in background ambient air. A recent study published by the CARB shows similar carbonyl emissions below instrument detection limits from exhaust of a heavy-duty natural gas transit bus (Yoon et al., 2014). Oxidation catalysts are highly effective in controlling tailpipe carbonyl emissions even at lower exhaust temperatures than observed in stoichiometric engines (Yoon et al., 2014). The stoichiometric platform of current technology natural gas engines provide conditions for superior after-treatment catalytic activity even at lower engine loads and idle conditions. As a result the tailpipe emission rates of all carbonyl species are below levels found in background ambient air.

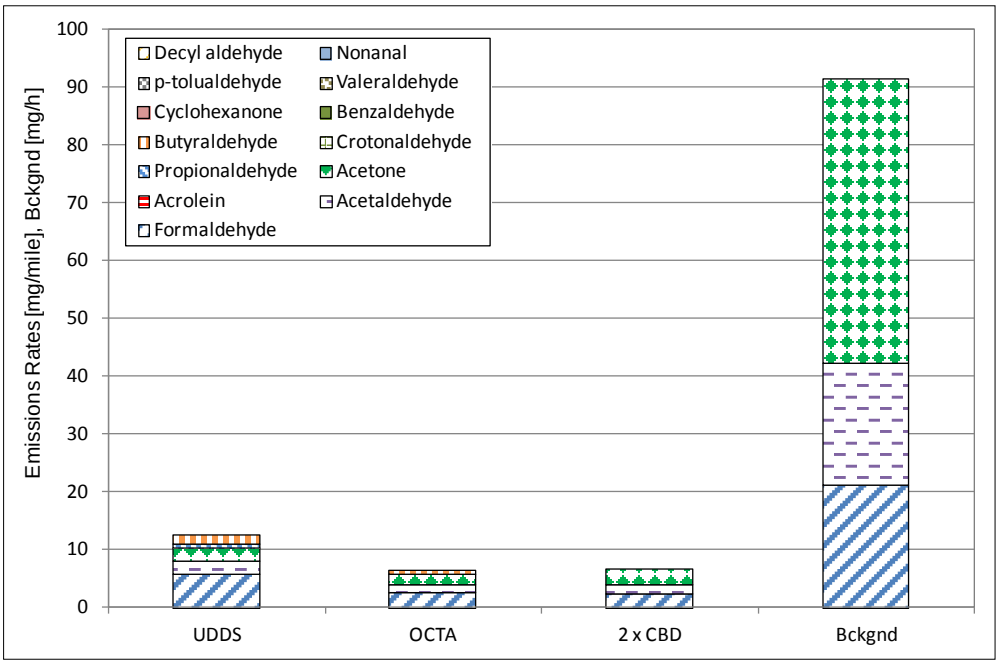


**Figure 59 Distance-specific carbonyl emissions results from a natural gas transit bus**

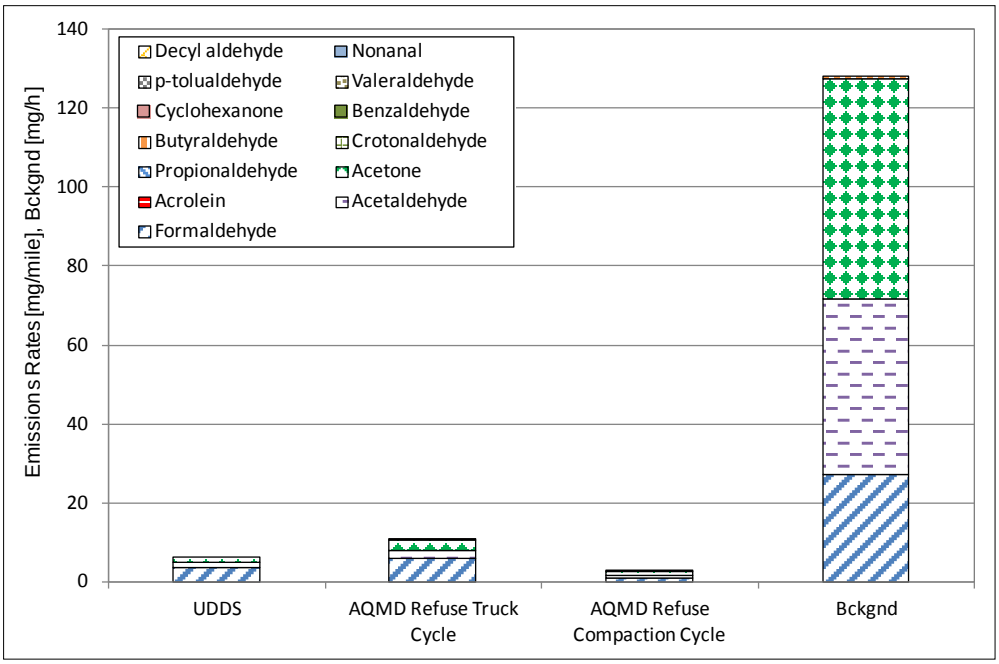


**Figure 60 Distance-specific carbonyl emissions results from a natural gas refuse truck**

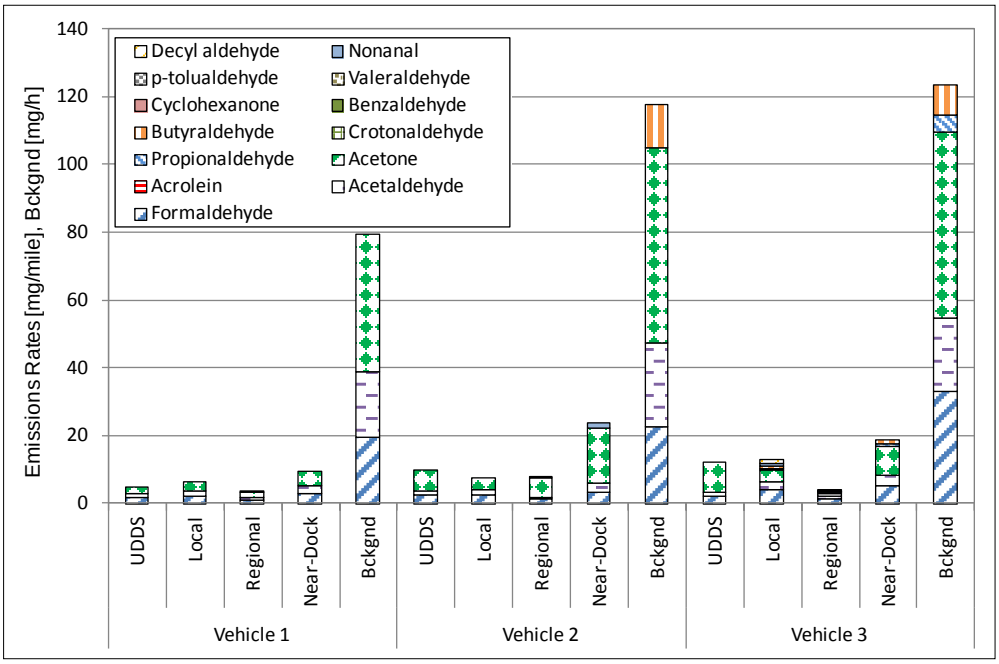


**Figure 61 Distance-specific carbonyl emissions results from three natural gas fueled goods movement vehicles**

Figure 60 and Figure 61 show the distance-specific carbonyl emissions from the natural gas refuse truck and goods movement vehicles respectively. The results show a similar profile as observed from the transit bus, wherein the tailpipe emission rate of carbonyl species from both vocation, and on all driving cycles are below levels observed in background air. The differences in catalyst lifetime between Vehicle 1, 2 and 3 in the goods movement vocation do exhibit a trend in the tailpipe carbonyl emissions rate, with

Vehicle 1 (200 miles) having the least mileage exhibiting the lowest emission rate. Vehicles 2 (45,000 miles) and 3 (65,000 miles) with significantly higher mileage show higher acetone emissions than Vehicle 1.

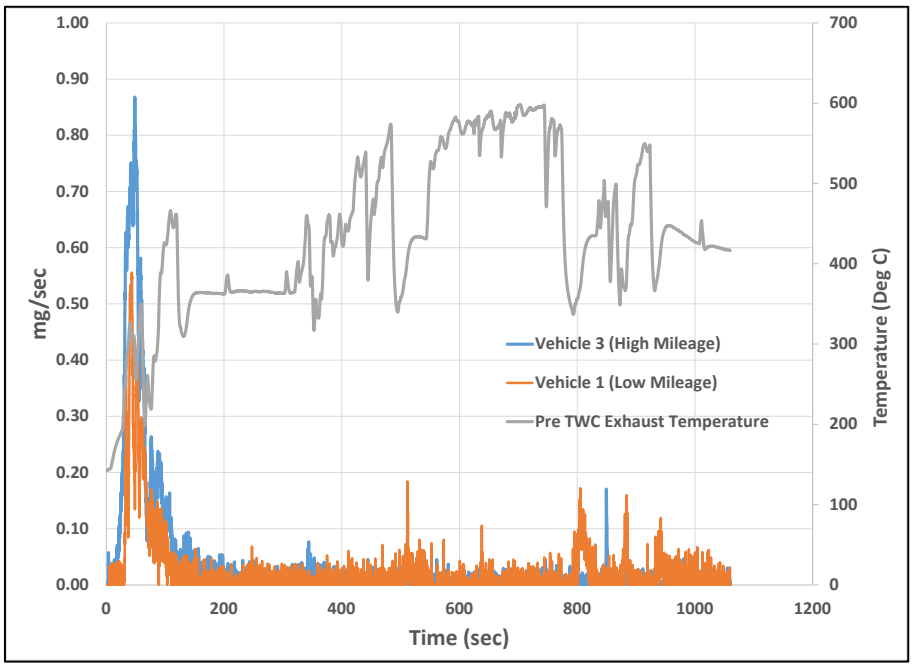


**Figure 62 Cold start formaldehyde emissions rate from two natural gas goods movement vehicles over the UDDS cycle**

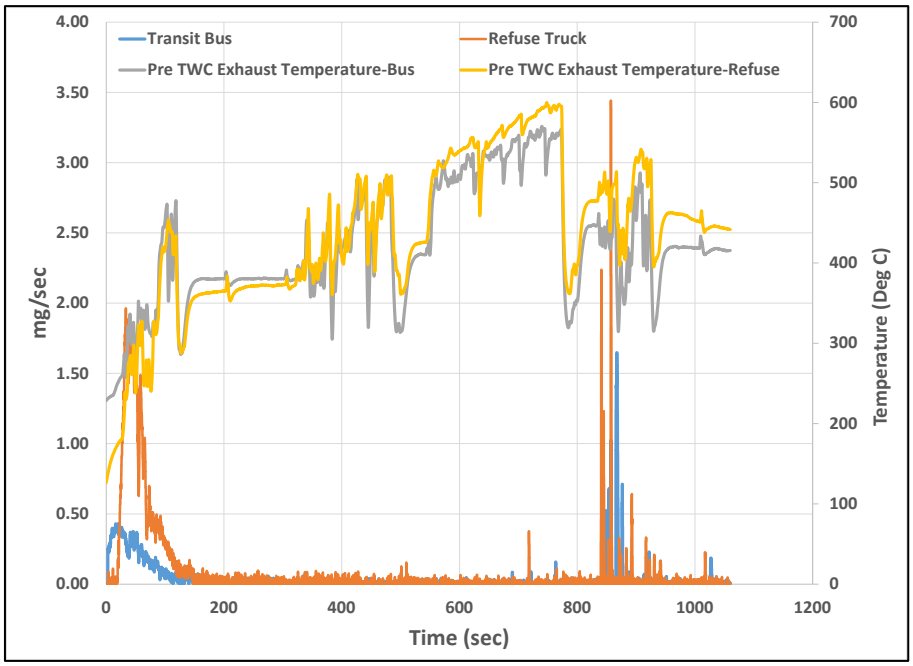


**Figure 63 Cold start formaldehyde emissions rate from transit bus and refuse truck over the UDDS cycle**

Figure 62 and Figure 63 show the instantaneous formaldehyde emissions measured using the MKS 2030 high speed FTIR during a cold start UDDS test. The results show significant emissions of formaldehyde during the brief warm-up period of the TWC. The exhaust temperatures plotted in the figure show that catalytic activity peaks close to 250 °C, after which formaldehyde emissions are observed to drop to below detection limits of the instrument.

#### *3.8.2.2 DIESEL VEHICLES*

Figure 64 shows the distance-specific carbonyl emissions from MY 2009 and MY 2011 diesel vehicles operating in the goods movement vocation. The results show formaldehyde emissions as the major constituent of the carbonyl species. The regional driving cycle characterized by the highest exhaust temperatures resulted in the lowest carbonyl emissions compared to other drayage cycles and the UDDS. It is to be noted that emissions of carbonyl compounds were lower than levels measured in the background air. Diesel truck with SCR exhibited higher formaldehyde emissions over the local and near-dock cycle than levels observed in background air.

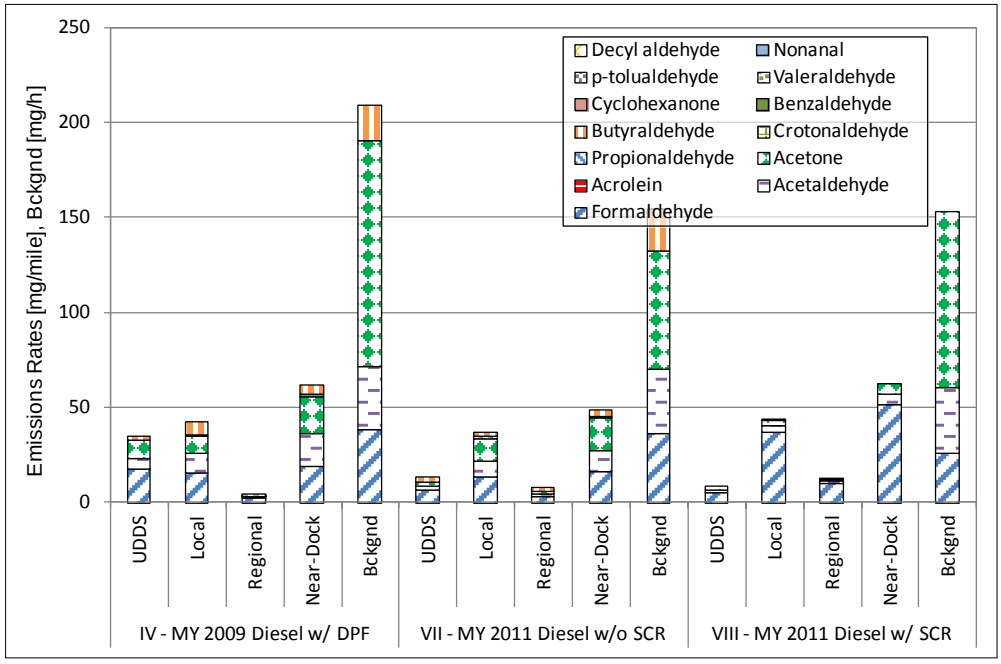


**Figure 64 Distance-specific carbonyl emissions results from diesel goods movement vehicles**

#### *3.8.2.3 DUAL FUEL VEHICLES*

Figure 65 shows the distance-specific carbonyl emissions from MY 2009 and MY 2011 dual-fuel HPDI vehicles. Vehicles 2 and 3 reported the highest formaldehyde emissions over the near-dock cycle,

indicative of incomplete combustion. Lower exhaust temperature due to dual-fuel strategy could be attributed to lower catalytic activity in comparison to stoichiometric natural gas engines.

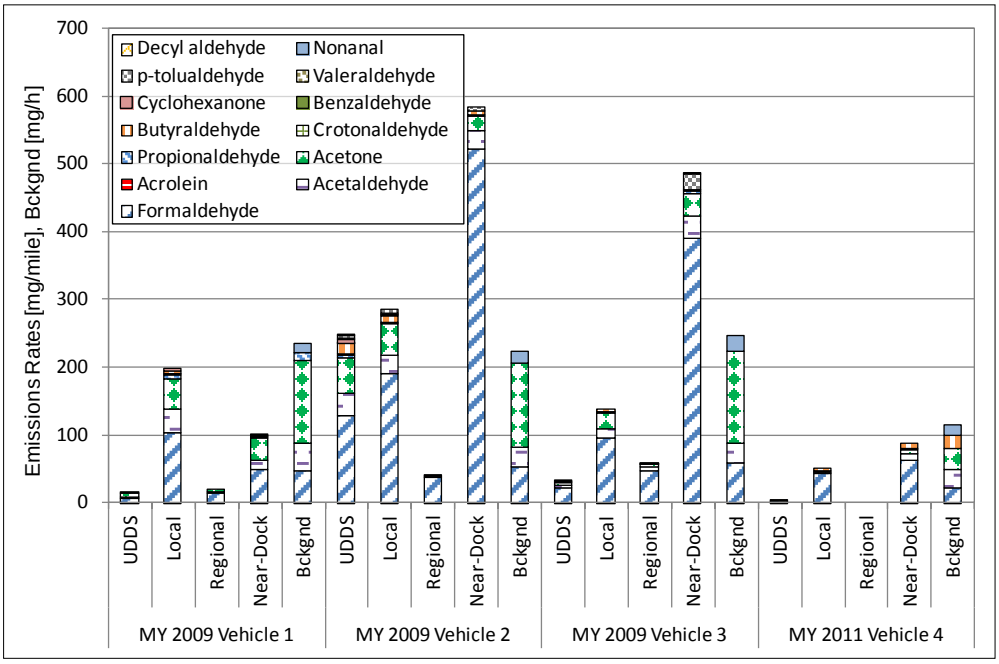


**Figure 65 Distance-specific carbonyl emissions results from three MY 2009 and one MY 2011 dual-fuel HPDI goods movement vehicles**

### *3.8.3 ELEMENTAL CARBON/ORGANIC CARBON (EC/OC) EMISSIONS*

EC/OC emissions were quantified using thermal/optical carbon analysis method of samples collected on pre-fired quartz filters. The analysis reports the elemental carbon mass and the volatile organic carbon mass of the total PM emissions.

#### *3.8.3.1 STOICHIOMETRIC NATURAL GAS VEHICLES*

The soot free combustion of natural gas fuel contributes to significantly lower soot emissions than diesel engines. As a result the OC fraction of PM is more dominant in the exhaust of natural gas engines (Okamoto et al., 2006). Also, studies have previously reported the effect of an oxidation catalyst in reducing organic carbon fraction in the exhaust. A recent study has shown the effect of oxidation catalyst and TWC in reducing the OC emissions by orders of magnitude compared to uncontrolled lean-burn natural gas engines (Yoon et al., 2014).

Figure 66 and Figure 67 show the distance-specific total elemental carbon (TEC) and total organic carbon (TOC) emissions from transit bus and refuse truck vocations, respectively. The results show a predominant OC composition of the total particulate matter with trace levels of elemental carbon

composition. Almost all of the EC emissions could be attributed to in-cylinder combustion of lubrication oil.

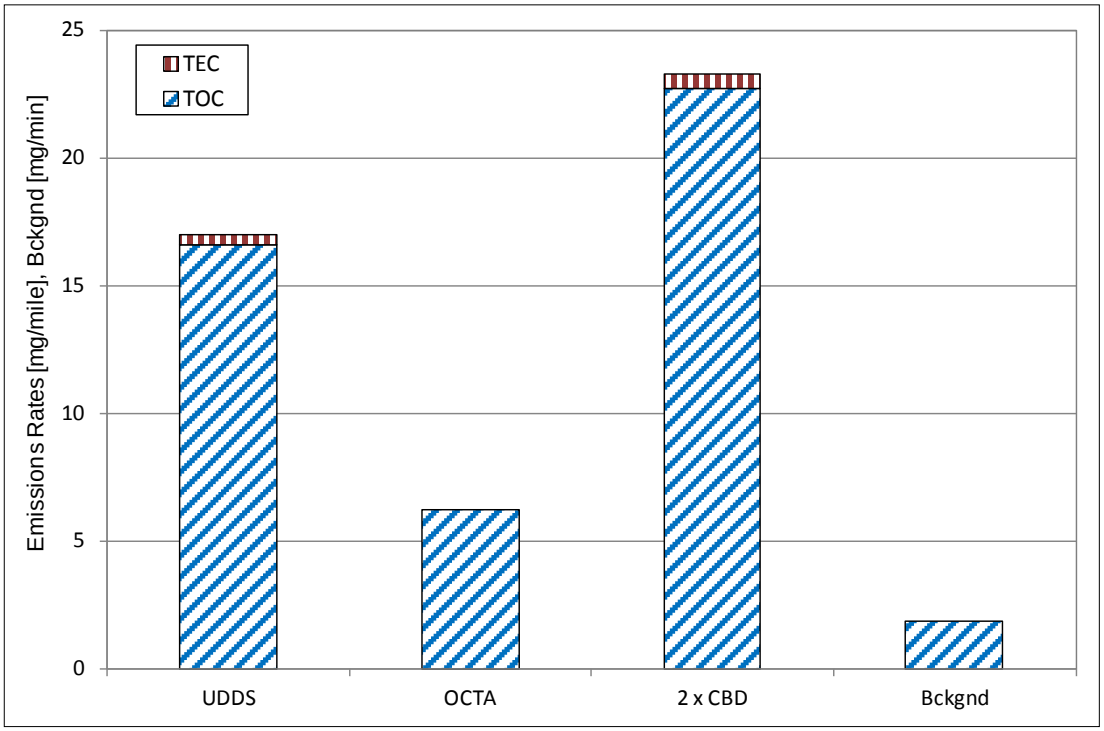


**Figure 66 Distance-specific EC/OC emissions results from a natural gas transit bus**

Figure 68 shows the TEC/TOC emissions from the three goods movement vehicles. The results show that the regional cycle characterized with the highest exhaust temperatures resulted in the lowest OC composition of the PM. While the near-dock cycle with the lowest exhaust temperature and extended idling periods contributed to the highest OC emissions from the goods movement application. The results also indicate a direct correlation of OC emissions to exhaust temperature characteristics and consequently catalytic activity. From the three goods movement vehicles tested under this category, the results show that the OC emissions from Vehicle 1 with the least mileage to be almost twice that observed from Vehicles 2 and 3. This can be attributed to the new after-treatment system that typically achieves peak catalytic activity to hydrocarbon species with continuous ageing.

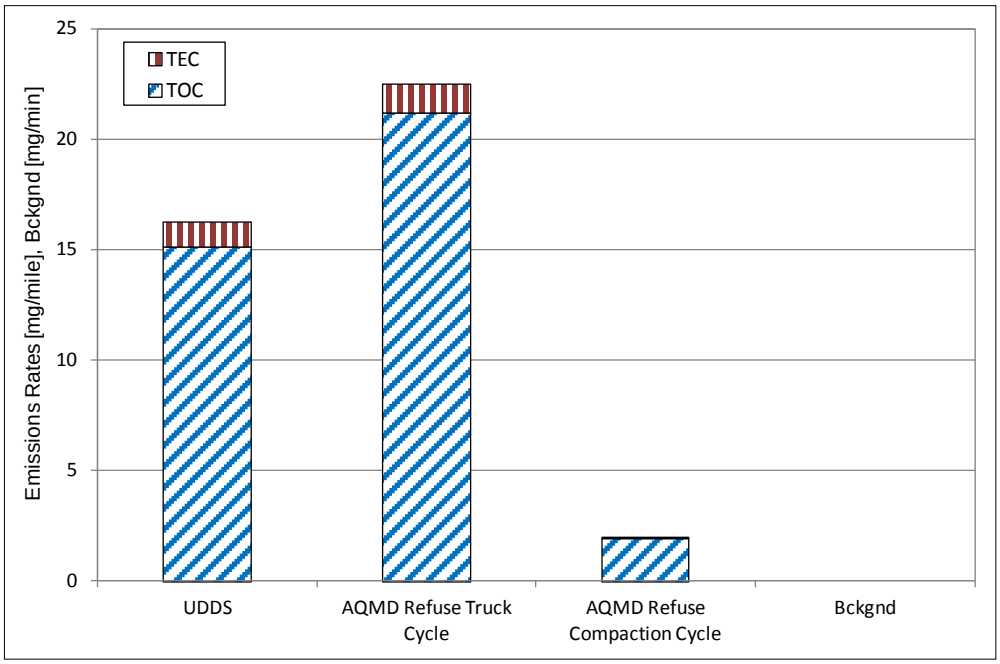


**Figure 67 Distance-specific EC/OC emissions results from a natural gas refuse truck**

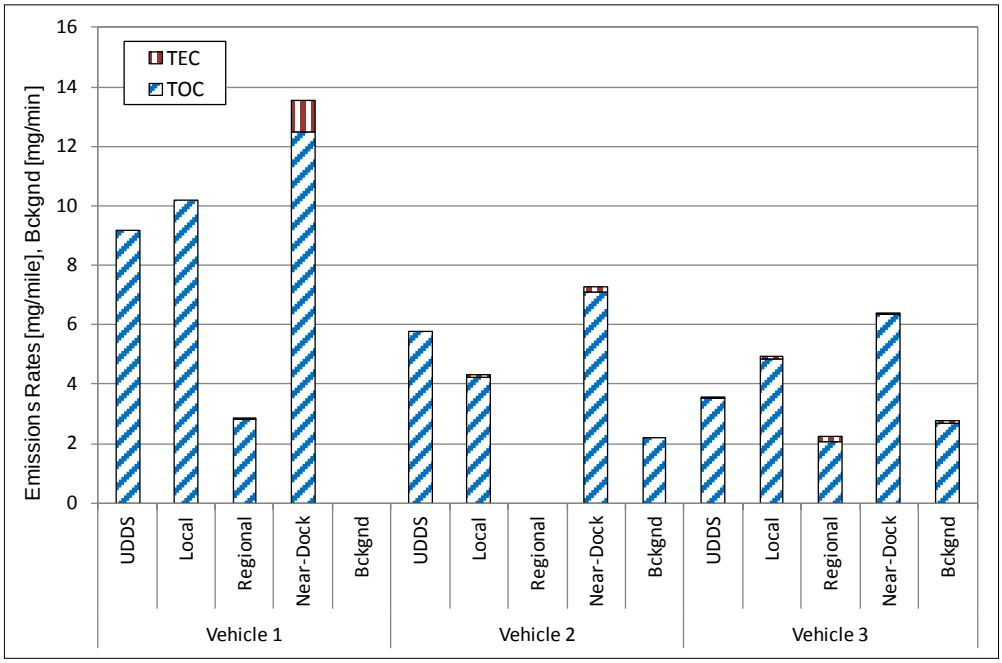


**Figure 68 Distance-specific EC/OC emissions results from three natural gas fueled goods movement vehicles**

### *3.8.3.2 DIESEL VEHICLES*

Figure 69 and Figure 70 show the distance-specific EC/OC emissions from diesel goods movement and refuse truck applications. The results show a complete OC contribution to the total PM from all model year diesel vehicles. This can be attributed to the use of DPF to remove soot from the exhaust. DPF filtration efficiencies close to 99% result in EC fractions close to detection limits. In some cases filtration efficiency of a DPF decreases during periods subsequent to an active DPF regeneration event. Such periods will be characterized by higher levels of EC emissions. This high level of EC emissions is due to the burning of the soot cake layer in the DPF which generally aids in particulate filtration. The effect of loss in filtration efficiency on EC emissions can be observed in the exhaust of the diesel refuse truck without SCR (Figure 70). The high EGR strategy of this engine resulted in frequent DPF loading and regeneration activity due to which the PM composition also reflected a higher EC fraction compared to diesel truck with SCR.

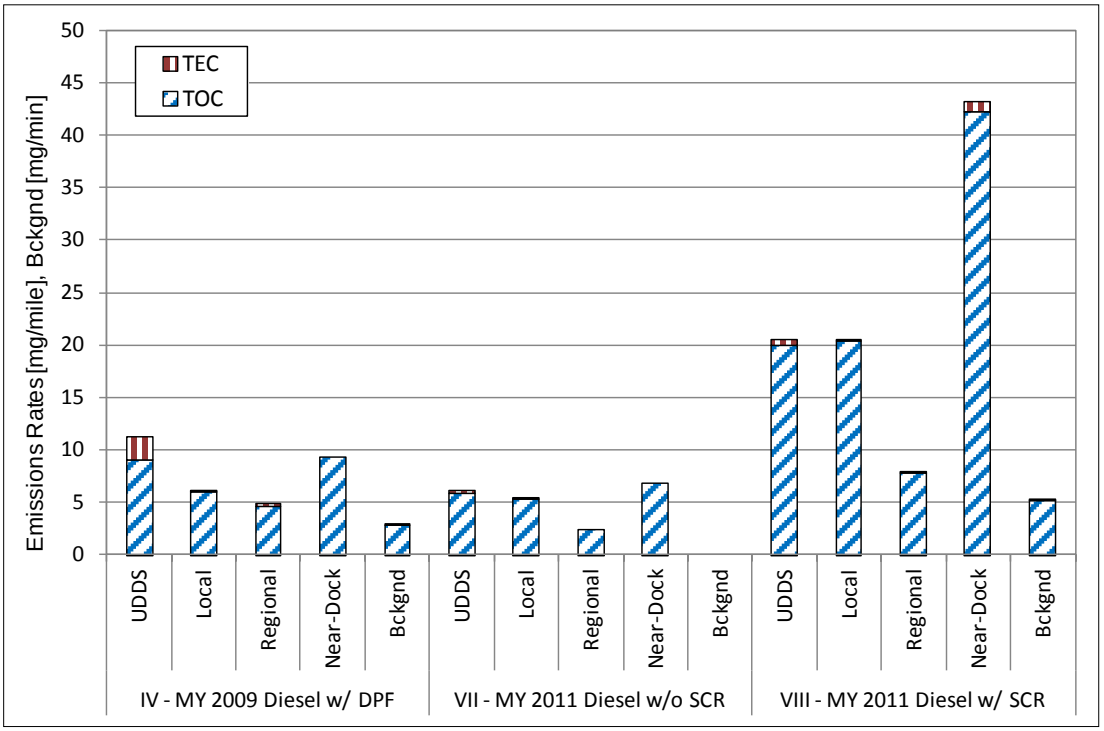


**Figure 69 Distance-specific EC/OC emissions results from diesel goods movement vehicles**

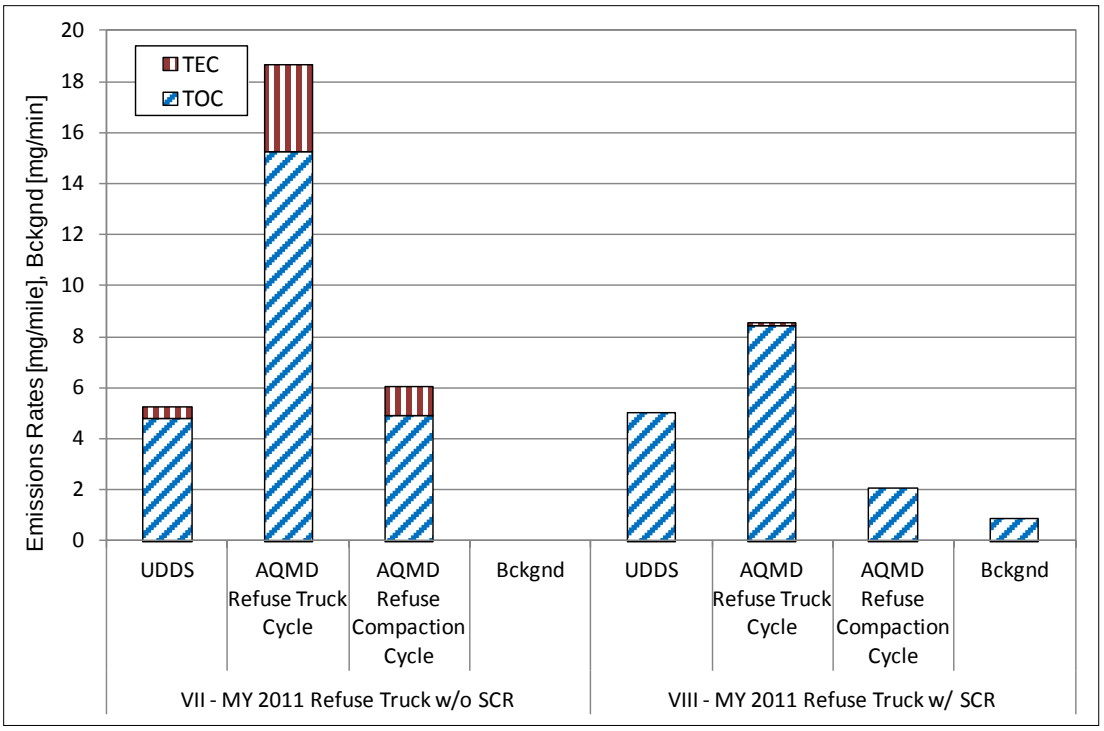


**Figure 70 Distance-specific EC/OC emissions results from a diesel refuse truck**

#### *3.8.3.3 DUAL-FUEL VEHICLES*

Figure 71 shows the distance-specific EC/OC emissions from MY 2009 and MY 2011 dual-fuel HPDI goods movement vehicles. The PM composition of the dual-fuel vehicles also indicate a predominant OC fraction. Vehicle 1 from the MY 2009 category presented a DPF full engine code prior to testing and hence the testing team had to perform a parked regeneration of the vehicle to clear the active engine code. Since, the local driving cycle was performed subsequent to this regeneration event, the PM composition could be influenced by the lower DPF efficiency and hence higher EC fraction.

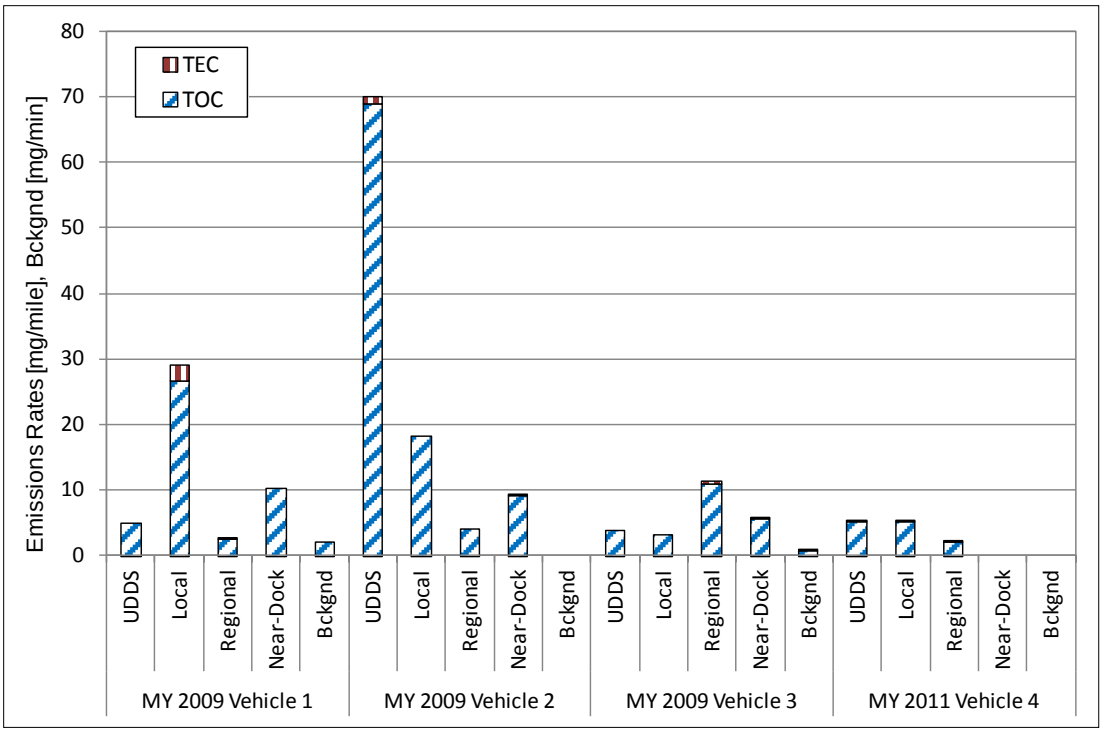


**Figure 71 Distance-specific EC/OC emissions results from three MY 2009 and one MY 2011 dual-fuel HPDI goods movement vehicles**

### 3.9 PARTICLE SIZE DISTRIBUTION

Instantaneous particle size distribution and concentrations were measured using the TSI EEPS. The particle size distribution and concentration are presented as average tailpipe particle concentration and distribution observed during operation over a given cycle. The TSI EEPS was setup for sampling at the CVS dilution tunnel, hence the measured particle concentrations were dilution corrected using the instantaneous dilution ratio measured from the CVS flow and exhaust flow rates.

Figure 72 shows the particle size distribution of all natural gas vehicles serving under different vocation for the UDDS driving cycle.

Dual-fuel vehicles with and without SCR after-treatment system exhibit a similar particle sized distribution. Particle concentrations measured from the dual-fuel vehicles range from approximately 1.5E+3 to 1.0E+4 particles/cm$^3$. This particle concentration typically corresponds to concentrations observed in ambient air. Studies have reported higher particle concentrations from catalyzed DPF and SCR equipped engines, during exhaust temperature greater than 380$^o$C (Thiruvengadam et al., 2011a, Kittelson et al., 2008). Since these particle formation is temperature dependent requiring exhaust temperature conditions greater than 380$^o$C, this particle formation was not detected in the exhaust of HPDI vehicles in which the conditions for particle formation was not achieved.

The natural gas transit bus powered by the stoichiometric fueled natural gas engine exhibited the highest particle concentration compared to the goods movement and refuse truck application. The particle size distribution showed nanoparticle emissions both in the nucleation mode (<30 nm) and accumulation mode (30-500 nm)(Kittelson et al., 2006). The observed particle size distribution could be a result of lubrication oil combustion manifesting itself as metals and elemental emissions of lubrication oil additives. A recent study presented by WVU showed that nanoparticle emissions observed in the exhaust of natural gas transit bus could be dominated by high levels of metals and inorganic species that could be traced to lubrication oil additives as its source (Thiruvengadam et al., 2013). The EC/OC emissions shown in Figure 66 also indicate the elemental carbon emissions during the UDDS cycle. Therefore the EC/OC emissions corroborate the accumulation mode particles observed from the transit bus tailpipe particle size distribution. Particle size distribution results shown in Figure 73 indicate instrument noise due to low particle concentrations detected over the CBD and the OCTA driving cycle. The high particle concentrations as result of possible lubrication oil entry were detected only during the UDDS cycle. This could be possibly attributed to differences in driving cycle metrics.

Particle size distribution characterized for the refuse truck and goods movement application over the UDDS cycle indicate instrument noise associated with measurement of low particle concentrations. No significant particle emissions in the nucleation and accumulation modes were detected from the goods movement and refuse trucks.

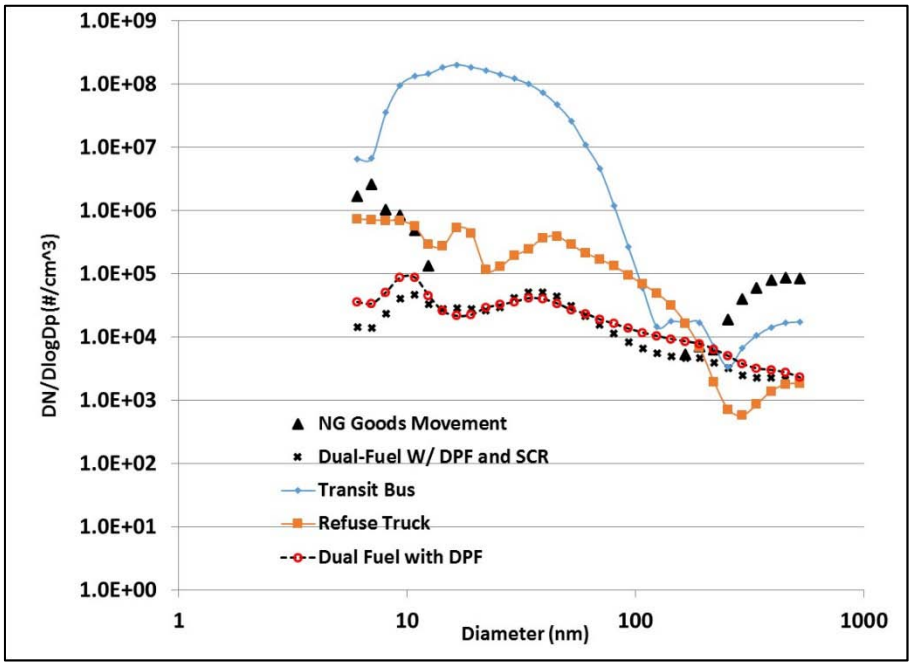


**Figure 72 Particle size distribution and concentration of natural gas vehicles over UDDS driving cycle.**

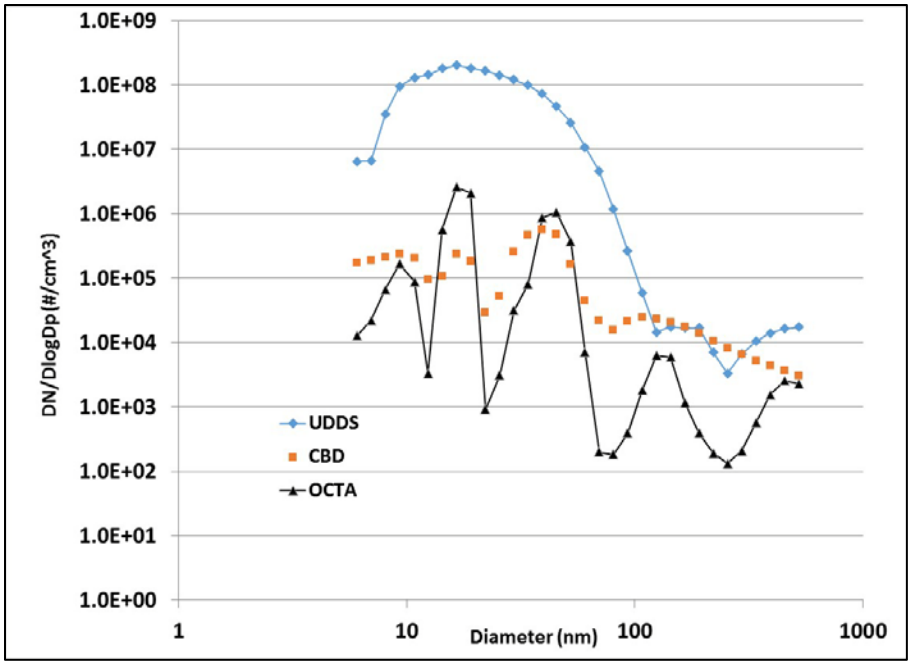


**Figure 73 Particle size distribution and concentration from natural gas transit bus**

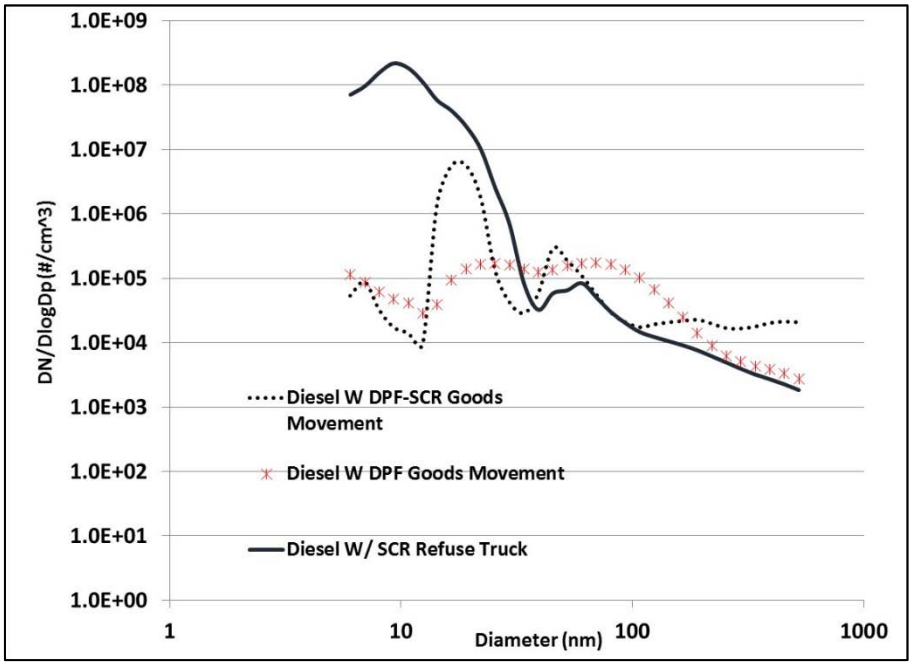


**Figure 74 Particle size distribution and concentration of diesel refuse truck and goods movement vehicles over UDDS cycle**

Figure 74 show the results of the particle size distribution and concentration measured for the diesel vehicles operating under goods movement and refuse truck applications. Diesel vehicles equipped with SCR exhibited high particle concentrations in the nucleation mode centered close to 10 nm. Studies have shown this observed particle emissions in the nucleation region to be linked to possible sulfuric acid

droplets formed as result of successive oxidation of sulfur in lubrication oil over catalyzed surface of DPF and SCR after-treatment systems (Thiruvengadam et al., 2011a, Kittelson et al., 2008). Studies have also shown that these particle emissions are highly temperature dependent and the onset of this particle emissions is only observed at exhaust temperatures over 380°C (Thiruvengadam et al., 2011a, Vaaraslahti et al., 2005). Diesel vehicles with only DPF did not exhibit any particle emissions in the nucleation mode, with particles only in the accumulation mode measured at a concentration range of 1E+5 particles/$cm^3$.

The results of particle size distribution and concentrations from heavy-duty diesel and natural gas vehicles show that the ultrafine particle emissions from both current technology diesel and natural gas engines to be in the same order of magnitude, with diesel engines exhibiting higher accumulation mode particles subsequent to regeneration activities. The age of natural gas engines, specifically in vocations related to transit bus and refuse truck, could be attributed to increase particle emissions due to the absence of DPF to control possible lubrication oil combustion. However, a previous study from CARB has documented close to 99% reduction in PM mutagenicity in comparison to legacy natural gas engines (Yoon et al., 2014).

Diesel engines equipped with SCR have exhibited a temperature dependent ultrafine particle emission in the 10 nm size range. However, the toxicological properties of these particles have also not been clearly established. A study by Herner et al. showed toxicity to decrease with an increase in particle emissions (Herner et al., 2011). Although the results of the study could be influenced by noise in the characterized data, it is important to note that the tailpipe concentrations of these ultrafine particle emissions do not provide sufficient mass for a conclusive toxicological assessment.

## 3.10 IN-USE CROSS COUNTRY EVALUATION OF A HEAVY-DUTY TRACTOR

The cross country test was conducted over a duration of six days. The results are presented for each day describing the vehicle operating conditions, terrain, the ambient conditions of the region in which the vehicle was operated, and the measured emissions of GHGs along with regulated pollutants in terms of payload-distance and brake specific values. The data for each day is further divided into micro-trips, which is defined as the distance covered between an engine on and off event.

### *3.10.1 RESULTS DAY 1*

The trip started at WVU in Morgantown, WV on the first day and ended at Terre Haute, IN. The trip consisted of five micro-trips, indicated by segments between the red bubbles over the route map shown Figure 75, covering a total distance of 457 miles.

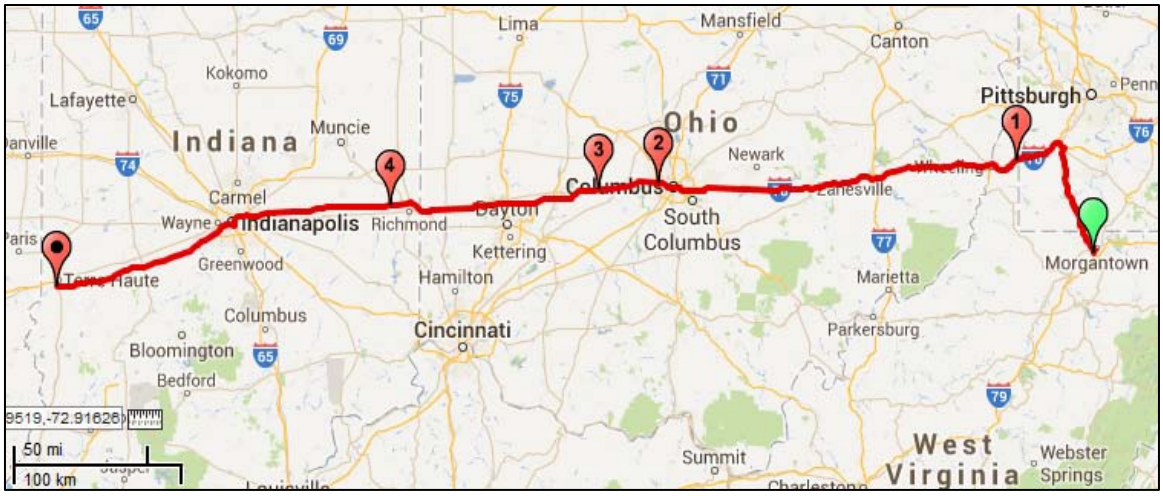


**Figure 75 Route Map of the Distance Covered in Day 1**

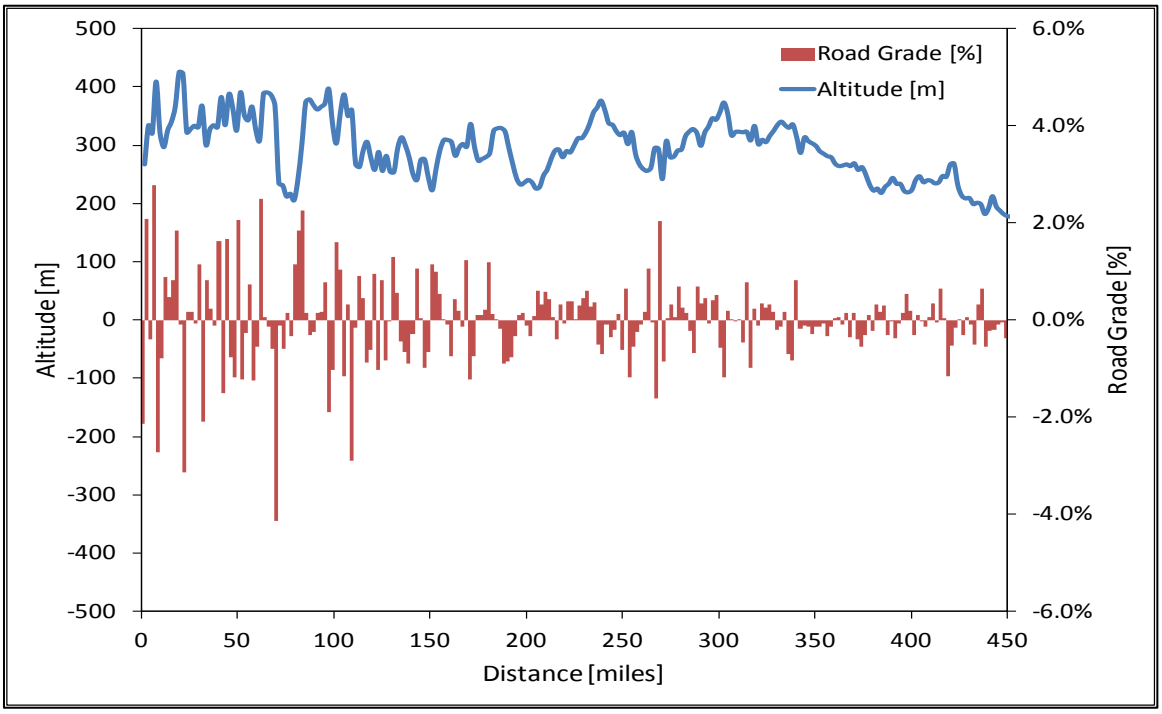


**Figure 76 Altitude and Road Grade Trace for Day 1 Route**

The road grade of the route traversed on Day 1 consisted of a maximum positive grade of 2.8% and negative grade of 4.1%. The grades are calculated based on change in elevation over a distance of 2 miles using GPS altitude data. The altitude and road grade trace for Day 1 revealed that the destination was lower than the starting point and total distance travelled with a negative gradient was 230 miles of which 12 miles were below -2.0% grades. The terrain included the rolling hills of the Appalachian valleys in West Virginia and Pennsylvania, crossing into the low lands of Ohio and Indiana. The ambient temperature and relative humidity ranged between 16 to 26 °C, and 28 to 77%, respectively over a period of 10 hours. The vehicle specific $CO_2$ emissions measured during Day 1 of the test campaign for each

micro-trip is shown in Table 23. The fuel consumption values were determined from measured $CO_2$ emissions using a factor of 10,180 [g/gal] for diesel fuel, and assuming complete combustion. The difference between measured values of payload-distance specific $CO_2$ emissions from micro-trips and the future GHG emissions standards for MY 2014 Class 8 combination sleeper cab with high roof, set at 75.0 g/ton-mile, ranged between -7% to 20% (negative sign signifies measured emissions being lower than the standard). However, the overall difference between measured $CO_2$ emissions and GHG standards for Day 1 was 2%.

Engine specific GHG emissions shown in Table 24 illustrates that the engine powering the test vehicle is compliant with future GHG certification standards as applied to MY 2017 and later engines, for all three GHG constituents. Also, $NH_3$ emissions were well controlled and brake specific emissions were in the range of milligrams. However, the same engine when used to power a MY 2011 tractor combination fails to meet future MY 2014 standards., This could be attributed to the vehicle design factors, primarily aerodynamic features, which account for up to 22% of energy to aerodynamic loss, also tire rolling resistance which accounts for up to 16% of the total energy when cruising at interstate speeds and other losses inherent to the vehicle. Hence, $CO_2$ emissions are regulated on both engine and vehicle specific basis leading to improved vehicle aerodynamics, transmission, auxiliaries, and tire design reducing energy loss associated with them.

### *3.10.2 RESULTS DAY 2*

The test route for Day 2 shown in Figure 77 consisted of four micro-trips over a total distance of 591 miles. The route passed through the great plains of the Mid-West regions of Illinois, Missouri, and Kansas. The elevation of the test route rises gradually from 150 m (492 ft) to 374 m (1,227 ft) above sea level resulting in a road grade of near 0%, with a maximum and minimum grade of 1.9% as shown in Figure 78. The ambient temperature and relative humidity ranged between 16 to 28 °C, and 42 to 75% over a period of 12 hours driving.

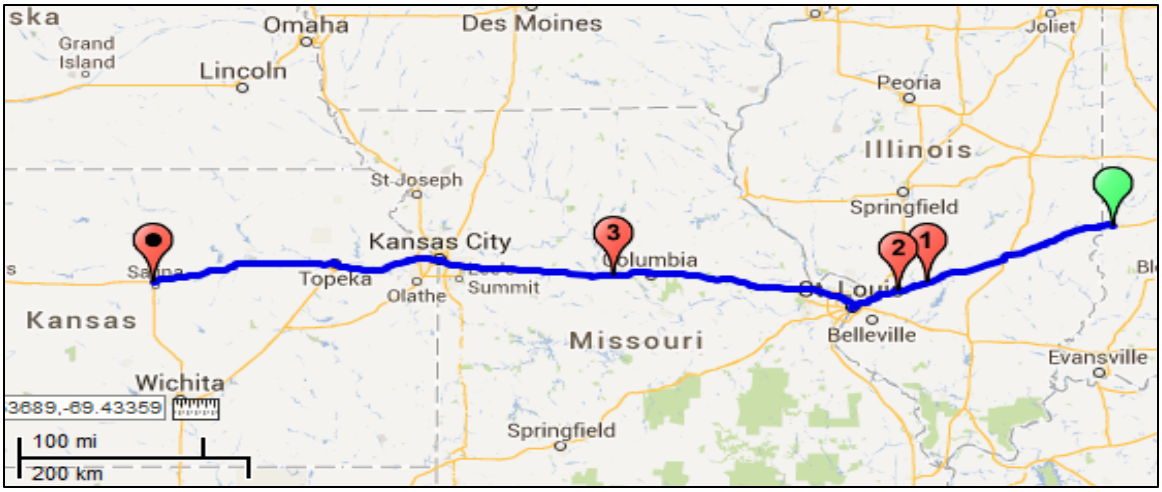


**Figure 77 Map of the Distance Covered on Day 2**

The payload distance specific $CO_2$ emissions for Day 2 were higher than the MY 2014 GHG standards, and ranged between 10 to 21% over four micro-trips with an average difference of 12% for the entire day. However, the difference between measured and simulated payload distance specific $CO_2$ emissions ranged between -16 to -4%, with an overall difference of -13% for Day 2. The brake specific GHG emissions shown in Table 24 illustrates that the engine is compliant with future emissions standards.

The test vehicle demonstrated compliance with MY 2010 regulated emissions standards as shown in Table 24, except for the last micro-trip, with the longest trip mileage of 275 miles. During this micro-trip the vehicle experienced an after-treatment event involving deactivation of diesel exhaust fluid (DEF) injection leading to increased NOx emissions. The measured brake specific NOx emission for this trip was 0.42 g/bhp-hr, of which 30% of the emissions was due to this event.

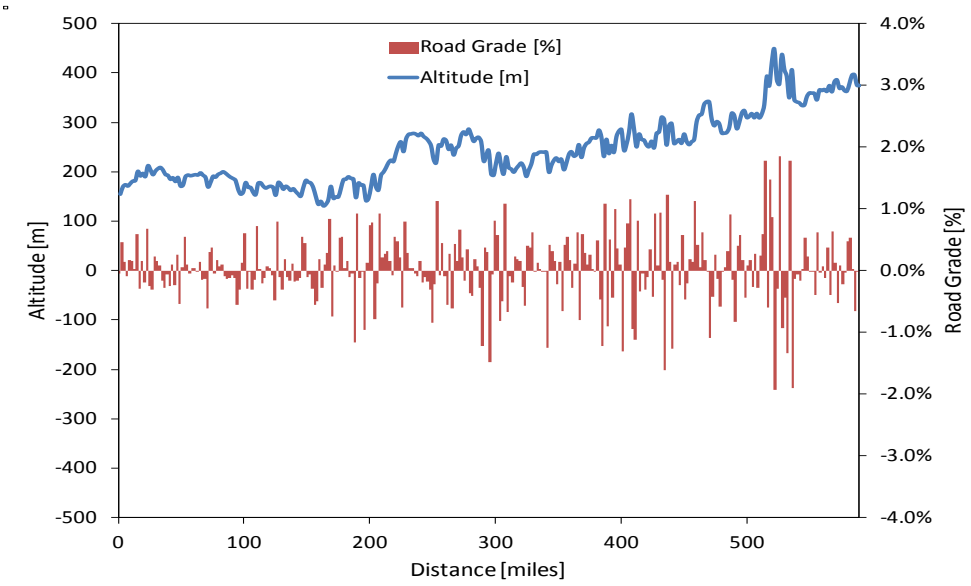


**Figure 78 Altitude and Road Grade Trace for Day 2 Route**

### *3.10.3 RESULTS DAY 3*

Day 3 test schedule involved three micro-trips covering a total distance of 440 miles, passing through the plains of Kansas for the majority of the test route, and stopping in Colorado at an elevation of 1,727 m (5,666 ft). The ambient temperature and relative humidity ranged between 15 to 37 °C and 24 to 79% over a period of 11 hours. Day 3 test route is shown in Figure 79. Although the rise in the altitude between the start and end of the test was more than 1,350 m (4,430 ft) it was gradual resulting in an average grade of 0.2% for the entire trip as illustrated in Figure 80.

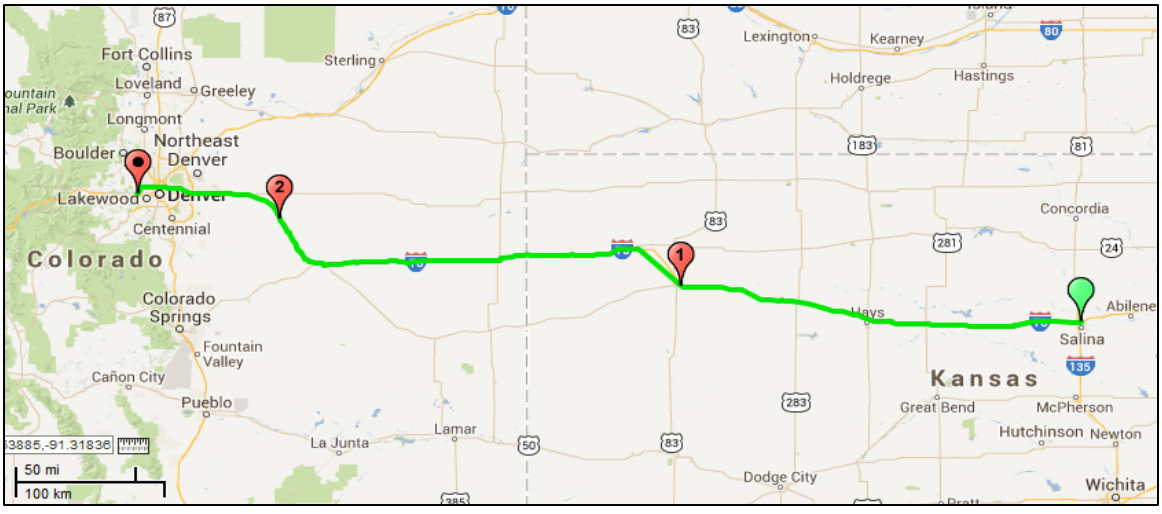


**Figure 79 Route Map of the Distance Traversed on Day 3**

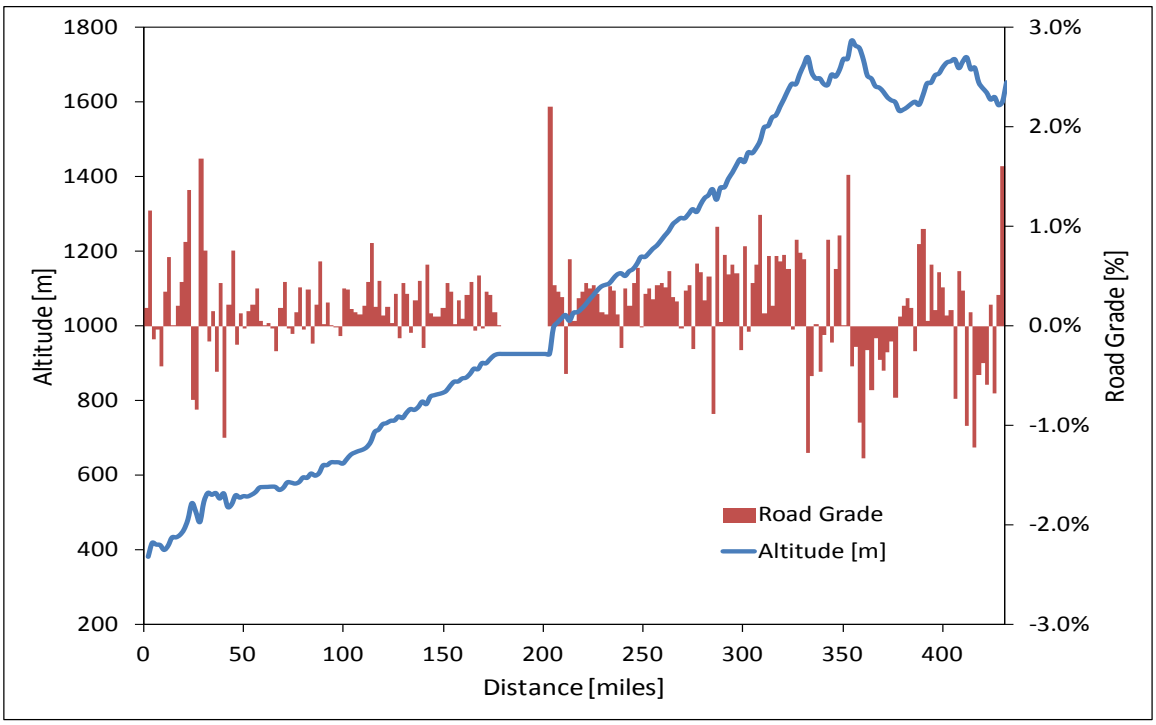


**Figure 80 Altitude and Road Grade of Day 3 Route**

Table 24 shows that the vehicle fails to meet future vehicle GHG standards. The difference between the measured and standard $CO_2$ emissions over 3 micro-trips ranged from 4 to 23% with an overall difference of 15% for whole day. The brake specific emissions of GHG and non-GHG emissions constituents' shown in Table 24 meet future GHG standards and existing non-GHG regulations.

### *3.10.4 RESULTS DAY 4*

Day 4 testing involved driving only in the state of Colorado passing over the high peaks of the Rocky Mountains. The route is illustrated in Figure 81. It consisted of 5 micro-trips of short distances totaling only 176 miles. The road grades ranged from 6% to -6%, with over 16 miles between 4 to 5% in both upward and downward directions, illustrated in Figure 82. The ambient temperature and relative humidity ranged between 3 to 19 °C and 15 to 43% respectively over test duration of 9 hours. The emissions measurement system required trouble-shooting for issues related to high altitudes leading to a change in the setup to operate effectively at high altitudes delaying the testing and resulted in shortest distance being covered in the entire test campaign.

The first three micro-trips included only ascent of the Rocky Mountains consisting of grades greater than 2% for 30 miles resulting in higher payload distance specific $CO_2$ emissions and fuel consumptions. The difference between measured and the MY 2014 $CO_2$ emissions standards ranged from -12% to 162% with an average of 32% higher $CO_2$ emissions over a distance of 159 miles. This shows that road grade has significant effect on NOx and $CO_2$ emissions when the road grades are greater than 2% and the

increase in emissions caused during the ascent is not negated by the decrease in emissions during descent. The results are illustrated in

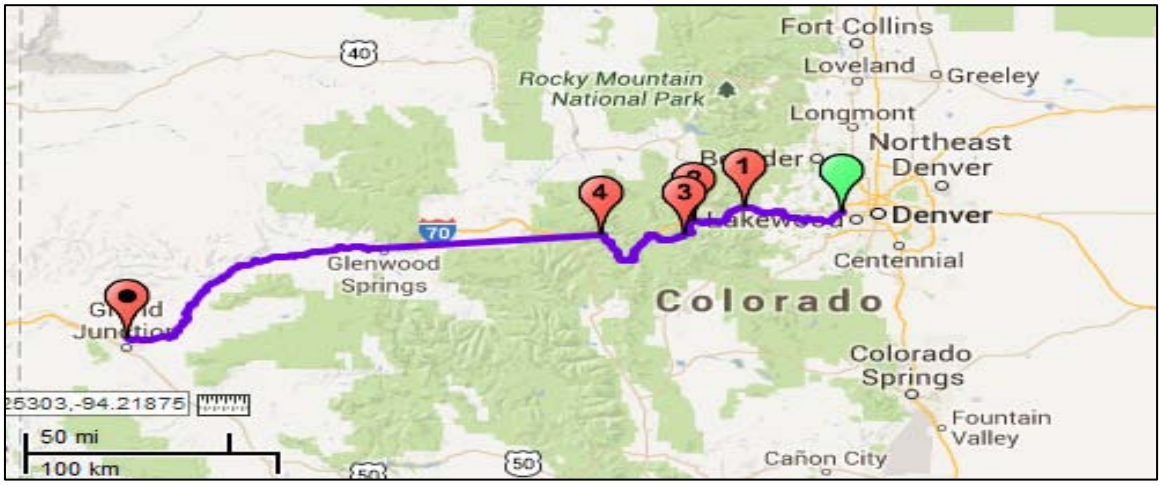


**Figure 81 Map of the Route Traversed on Day 4**

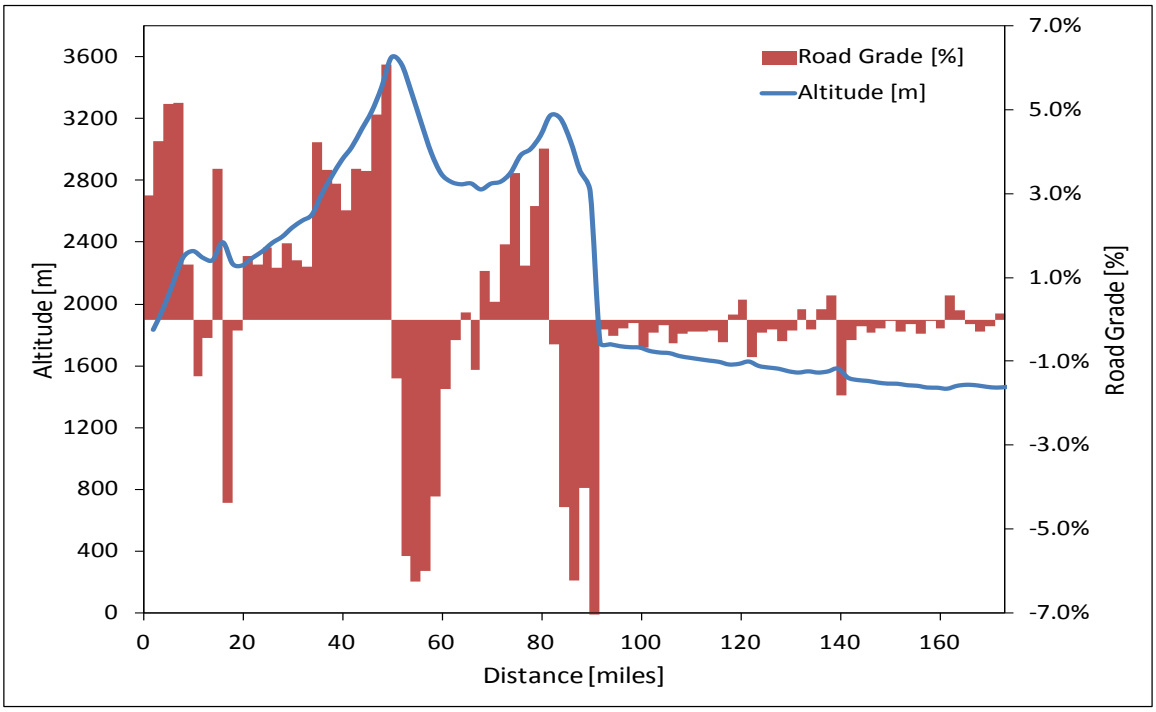


**Figure 82 Altitude and Road Grade trace of Day 4 Route**

The brake specific NOx emissions were an order of magnitude higher than certification values 0.2 g/bhp-hr since injection of DEF, required for SCR after-treatment operation, was de-activated due to engine operation at altitudes greater than 1,676 m (> 5,500 ft). This is observed due to the fact that US-EPA does not regulate NOx emissions at high altitudes (above 1,676 m) allowing engines to be operated conservatively and increasing its useful life. The brake specific emissions of GHG and regulated emissions are shown in Table 24 along with altitude.

### 3.11 RESULTS DAY 5

The test route on Day 5 passed through the plateaus of Utah and arid deserts of Nevada. The trip consisted of 5 micro-trips covering a total distance of 500 miles, as shown in Figure 83. The elevation of the route decreased from 1,400 m (4,593 ft) to 575 m (1,886 ft) with intermediate peaks ranging between 1,600 to 2,400 m (5,249 to 7,874 ft) presenting with road gradients of greater than 2% up to 6% for a distance of 80 miles with a maximum of 6% gradient for 4 miles including ascent and descent portions as shown in Figure 84. The ambient temperature and relative humidity for the test duration of 10 hours ranged between 8 to 34 °C and 12 to 45% respectively.

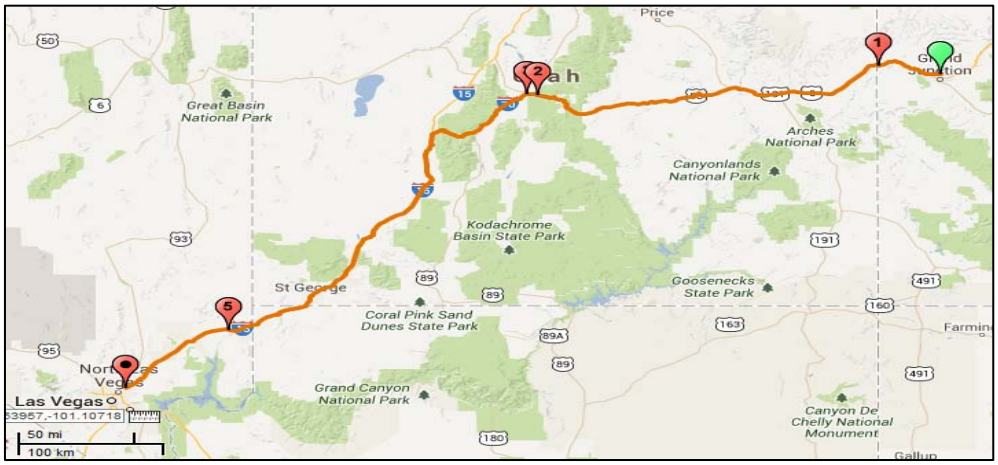


**Figure 83 Map of the Route Traversed on Day 5**

The measured payload distance specific $CO_2$ and fuel consumption values for all micro-trips on Day 5 are illustrated in Table 23. The difference between measured and MY 2014 standard payload distance specific $CO_2$ emissions ranged between -33% to 22%, for micro-trips, with an overall difference of 3% for the entire day.

Note that the micro-trip number 3 involving descent for a short distance resulted in lower $CO_2$, both payload-distance and brake specific emissions, shown in Table 24 but higher brake specific NOx emissions as there was no SCR activity due to low exhaust gas temperatures.

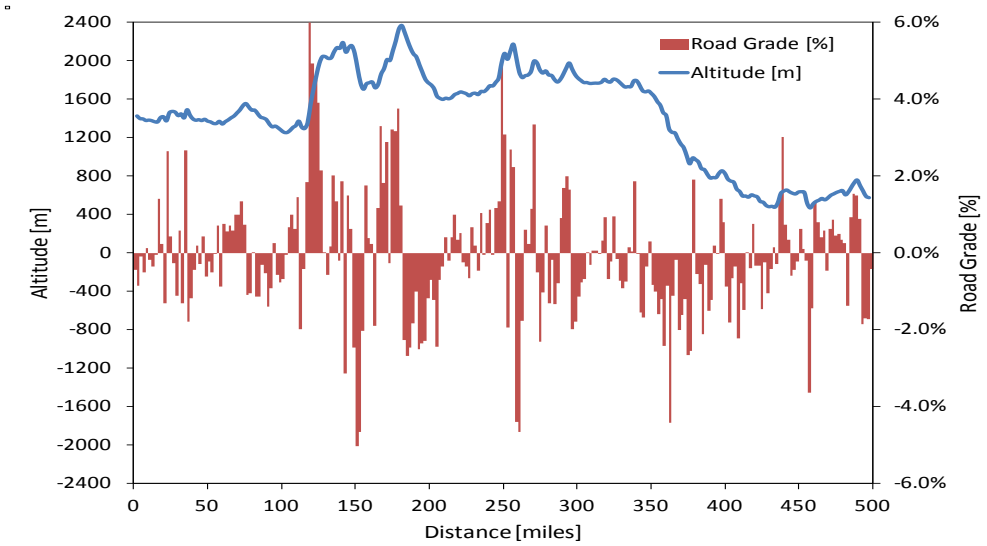


**Figure 84 Day 5 Route's Altitude and Road Grade Trace**

### *3.11.1 DAY 6*

The last day of the test campaign, shown in Figure 85, transited mostly through the Mojave Desert and Death Valley in the south east portion of California. It included 4 micro-trips passing over two peaks of altitude 1,400 m (4,593 ft) and 1,200 m (3,937 ft) traversing through the Mojave Valley and ending the trip at Riverside, CA, situated in Moreno Valley, at an elevation of 450 m (1,476 ft), as shown in Figure 86. The total distance covered on Day 6 was 323 miles. Over 60 miles of the test route had a road grade of higher than ±2% of which 4 miles had a maximum road grade of ±6%. The ambient temperature and relative humidity ranged between 20 to 36 ℃ and 10 to 28% respectively over test duration of 8 hours.

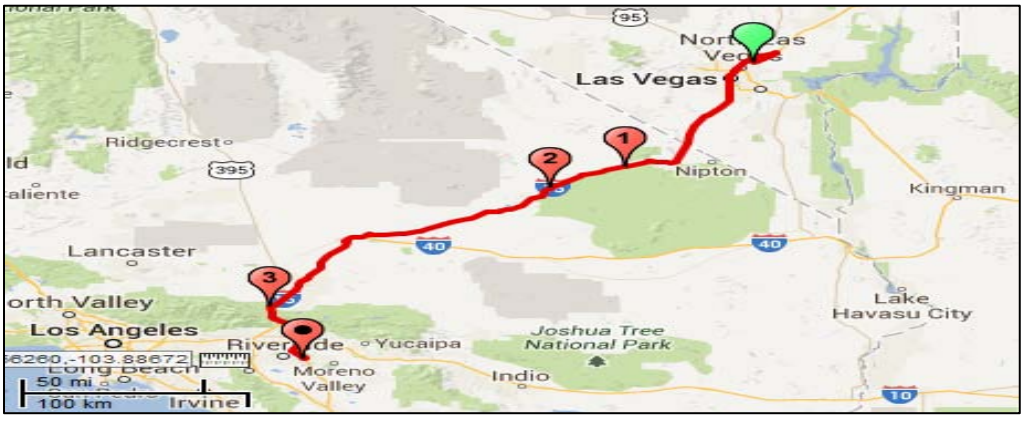


**Figure 85 Map of the Route to Final Destination on Day 6**

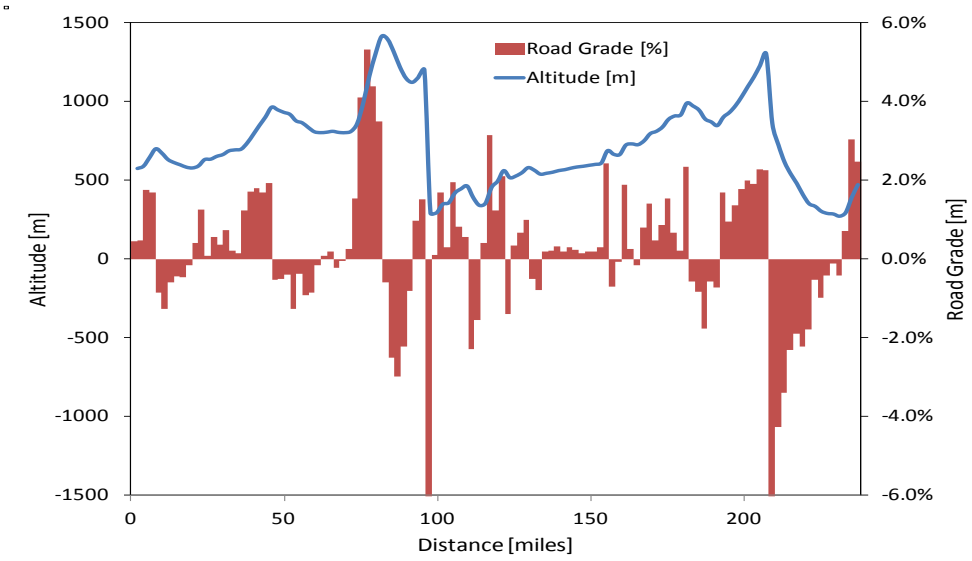


**Figure 86 Altitude and Road Grades through California**

Measured payload-distance specific $CO_2$ emissions and fuel consumption results shown in Table 23 confirms that the MY 2010 vehicle fails to meet future payload-distance specific GHG emissions standards, since the measured emissions were 18% higher than the standard for MY 2014 on Day 6.

### 3.12 RESULTS SUMMARY

The test campaign, which involved measuring both GHG and non-GHG emissions using lab grade analyzers along with other independent measurement systems while the vehicle was operated on the US Interstate Highway system travelling from east to west coast, was completed successfully. The effort was a first of its kind involving lab grade emissions measurement over a distance of more than 2,400 miles. The entire test route, designated in different colors representing different test days along with the stops demarcating micro-trips, is illustrated in Figure 16. The trace of altitude change with distance for the entire test route is shown in Figure 87.

The test vehicle, a MY 2011 Class 8 Combination-Sleeper Cab with high-roof powered by a heavy-duty diesel engine compliant with US-EPA MY 2010 non-GHG emissions regulation, fails to meet future (MY 2014 and later) payload-distance specific $CO_2$ emissions and fuel consumption standards. However, the brake specific GHG emissions meet future standards, even MY 2017 and later, by a wide margin. This shows that a greater emphasis should be placed on improving the design of the whole vehicle, such as reducing aerodynamic losses, rolling friction of tires, weight of the vehicle, use of vehicle speed limiter, and improving efficiency of transmission, in order to reduce payload-distance specific $CO_2$ and fuel consumption values.

At high altitudes, greater than 1,524 m (5,000 ft), the brake specific NOx emissions were higher than certification standards by an order of magnitude. This is due to engine protection strategies adopted to

overcome the operational limitations encountered at high altitudes, and also due to the fact that engine manufacturers are exempted from complying with NOx emissions standards at altitudes greater than 5,500 feet above sea level. It was also observed that the NOx emissions were higher when measured over short distances due to low exhaust temperatures, a constraint for effective SCR operation. The un-regulated $NH_3$ emissions, a byproduct of SCR after-treatment systems, was well controlled and were in the range of milligrams with average concentrations of less than 4 ppm across all micro-trips. Also $N_2O$, a potent GHG emission, was negligible and was measured at 1.7% of $CO_2$ equivalent over the entire trip.

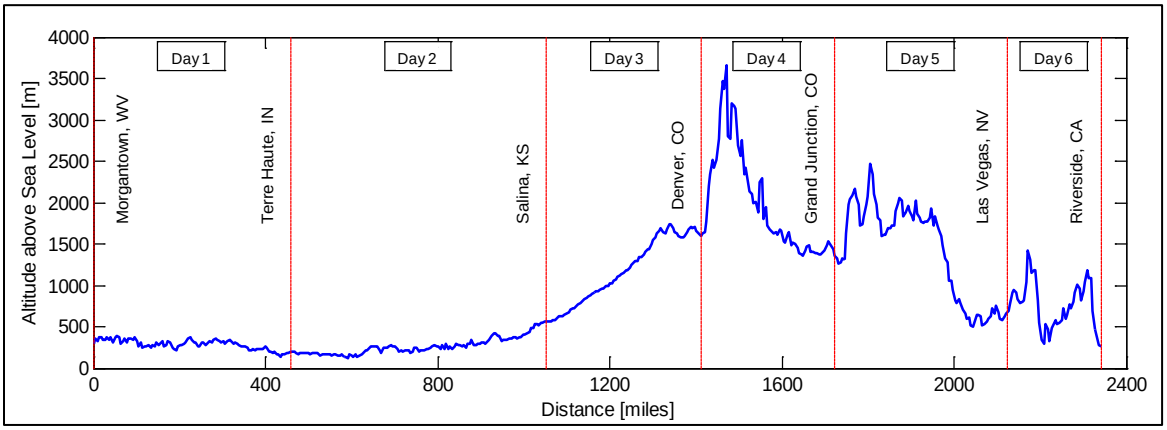


**Figure 87 Altitude Trace of the Complete Test Route**

**Table 24 Measured Payload-Distance Specific $CO_2$ Emissions and Fuel Consumption for the Cross-Country Trip**

| Trip Day | Micro-trip | Dist. [mi] | Dist. > 2% Grade [mi] | Max. Upward Grade [%] | Avg. Velocity [mph] | $CO_2$ [g/ton-mi] | Fuel [gal/$10^3$ ton-mi] |
|---|---|---|---|---|---|---|---|
| **Day 1** | 1 | 67.00 | 8 | 2.8 | 58 | 89.79 | 8.82 |
| | 2 | 146.00 | 2 | 2.2 | 60 | 75.08 | 7.38 |
| | 3 | 24.00 | 0 | 0.6 | 42 | 84.17 | 8.27 |
| | 4 | 83.00 | 0 | 1.8 | 62 | 69.71 | 6.85 |
| | 5 | 137.00 | 0 | 1.0 | 53 | 74.05 | 7.27 |
| **Overall Day 1** | | **457.00** | **10** | **2.8** | **57** | **76.43** | **7.51** |
| **Day 2** | 1 | 118.00 | 0 | 0.7 | 61 | 86.31 | 8.48 |
| | 2 | 19.00 | 0 | 0.7 | 48 | 90.38 | 8.88 |
| | 3 | 179.00 | 2 | 2.2 | 62 | 83.45 | 8.20 |
| | 4 | 275.00 | 4 | 2.3 | 64 | 82.72 | 8.13 |
| **Overall Day 2** | | **591.00** | **16** | **2.8** | **62** | **83.90** | **8.24** |
| **Day 3** | 1 | 178.00 | 0 | 1.7 | 65 | 92.17 | 9.05 |
| | 2 | 192.00 | 0 | 1.5 | 63 | 83.97 | 8.25 |
| | 3 | 70.00 | 0 | 1.6 | 58 | 78.02 | 7.66 |
| **Overall Day 3** | | **440.00** | **20** | **2.8** | **63** | **86.34** | **8.48** |
| **Day 4** | 1 | 29.00 | 10 | 5.2 | 44 | 136.42 | 13.40 |
| | 2 | 12.00 | 8 | 6.1 | 24 | 163.76 | 16.09 |
| | 3 | 8.00 | 6 | 5.6 | 23 | 196.73 | 19.32 |
| | 4 | 26.00 | 6 | 3.8 | 41 | 104.27 | 10.24 |
| | 5 | 84.00 | 0 | 0.9 | 61 | 66.13 | 6.50 |
| **Overall Day 4** | | **159.00** | **30** | **6.1** | **44** | **99.13** | **9.74** |
| **Day 5** | 1 | 31.00 | 2 | 2.6 | 47 | 91.18 | 8.96 |
| | 2 | 171.00 | 24 | 5.3 | 58 | 79.92 | 7.85 |
| | 3 | 5.00 | 0 | -1.7 | 55 | 50.11 | 4.92 |
| | 4 | 230.00 | 12 | 4.5 | 66 | 71.27 | 7.00 |
| | 5 | 63.00 | 2 | 3.2 | 60 | 84.22 | 8.27 |
| **Overall Day 5** | | **500.00** | **40** | **5.3** | **60** | **76.88** | **0.00** |
| **Day 6** | 1 | 92.00 | 8 | 5.3 | 58 | 87.73 | 8.62 |
| | 2 | 5.00 | 0 | 1.5 | 56 | 146.39 | 14.38 |
| | 3 | 111.00 | 16 | 3.2 | 46 | 92.48 | 9.08 |
| | 4 | 31.00 | 2 | 3.3 | 43 | 64.91 | 6.38 |
| **Day 6** | | **239.00** | **66** | **5.3** | **51** | **88.20** | **8.66** |
| **Overall Trip** | | **2386.00** | **182** | **6.1** | | **82.90** | **8.14** |

Table 23 tabulates the distance traveled for more than 2% grade, maximum road grade experienced by vehicle, average velocity for each segment, payload-distance specific $CO_2$ emissions and payload-distance specific fuel consumption for each data segment within a given day of the cross country trip. Table 24 shows the brake-specific emissions of regulated, greenhouse gases and ammonia emissions for each segment of each day of the cross country trip.

**Table 25 Brake Specific GHG Emissions, $NH_3$ and Regulated Gaseous Emissions Results for the Cross-Country Trip**

| Test Day | Micro-trip | Work | Avg. Altitude | $CO_2$ | $CH_4$ | $N_2O$ | $NH_3$ | NOx | NMHC | CO |
|---|---|---|---|---|---|---|---|---|---|---|
| | | [bhp-hr] | [ft] | [g/bhp-hr] | | | [g/bhp-hr] | [g/bhp-hr] | | |
| Day 1 | 1 | 275.47 | 1134.25 | 327.58 | 0.02 | 0.023 | 0.008 | 0.06 | 0.03 | 0.03 |
| | 2 | 502.82 | 953.11 | 327.01 | 0.01 | 0.027 | 0.005 | 0.06 | 0.02 | 0.02 |
| | 3 | 89.00 | 1021.38 | 340.43 | 0.01 | 0.000 | 0.000 | 0.18 | 0.03 | 0.02 |
| | 4 | 255.93 | 1035.87 | 339.13 | 0.01 | 0.000 | 0.000 | 0.06 | 0.02 | 0.02 |
| | 5 | 418.67 | 805.61 | 363.49 | 0.03 | 0.026 | 0.001 | 0.05 | 0.01 | 0.04 |
| **Overall Day 1** | | **1541.89** | **949.39** | **339.81** | **0.02** | **0.026** | **0.004** | **0.06** | **0.02** | **0.03** |
| Day 2 | 1 | 441.93 | 602.16 | 345.68 | 0.01 | 0.016 | 0.003 | 0.03 | 0.01 | 0.03 |
| | 2 | 70.75 | 555.72 | 364.11 | 0.02 | 0.008 | 0.000 | 0.11 | 0.01 | 0.02 |
| | 3 | 654.68 | 688.43 | 342.26 | 0.01 | 0.021 | 0.004 | 0.02 | 0.01 | 0.02 |
| | 4 | 1038.97 | 975.84 | 328.41 | 0.01 | 0.022 | 0.002 | 0.42 | 0.01 | 0.03 |
| **Overall Day 2** | | **2206.32** | **793.33** | **337.13** | **0.01** | **0.020** | **0.003** | **0.21** | **0.01** | **0.03** |
| Day 3 | 1 | 789.33 | 2087.61 | 311.76 | 0.00 | 0.016 | 0.003 | 0.02 | 0.01 | 0.03 |
| | 2 | 806.88 | 4277.53 | 299.72 | 0.00 | 0.012 | 0.002 | 0.04 | 0.02 | 0.03 |
| | 3 | 269.50 | 5415.92 | 303.97 | 0.00 | 0.016 | 0.002 | 0.07 | 0.02 | 0.03 |
| **Overall Day 3** | | **1865.71** | **3588.54** | **305.43** | **0.00** | **0.015** | **0.003** | **0.04** | **0.01** | **0.03** |
| Day 4 | 1 | 186.26 | 7292.23 | 318.60 | 0.00 | 0.015 | 0.006 | 0.52 | 0.02 | 0.04 |
| | 2 | 93.81 | 9635.57 | 314.23 | 0.00 | 0.005 | 0.000 | 1.16 | 0.02 | 0.03 |
| | 3 | 71.47 | 11301.08 | 330.30 | 0.00 | 0.010 | 0.000 | 1.94 | 0.02 | 0.07 |
| | 4 | 126.70 | 9569.94 | 320.96 | 0.00 | 0.009 | 0.000 | 1.47 | 0.02 | 0.04 |
| | 5 | 233.51 | 5155.72 | 356.84 | 0.00 | 0.032 | 0.000 | 0.12 | 0.03 | 0.06 |
| **Overall Day 4** | | **711.75** | **7896.80** | **332.16** | **0.00** | **0.018** | **0.002** | **0.78** | **0.02** | **0.05** |
| Day 5 | 1 | 117.35 | 4637.37 | 286.95 | 0.03 | 0.032 | 0.002 | 0.14 | 0.02 | 0.06 |
| | 2 | 621.03 | 5578.09 | 330.08 | 0.01 | 0.012 | 0.003 | 0.14 | 0.02 | 0.04 |
| | 3 | 10.08 | 5310.08 | 372.78 | 0.02 | 0.015 | 0.001 | 1.36 | 0.03 | 0.15 |
| | 4 | 723.52 | 4747.38 | 339.85 | 0.02 | 0.014 | 0.001 | 0.08 | 0.02 | 0.05 |
| | 5 | 233.19 | 2002.47 | 341.28 | 0.04 | 0.000 | 0.000 | 0.06 | 0.02 | 0.04 |
| **Overall Day 5** | | **1705.17** | **4770.97** | **333.04** | **0.02** | **0.014** | **0.002** | **0.11** | **0.02** | **0.05** |
| Day 6 | 1 | 352.34 | 2737.62 | 343.61 | 0.01 | 0.024 | 0.002 | 0.05 | 0.02 | 0.04 |
| | 2 | 36.51 | 2653.48 | 300.72 | 0.00 | 0.004 | 0.001 | 0.31 | 0.01 | 0.02 |
| | 3 | 439.39 | 2250.33 | 350.44 | 0.00 | 0.019 | 0.001 | 0.07 | 0.02 | 0.04 |
| | 4 | 81.48 | 1380.65 | 370.44 | 0.03 | 0.021 | 0.001 | 0.04 | 0.02 | 0.09 |
| **Overall Day 6** | | **909.71** | **2427.96** | **347.59** | **0.01** | **0.021** | **0.001** | **0.07** | **0.02** | **0.04** |
| **Overall Trip** | | **8940.56** | | **330.86** | **0.010** | **0.019** | **0.003** | **0.16** | **0.02** | **0.03** |

Figure 88 shows the SCR intake gas temperatures and the calculated NOx conversion efficiency during the course of the cross-country study. The results show that SCR efficiency in reducing NOx was calculated to be on average 83-88%. Sustained highway vehicle speeds resulted in high exhaust temperatures conducive for high SCR activity.

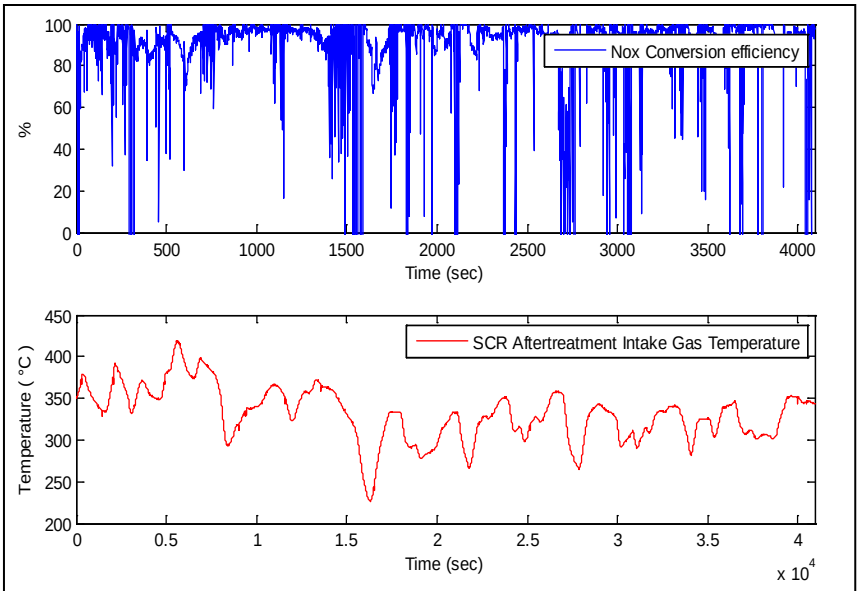


**Figure 88 NOx conversion efficiency and Pre-SCR exhaust temperature during in-use trip**

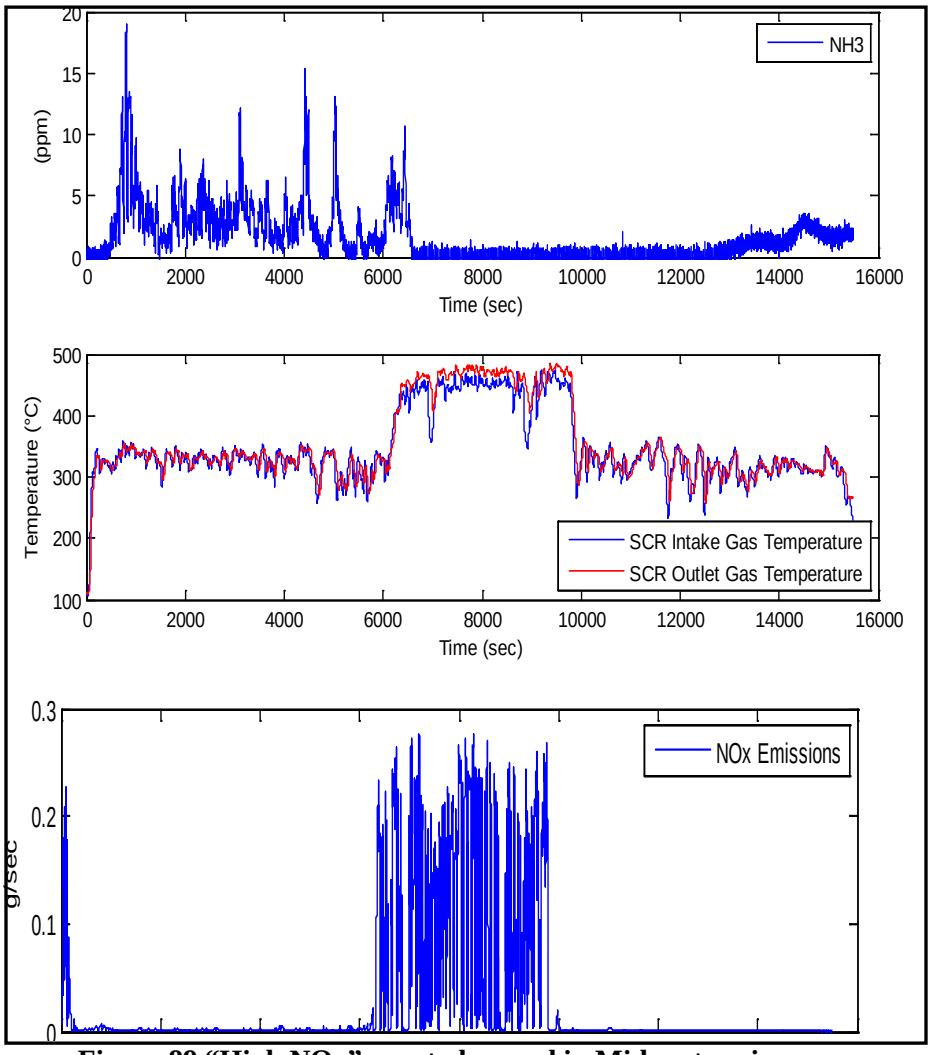


**Figure 89 "High NOx" event observed in Midwest region**

Figure 89 shows the “high NOx” event that was observed during a micro trip in the Midwest region. The entire duration of the micro trip was 4.4 hrs and 92% of the NOx emissions of this micro trip was emitted in a duration of 1 hour of this “high NOx” event. The figure above shows the change in exhaust temperature during this “high NOx” event through possible engine management strategy. The exhaust temperature during this event is observed to be in the range of 450 °C. This event could be related to SCR maintenance procedures that OEMs perform in order to preserve the health of the after-treatment system. This event was not an active regeneration system as the ECU broadcast did not indicate a regeneration activity. The figure also shows an interesting trend in the ammonia emissions prior to and subsequent to this “high NOx” event. Prior to the 7,000 second timestamp that marks the beginning of this “high NOx” event, it can be observed that tailpipe concentration of ammonia is measured to be in the range of 10-20 ppm. Subsequent to the event, the ammonia concentrations decrease to near-zero levels. The detection of ammonia slip could be attributed to the lower adsorption of urea by the SCR catalyst due to hydrocarbon or urea crystal deposition on the active surfaces of the SCR. The after-treatment maintenance strategy could have been employed to regenerate the active surfaces of the SCR through addition of exhaust energy. OEMs perform these procedures periodically to maintain the health of the after-treatment system and emissions during such events are quantified by the OEM, but however might be excluded from in-use emissions considerations.

# 4 - CONCLUSION

Results of this study show that NOx emissions from natural gas vehicles with TWC and the dual-fuel HPDI equipped with DPF and SCR to be significantly lower both in distance-specific and brake-specific emissions metric than US-EPA 2010 compliant diesel engines. Sustained activity of the TWC under all operating conditions contributed NOx emissions that were lower by 50% to 95% compared to diesel vehicles with SCR depending on the driving cycle. The overall lower engine out NOx emissions from the dual-fuel HPDI engine reduced the effect of SCR inactivity on the NOx emissions from this engine.

Exhaust temperature characteristics over the drayage cycle do not support sustained SCR activity for the diesel with SCR, while the stoichiometric natural gas with TWC exhibit orders of magnitude lower NOx emissions over all three drayage activities. The dual-fuel HPDI vehicles exhibited lower NOx, even during periods of no SCR activity while compared to diesels with similar aftertreatment technology. From a perspective of port drayage application, the natural gas fueled vehicles will contribute to lower NOx emissions during activities inside the port and local urban type operation. Diesel vehicles with SCR require sustained vehicle speeds and higher operating loads to achieve lower NOx emissions.

The PM mass emissions from DPF equipped diesel and natural gas with TWC were of the same order of magnitude, with low mass emissions that contribute to high levels of measurement uncertainty. It is to be noted that since diesel vehicles undergo periodic DFP regeneration to prevent exhaust backpressure and integrity of the DPF, regeneration activities did contribute to higher PM mass and number emissions. Since natural gas combustion is soot free compared to diesel combustion, natural gas vehicles are able to achieve USEPA 2010 PM emissions limit without the use of DPF.

Diesel vehicles with SCR exhibited a NOx emissions profile similar to natural gas with TWC in the refuse truck platform. The lower NOx emissions from the diesel with SCR can be attributed to a down sized engine and the use of active SCR thermal management to achieve reduce NOx emissions. It should be noted that the natural gas refuse truck operates at a 32% better fuel economy (DGE) than the diesel refuse truck.

Stoichiometric natural gas engines were characterized by ammonia emissions close to 1 mg/mile over all driving cycles. No ammonia emissions were observed from diesel equipped with SCR. $N_2O$ emissions from natural gas engines were observed only during the warm-up phase of the TWC. No significant $N_2O$ emissions were detected from any diesel technology vehicles.

Carbonyl and BTEX emissions results indicated a superior activity of the TWC in controlling emissions of tailpipe toxic air contaminants to levels below ambient air. Significant levels of

formaldehyde emissions were observed during the warm-up phase of the TWC. Diesel vehicles operating with a high EGR strategy indicated the presence of benzene in the exhaust that could be linked to active regeneration activities. EC/OC emissions showed a predominant OC fraction of total PM from both natural gas and DPF equipped diesels. However, natural gas engines operating in transit bus and refuse trucks with significantly high mileage revealed the possibility of lubrication oil consumption, indicated by the detection of EC fraction in the PM samples.

Particle size distribution analysis showed particle emissions from stoichiometric natural gas engines and DPF equipped diesel engines to be of the same order of magnitude as ambient air concentrations. The observed particle size distribution and concentrations from the transit bus suggests an influence of engine component ageing on PM emissions. Since, the natural gas engines operate without a particulate filter, changes in oil consumption, engine wear and catalyst degradation can manifest itself as organic or inorganic PM emissions in the exhaust. High nucleation mode particle concentrations observed from the DPF and SCR equipped vehicles, corroborates previous studies that have documented similar events. However, it is to be noted that the fate of these particles or their impending health effects have not been completely understood yet.

The $NO_2$ fraction in total NOx emissions from stoichiometric natural gas engines is insignificant compared to HPDI and diesel with DPF and SCR. With NMHC emissions close to detection limits, it can be concluded that the ground level ozone formation potential of stoichiometric natural gas exhaust to be significantly lower than diesel vehicles.

The GWP of natural gas vehicles were lower than diesel vehicles for both refuse truck and goods movement application. Methane emissions from natural gas vehicles was not a major contributor to the GWP of exhaust.

The study presents a comprehensive analysis of current emissions rates of heavy-duty diesel, natural gas, and dual-fuel engines while operating under different vocations. The overall results of the study indicate orders of magnitude lower emission rates of NOx from stoichiometric natural gas engines when compared to heavy-duty diesel engines. The study clearly illustrates the differences in emission rates of diesel engines equipped with SCR while operating in and out of conditions favoring SCR activity.

The results of the study raises important questions regarding ammonia emissions from the stoichiometric natural gas engines and the impact of this mobile source emissions to secondary particulate matter formation. WVU is conducting research on a passive SCR strategy to control ammonia emissions and further reduce NOx emissions from stoichiometric natural gas engines.

## References


2012. *Background and Justification for Handbook 130 Definition of "Diesel Gallon Equivalent (DGE)" of Natural Gas as a Vehicular Fuel* [Online]. Available: www.cleanvehicle.org/linked/GGE_DGE_Background_Document.pdf [Accessed 6/29/2013].

ANEJA, R., BOLTON, B., OLADIPO, B. A., MACKINNON, P. Z. & RADWAN, A. Year. Advanced diesel engine and aftertreatment technology development for Tier 2 emissions. *In:* Diesel Engine Emission Reduction Workshop, 2003 Newport, Rhode Island.

ARDANESE, R., ARDANESE, M., BESCH, M., ADAMS, T., THIRUVENGADAM, A., SHADE, B., GAUTAM, M., OSHINUGA, A. & MIYASATO, M. 2009. PM Concentration and Size Distributions from a Heavy-duty Diesel Engine Programmed with Different Engine-out Calibrations to Meet the 2010 Emissions Limits. *SAE Technical Paper,* 2009-01-1183.

AYALA, A., KADO, N., OKAMOTO, R., HOLMEN, B., KUZMICKY, P., KOBAYASJI, R. & STIGLITZ, K. 2002. Diesel and CNG Heavy-duty Transit Bus Emissions over Multiple Driving Schedules: Regulated Pollutants and Project Overview. *SAE Technical Paper,* 2002-01-1722.

COUCH, P. 2011a. Charcaterization of Drayage Truck Duty Cycles at the Port of Long Beach and Port of Los Anegeles. Irvine, CA: TIAX LLC.

COUCH, P. 2011b. Development of a Drayage Truck Chassis Dynamometer Test Cycle. Irvine, CA: TIAX LLC.

COUCH, P. & LEONARD, J. 2011. *Characterization of Drayage Truck Duty Cycles at the Port of Long Beach and Port of Los Angeles* [Online]. Irvine, CA: TIAX LLC. [Accessed].

DEFOORT, M., OLSEN, D. & WILLSON, B. 2003. The effect of air-fuel ratio control strategies on nitrogen compound formation in three-way catalysts. *International Journal of Engines Research,* 5**,** 115-122.

HERNER, D. J., HU, S., ROBERTSON, H. W., HUAI, T., CHANG, O. M. C., REIGER, P. L. & AYALA, A. 2011. Effect of Advanced Aftertreatment for PM and NOx Reduction on Heavy-Duty Diesel Engine Ultrafine PArticle Emissions. *Environmental Science and Technology,* 45**,** 2413-2419.

IPCC. 2007. *IPCC Fourth Assessment Report: Climate Change 2007* [Online]. [Accessed 3/21/2014 2014].

JOHNSON, T. 2009. Diesel Emissions Control in Review. *SAE Journal,* SAE 2009-01-0121.

KAMASUNDARAM, K., HENRY, C. & YEZERETS, A. Year. N2O Emissions from 2010 SCR systems. *In:* Directions in Engine-Effeciency and Emissions Research Conference-DEER 2011. U.S DOE.

KITTELSON, D. B., F., W. W. & JOHNSON, J. P. 2006. On-road and laboratory evaluation of combustion aerosols-Part 1: Summary of diesel engine results. *Journal of Aerosol Science,* 37**,** 913-930.

KITTELSON, D. B., WATTS, W. F., JOHNSON, J. P., THORNE, C., HIGHAM, C., PAYNE, M., GOODIER, S., WARRENS, C., PRESTON, H., ZINK, U., PICKLES, D., GOERSAMNN, C., TWIGG, M. V., WALKER, A. P. & BODDY, R. 2008. Effect of fuel and lube oil sulfur on the performance of a diesel exhaust gas regenerating trap. *Environmental Science and Technology,* 42**,** 9276-9282.

ODAKA, M., KOIKE, N. & SUZUKI, H. 1998. Deterioration Effect of Three-way Catalyst on Nitrous Oxide Emission. *SAE Technical Paper,* SAE-980676.

OKAMOTO, R., KADO, N., KUZMICKY, P., AYALA, A. & KOBAYASJI, R. 2006. Unregulated Emissions from Compressed Natural Gas (CNG) Transit Buses Configured with and without Oxidation Catalyst. *Environmental Science and Technology,* 40**,** 332-341.

REXEIS, M. & HAUSBERGER, S. 2009. Trend of vehicle emission levels until 2020-Prognosis based on current vehicle measurements and future emission legislation. *Atmospheric Environment,* 43**,** 4689-4698.

THIRUVENGADAM, A. 2013. *Characterization of the composition and toxicity of particulate matter emissions from advanced heavy-duty natural-gas engines.* Doctor of Philosophy, West Virginia University.

THIRUVENGADAM, A., BESCH, C. M., CARDER, D., OSHINUGA, A. & GAUTAM, M. 2011a. Influence of Real-World Engine Load Conditions on Nanoparticle Emissions from a DPF and SCR Equipped Heavy-Duty Diesel Engine. *Environmental Science and Technology,* 46**,** 1907-1913.

THIRUVENGADAM, A., BESCH, M., CARDER, D. & GAUTAM, M. 2013. Characterization of the composition and toxicity of particulate matter emissions from advanced heavy-duty natural gas engines. *17th ETH Conference on Combustion Generated Nanoparticles.* Zurich, Switzerland.

THIRUVENGADAM, A., CARDER, D., KRISHNAMURTHY, M., OSHINUGA, A. & GAUTAM, M. 2011b. Effect of an economical oxidation catalyst formulation on regulated and unregulated pollutants from natural gas fueled heavy duty transit buses. *Transportation Research Part D,* 16**,** 469-473.

USEPA 2004. Draft Techincal Support Document: In-Use Testing for Heavy-Duty Diesel Engines and Vehicles. Office of Transportation and Air Quality, U.S.. Environmental Protection Agency.

VAARASLAHTI, K., J, K., GIECHASKIEL, B., A, S., T, M. & H, V. 2005. Effect of Lubricant on the formation of Heavy-Duty Diesel Exhaust Nanoparticles. *Environmental Science and Technology,* 39**,** 8497-8504.

YOON, S., HU, S., KADO, N., THIRUVENGADAM, A., JOHN, C., GAUTAM, M., HERNER, J. & AYALA, A. 2014. Chemical and toxicological properties of emissions from CNG transit buses equipped with three-way catalysts compared to lean-burn engines and oxidation catalyst technologies. *Atmospheric Environment,* 83**,** 220-228.